JIMMA UNIVERSITY

JIMMA INSTITUTE OF TECHNOLOGY(JIT)

DEPARTMENT OF CIVIL AND ENVIRONMENTAL ENGINEERING

GEOTECHNICAL ENGINEERING STREAM.

ASSESSMENT OF LANDSLIDE SUSCEPTIBILITY AND ROCK-SOIL SLOPE STABILITY ANALYSIS (RSSSA): USING GIS AND ROCSCIENCE (SLIDE) SOFTWARES

A Final MSc Thesis submitted to the school of Graduate studies of Jimma University In Partial Fulfillment of the Requirements for the Master's Degree in Geotechnical Engineering

BY

Mr. GASHAW HAILE FIKADU

JANUARY, 2022

JIMMA, ETHIOPIA

JIMMA UNIVERSITY

JIMMA INSTITUTE OF TECHNOLOGY(JIT)

DEPARTMENT OF CIVIL AND ENVIRONMENTAL ENGINEERING

GEOTECHNICAL ENGINEERING STREAM.

ASSESSMENT OF LANDSLIDE SUSCEPTIBILITY AND ROCK-SOIL SLOPE STABILITY ANALYSIS (RSSSA): USING GIS AND ROCSCIENCE (SLIDE) SOFTWARES

A Final MSc Thesis submitted to the school of Graduate studies of Jimma University In Partial Fulfillment of the Requirements for the Master's Degree in Geotechnical Engineering

BY

Mr. GASHAW HAILE FIKADU

Advisor: DAMTEW TSIGE (PhD)

Co-Advisor: TEWODROS TSEGAYE (MSc)

JANUARY, 2022

JIMMA, ETHIOPIA

JIMMA UNIVERSITY

JIMMA INSTITUTE OF TECHNOLOGY(JIT)

DEPARTMENT OF CIVIL AND ENVIRONMENTAL ENGINEERING

GEOTECHNICAL ENGINEERING STREAM.

ASSESSMENT OF LANDSLIDE SUSCEPTIBILITY AND ROCK-SOIL SLOPE STABILITY ANALYSIS (RSSSA): USING GIS AND ROCSCIENCE (SLIDE) SOFTWARES

A Final MSc Thesis submitted to the school of Graduate studies of Jimma University In Partial Fulfillment of the Requirements for the Master's Degree in Geotechnical Engineering

BY

Mr. GASHAW HAILE FIKADU
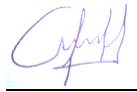
<u>APPROVED BY BOARD OF EXAMINERS</u>

1. ENDALU TADELE (PhD)		08/03/ 2022 G.C.
External Examiner	Signature	Date
2. HASHIM WARE (MSc)		10/03/ 2022 G.C.
Internal Examiner	Signature	Date
3. HABTE TAMRAT (MSc)		09/03/ 2022 G.C.
Chairman of Examiner	Signature	Date
4. DAMTEW TSIGE (PhD)		08/03/2022 G.C.
Main Advisor	Signature	Date
5. TEWODROS TSEGAYE(MSc)		07/03/2022 G.C.
Co- Advisor	Signature	Date

DECLARATION

I, the undersigned, declare that this study, titled "Assessment of landslide susceptibility and rock-soil slope stability analysis (RSSSA) along Zabidar mountain road corridors using GIS AND ROCSCIENCE (SLIDE) softwares," is my original work and has not been submitted to a degree by anyone else. In addition, all tools and materials used in this study must be duly recognized.

Candidate:

Mr. GASHAW HAILE FIKADU   06/01/2022 G.C.

                          Signature   Date

We, the Master's Research Advisors, hereby certify that we have read and evaluated Mr. GASHAW HAILE FIKADU's MSc thesis entitled "ASSESSMENT OF LANDSLIDE SUSCEPTIBILITY AND ROCK-SOIL SLOPE STABILITY ANALYSIS (RSSSA): USING GIS AND ROCSCIENCE (SLIDE) SOFTWARES" along Zabidar Mountain road corridor: (GURAGE AND SILT'E ZONE, SNNPR, ETHIOIA).

It is recommended that it be submitted as fulfilling the MSc thesis requirements.

DAMTEW TSIGE (PhD).   06/01/2022 G.C.

  Main Advisor   Signature   Date

TEWODROS TSEGAYE (MSc).   06/01/2022 G.C.

 Co- Advisor   Signature   Date

ACKNOWLEDGEMENTS

ABSTRACT

A landslide is a downhill movement of rock or soil, or both, over the ground surface's crust in the form of a curved (rotational) or planar (translational) rupture. There is still a lack of realistic policies for landslide risk management due to a lack of (rare) landslide assessment, knowledge of various causative factors, triggering factors, methods of counting, measuring, analysis, and landslide susceptibility mapping practices. Two of the most common approaches to landslide mapping are field surveys and visual analysis of stereoscopic aerial imagery. These procedures, on the other hand, not only take a long time, but are costly, labor-intensive, and physically exhausting operations in a large area. Therefore, to overcome this problem, it is better to use remote sensing software to save time and money for survey data collection processes and omit errors due to landslide assessments, like during counting, measuring the area or size and analysis of landslides, estimation of the time it occurred.

The objective of this research was to study different causative and triggering factors, evaluate frequently experienced landslides/slope failure points and prepare a landslide hazard zone map for the entire study area using a bivariate statistical and numerical approach. For this study, removed/lost surfaces along the Zabidar Mountain road corridor were extracted by the cut/fill spatial analyst tool in GIS and their frequency ratio was evaluated for the past six consecutive years. The landslide hazard zone map was created on the Arch map using a customized raster calculation to identify regions vulnerable to landslides/slope stability failure.

According to the landslide hazard map, 27% (4.8 km2) of the area is free from the landslide zone, 29% (5.2 km2) is susceptible to the landslide zone, 23% (4.1 km2) is low to the landslide zone, and 21% (3.8 km2) is truly dangerous to the landslide zone. Based on the hazard map created, geotechnical characterization of selected points was studied by conducting sieve analysis, angle of repose, unconfined compressive strength and direct shear tests. Rocscience software (Slide) was applied for the limit ,equilibrium method analysis of weathered rock mass along the road corridor for cross check of the landslide hazard zone map. The result shows, 80% are unstable (factor of safety less than 1.5). In this study, it was also identified that 588 households are in the no-landslide danger zone, 555 households are living in the medium to landslide danger zone, 228 households are living in the low-risk landslide zone, and 61 households are living in the high-risk landslide zone. The findings of this study might be useful to guide a suitable method for survey data collection and its analysis, for decision-makers in future land management, hazard mitigation operations, selecting appropriate sites for infrastructure developments, flood control systems, and drainage canals.

Key words: ASSESSMENT, GIS, LANDSLIDES, STABILITY, SUSCEPTIBILITY

Table of Contents

List of tables

List of figures

ABREVIATIONS

ASTER   Advanced Spaceborne Thermal Emission and Reflection Radiometer

ASTM   American Society For Testing and Materials

AUC   Area Under the Curve

DEM   Digital Elevation Model

FR   Frequency ratio

GDEM   Global Digital Elevation Model

GIS   Geographical information system

Gps   Global positioning system

INT   Integer

KM   Kilometer

KM^2 Square Kilometer

M   Meter

M^2 Square Meter

MS   Micro Soft

KML   Keyhole Markup Language

LSI   Landslide susceptibility index

LSM   Landslide susceptibility map

UCS   Unconfined Compressive Strength

USGS   United state Geological Survey

PR   Probability Ratio

RF   Rate of Frequency

SNNPR   South Nations Nationalities and Peoples' Region

CHAPTER ONE
INTRODUCTION

1.1 Background

A landslide is a downward and outward movement of rock or soil, or both, that occurs on the crust of ground surface in the form of a curved (rotational) or planar (translational) rupture (1). Landslides on mountainous terrain often occur during or after heavy rains, causing death and disruption to the natural and built environment (or both). Landslide-prone areas should also be known ahead of time to minimize risk (2).

Natural and man-made landslide risks and associated failures have been observed in almost all regions of Ethiopia. Major infrastructural development (including roads and railways), urbanization, and comprehensive natural resource management are currently underway in the country (3).

Landslides are one of the most dangerous natural phenomena, causing not only extensive damage to civil engineering systems such as highways, railways, bridges, dams, bioengineering structures, and homes, but also death. As a result, landslide susceptibility mapping is required for the identification of potential landslide areas (4). In the last five decades, Ethiopia has resulted in the death of humans and animals, as well as infrastructure and property destruction. Between 1960 and 2010, 388 people died, 24 people were hospitalized, and a large area of cultivated and non-cultivated soil, buildings, and homes were all impacted. Despite the fact that Ethiopia's landslide issue is severe, there is still no comprehensive landslide susceptibility mapping in the country's various regions (5).

With careful project preparation and execution, landslide susceptibility mapping will provide most of the critical knowledge needed for hazard mitigation (2).

Zabidar Mountain is one of the problematic areas for landslides and slope failure occurrences along road corridor constructed through it. In order to manage this problem, this research was done to evaluate the landslide frequencies in entire study area. After the determination of frequency ratio of landslide for the entire study area, the landslide hazard map was prepared using the spatial analyst tool in GIS. Using GIS software increases the accuracy of constructing a landslide susceptibility map by omitting errors encountered during landslide counting, size measuring and estimation of the time it occurred. Finally, based on the landslide hazard zone map, geotechnical characterization was studied for selected points along the road corridor by conducting sieve analysis, angle of repose, unconfined compressive strength and direct shear tests. Rocscience (slide) software was also applied for limit equilibrium method of weathered rock slope stability analysis along road corridor for check up of GIS results.

1.2 Statement of problem

Natural disasters are a major impediment to economic development, especially in developing countries (6). Landslide hazards are among the world's most deadly natural disasters. Through taking effective steps, landslide threat mapping assists in reducing the danger of a landslide. Monitoring landslides in a vast region with a sparse population, on the other hand, can be a costly, labor-intensive, and physically exhausting activity (7). Landslides are often characterized as local issues, but their consequences and costs often exceed local governments, becoming State, Provincial, or national issues (8).

Since many landslides go unreported and no systematic estimate of casualties due to landslide hazards has been made so far, decision makers at different levels of government who are mainly interested in emergency issues including relocation and rehabilitation of people affected by landslide hazards have a poor knowledge of the severity of the problems. Furthermore, general understanding of landslide dangers is still limited, and many people still see those threats as acts of God (9).

The first and most important stage in determining landslide vulnerability is mapping landslide occurrence regions. Over a wide area, it is difficult to reliably forecast the time and location of landslides (10). In landslide studies, data quality is critical, and more reliable findings can be obtained if the data is sufficient, relevant, and taken from a diverse set of parameters (11). A field survey or visual analysis of stereoscopic aerial photography are two of the most popular techniques for landslide mapping (12). These approaches, on the other hand, are not only time consuming, but also resource consuming. Furthermore, they appear to need data on a wide range of areas (13).

The most important approaches for assessing landslide frequency and indicating landslide susceptibility zones include the use of a geographic information system (GIS). It enables rapid analysis of cartographic materials as well as the selection of methods that are appropriate for the target, size, and data available (14). Over the last few years, a number of countries have seen progress in minimizing the loss of human lives, property destruction, and infrastructure failure caused by landslide-related hazards by detecting and providing appropriate landslide safety systems using GIS-based landslide hazard zonation maps. Concerns regarding the causes of landslides, as well as estimates of when they will occur, differ greatly across the world's regions and countries, especially in developed countries, where landslides and associated hazards are seen as growing rather than decreasing in severity and danger (5).

Not only does the country lack a competent organization capable of leading the way in landslide hazard assessment and prevention, but it still lacks realistic policies for landslide risk management. This is due to a lack of (rare) landslide assessment, a knowledge deficit on various causative factors,

internal and external triggering factors, method of counting, measuring, analysis, landslide susceptibility mapping practices, and the lack of appropriate landslide protection mechanisms.

As a result, Zabidar Mountain is one of the most prone to landslides of various forms. In this area, flooding and landslides are the most serious issues affecting human and animal life, agricultural fields, infrastructure, and the social and economic elements of rural communities as a whole.

The work presented here contributes to the use of a spatial analyst tool cut/fill in GIS software to forecast landslides on Zabidar Mountain rather than counting landslides or measuring surface area manually. As a result, a susceptible landslide hazard map of the research area was created using the frequency ration (FR) approach, and vulnerable settlements and potential slope failure spots along the road corridor were found. This study's findings may be useful to surveyors and decision-makers in forecasting the likelihood of landslide occurrence zones as well as in future land management and hazard reduction programs.

1.3 Research questions

1. What are the causes and triggering factors of landslides?

2. Can infrastructure development be responsible for the occurrence of landslides?

3. Where do landslides/ slope failures are frequently occurred?

4. Who are in risk to landslide/Slope failures in the study area?

1.4 Objectives of the study

1.4.1 General objective

The general objective of the study is, to assess, predict and mapping of landslide hazard zone map using GIS software and analyze rock-soil slope stability along road corridor using Rocscience (Slide) software.

1.4.2 Specific objectives

1. To asses various landslide causative and triggering factors in the study area.

2. To characterize geotechnical conditions of rock and soil slope failure points along road.

3. To analysis weathered rock mass slope stability by limit equilibrium method along road corridor

4. To predict possible landslide/slope failure risk areas or points in entire study area.

1.5 Scope and Limitation of the study

In general, this research includes mathematical method modeling of a limited number of causative factor classes for landslide hazard prone mapping over a total study area of 17.9km^2, as well as limited number of laboratory tests for geotechnical characterization and limited number of points for numerical evaluation (Limit equilibrium method) of rock slope stability analysis along a 13.9km road corridor through the study area were used. In general, only area mentioned above, i.e. 17.9km^2, was used to construct a susceptible landslide hazard zone map.

1.6 Significance of the study

This study is important to identify different causative and triggering factors, methods of analysis for landslides and to map susceptible landslide prone areas as well as to evaluate weathered rock slope stability analysis by limit equilibrium method along the road corridor through Zabidar Mountain (GURAGE AND SILT'E ZONE, SNNPR, ETHIOPIA).

The following are some of the stakeholders who would benefit from the findings of this study:

1. The study will benefit the administrations of Gurage Zone and Silt'e Zone as a source of information and a basis for road maintenance and the temporary flood and landslide hazard state of emergency that they have for vulnerable societies who live around Zabidar Mountain every summer.
2. Provide a very simple method of data collection or extraction. Example: Survey data.
3. The thesis would help surveyors, environmentalists, geologists, and geotechnical engineers as a source of expertise and a foundation for consultancy in the construction industry, reducing the risks of landslide/slope collapse on human life and infrastructure.
4. Other researchers will use the results as a basis for more studies into landslide evaluation and slope stabilization analysis.
5. As a guide for flood and relative studies in the agricultural sector.
6. Provide responses to study questions or make recommendations for landslide/slope collapse prevention measures.

1.7 Justification of the study

The rationale for conducting this study to provide the baseline to reduce the cost and time for data collection and process by providing a very precise method of statistical analysis. Facts show that the Gurage and Silt'e zone administrations both allocate and consume massive budgets for road maintenance and as a result of the temporary flood and landslide hazard protection state of

emergency for vulnerable societies who live around Zabidar Mountain every summer. To mitigate this problem, assessing, predicting and mapping of susceptible landslides in the area is needed.

1.8 Methodology

Pre-field work, field work, and post-field work are the three primary parts of this study. A literature study and gathering all relevant material from diverse sources were the major activities in the Pre-fieldwork phase. During the field work stage, the ground verification of potential landslides, general layout of the study area, location, mode and condition of landslides/slopes failures in the study area and unconfined compressive strength of weathered rock mass on selected four points along road were conducted. During post field work, gradation (sieve analysis) and angle of repose and direct shear test to determine soil shear strength parameters such as cohesive force (C) and angle of internal friction (Φ) and unit weight (γ) for four points along road corridor were conducted and interpreted. A map of considered causative factors for lithology/soil mass, elevation, slope, aspect, curvature, and distance to stream were prepared with the help of ArcGIS and statistical analysis. Frequency ratio values were determined and used to prepare landslide susceptibility map. Based on the developed map, numerical analysis (Limit equilibrium method) of weathered rock mass slope stability for selected points along the road corridor were analyzed and interpreted as validation of developed landslide hazard zone map.

CHAPTER TWO
LITERATURE REVIEW

2.1 Introduction

Landslides are one of the most common natural catastrophes, posing serious risks to people, property, and the environment in a variety of locations. Landslide susceptibility mapping (LSM) has been found to be beneficial in developing landslide mitigation techniques for lowering catastrophe risk and social and economic losses, which is important for land use planning, hazard prevention, and risk management.

The literature on causes and triggering factors, types of landslides, vulnerability, landslide statistical analysis and rock-soil slope stability analysis is discussed in this chapter. The primary goal of a literature review is to identify the scholarly and research areas that are important to the topic under consideration. The following research were analyzed and referenced for this report, which includes material on landslide susceptibility assessment and slope stability evaluation.

2.2 General theoretical review

Falls, rotational and translational slips, flows, and creep are the most common mass-wasting mechanisms. Falls are sudden rock movements that break off from cliffs or steep slopes. Natural cracks, such as fractures and bedding planes, enable rocks to split. Free fall, bouncing, and spinning are also examples of movement. Gravity, mechanical weathering, and water have a major effect on dropping. Slow movement around a curved rupture surface is typical of rotational slides. Rapid motions along a plane of distinct instability between the overlying slide material and the more solid underlying material are often referred to as translational slides. Rock slides, debris slides, and planet slides are some of the types of slides (19, 20).
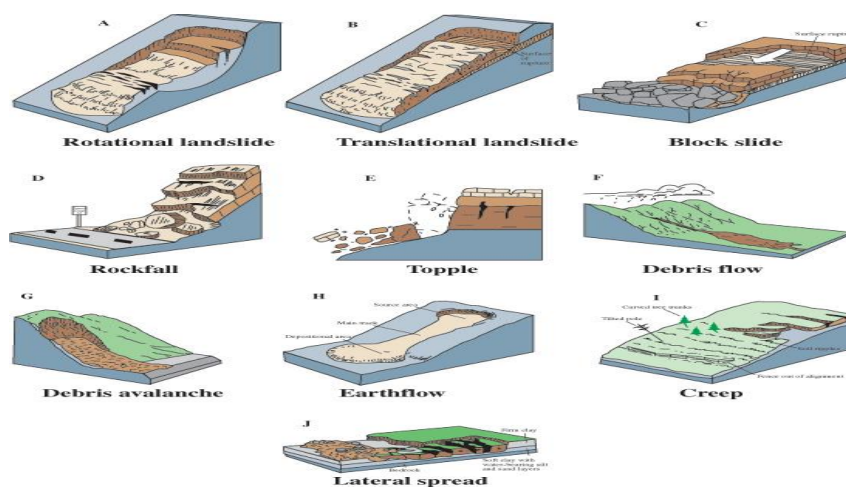
Figure1. Classification of landslide types based on classification of Varnes (1978)**.**

Soil types, stratification, groundwater, seepage, and slope geometry all play a role in slope failures. The following are some of the most common forms of slope failure in soil (17).

1. Translational Slide: A translational slip occurs when a slope fails along a poor zone of soil (Figure 2.a). Before coming to a stop, the sliding mass can travel a long distance. In coarse-grained soils, translational slides are common.

2. Rotational Failure: A rotational slip, with its point of rotation on an imaginary axis parallel to the slope, is a typical form of failure in homogeneous fine-grained soils. Rotational failure can take three forms.

i. Base Failure: Base failure can occur when a soft soil layer rests on a stiff soil layer (Figure 2.b).

ii. Toe Failure: When the fault surface runs through the slope's toe (Figure 2.c).

iii. Slope Failure: When the failure surface passes through the face of slope (Figure 2.d).

iv. Flow Slide: When internal and external pressures force a soil to behave like a viscous fluid and flow down even shallow slopes, spreading out in several directions, a flow slide occurs (Figure 2.e).

v. Block Slide: When a translational slide in which the moving mass consists of a single unit or a few closely related units that move downslope as a relatively coherent mass (figure 2.f).
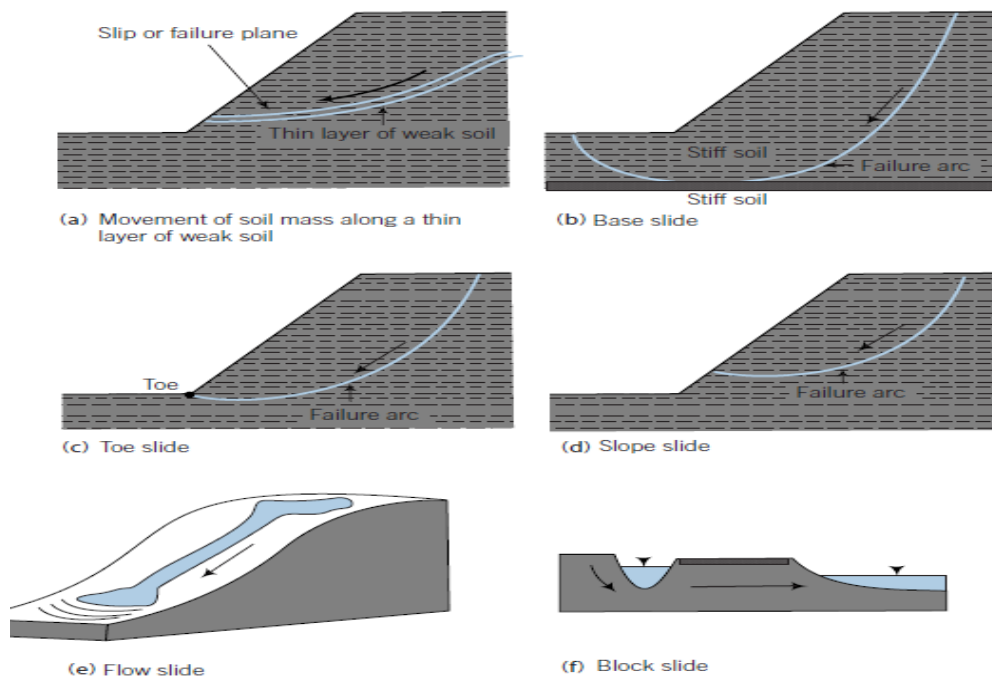
Figure 2. Common types of slope failure in soils

According to (18),16)

 A fall starts when soil or rock, or both, disconnects from a steep slope along a surface with little or no shear displacement. The material either falls, bounces, or rolls off.

Rack falls are sudden, downward movements of rock, soil, or both that separate steep slopes or cliffs. Bouncing occurs as falling debris reaches the lower slope at an angle that is less than the angle of fall. On impact, the dropping mass can crack, roll down steeper slopes, and continue until the terrain flattens.

Topple is the forward movement of a mass of soil or rock around a point or axis below the displaced mass is known as a topple. Toppling is frequently caused by the weight of material upslope from the displaced mass. Water or ice in cracks in the mass may cause toppling sometimes. Rock, rubble (coarse material), and earth materials may all cause topples (fine grained material). Complex and composite topples may occur.

A flow is a continuous spatial movement in which the shear surfaces are short-lived, closely spaced, and normally not maintained. The factor velocities of a flow's displacing mass are similar to that of a viscous liquid. Depending on the water content, mobility, and evolution of the movement, there is often a gradation of transition from slides to flows.

Debris Flows are type of rapid mass movement in which water, loose soil, and often organic matter combine to create slurry that flows downslope. Owing to the vast amount of fine material that could be found in the river, they have been named "mudslides" informally and inappropriately. A debris flow may form when a rotational or translational slide gains momentum and the internal mass loses cohesion or gains water. In cohesionless sand, dry flows may occur (sand flows). Debris floods can be dangerous because they can happen quickly and without warning.

Debris avalanches are massive, incredibly fast, often open-slope flows that occur when an unstable slope collapses and the scattered debris is quickly moved away from the slope. Generally speaking, there are two kinds of debris avalanches: "cold" and "hot." A cold debris avalanche occurs when a slope becomes unstable, such as when weathered cliffs in steep terrain collapse, or when bedrock disintegrates during a slide-type landslide moving downslope at high speed. The mass will then turn into a debris avalanche at this stage. A hot debris avalanche is one that occurs as a result of volcanic activities, such as volcanic explosions or magma injection, causing slope instability.

2.3 Landslide Causes and Triggering Mechanisms

The lithology, elevation, slope, aspect, plan curvature, and distance from the river all have a role in the spatial distribution and intensity of landslides. (13). When assessing the likelihood of landslides over a certain length of time and in a certain location, it's critical to understand the circumstances that might induce a landslide and the mechanism that might start the movement (11).

Researchers have discovered that soil erosion triggers landslides as a result of permanent challenges to slope stability and ecosystem functionality. According to (19), by changing the conditions that cause soil erosion, the rate of landslides may be decreased.

Fresh bedrock's susceptibility to rockfalls, rockslides, and block glides is determined by a variety of factors, including seepage forces during rainstorms. The weathered zone grows outward from the joints, isolating fresh rock blocks or boulders to form corestones. Corestones become remnants on the ground surface in some areas and can roll down hills during rainy seasons, causing severe damage. The rock fall landslide is the most common form of slide in this weathering stage. The danger of falling materials is real. Property under the fall-line of big rocks may be damaged by falls. Boulders have the ability to bounce or roll long distances, causing structural damage or death. Rockfalls can cause deaths in cars struck by rocks which can obstruct highways and railroads, causing significant damage to roads and railroads (16),22).

The Schmidt hammer (also known as the rebound or impact hammer) test is a non-destructive method for determining the quality of rock in terms of surface rebound hardness, which is linked to uniaxial compressive strength. The Schmidt hammer test is an essential index test for rock material characterization since it is fast, inexpensive, and non-destructive (21). Predicting the stability of rock slopes is a basic geotechnical engineering problem that is critical when constructing dams, highways, tunnels, and other engineering projects. In assessing the stability of a rock slope, the approach utilized to characterize the failure behavior of the rock mass is essential. The stress function of rock mass strength, on the other hand, is nonlinear. Hoek and Brown introduced the nonlinear Hoek–Brown (HB) criteria in 1980, based on a significant quantity of experimental data from field testing done on rocks. Following that, in 2002, Hoek et al. refined the fundamental Hoek–Brown (HB) criterion, resulting in the generalized Hoek–Brown (GHB) criterion, which has subsequently become extensively used for evaluating the strength of rock and rock masses. The GHB criterion can currently reflect a rock's inherent nature as well as the effect of certain factors on the strength of a rock mass, such as the rock's strength, the number of structural planes, and the stress state; thus, the GHB criterion is critical in studying the deformation and failure characteristics of rock slopes (22).

As shear stress exceeds the shear strength of slope material, landslides/slope collapses occur. The factors that lead to a rise in shear stress and factors that contribute to a decrease in shear strength can be categorized as landslide causative factors. However, water is another factor that contributes to both increasing and decreasing shear stress and shear strength of slope material, respectively (23).

Understanding the geological setting (lithological and structural), terrain characteristics, hydrological condition (surface and groundwater), land use/vegetation status, and other geomorphological processes is essential for understanding failure mechanisms and designing effective landslide mitigation measures (24).

Different causative variables (independent factors) such as lithology, elevation, slope, aspect, curvature, and distance from river can be used to construct landslide hazard zonation maps (25).

Lithology refers to the composition, texture, and degree of weathering of rocks and soils, as well as other characteristics that affect physico-chemical and engineering properties such as permeability, shear strength, and so on. The slope stability is affected by these features (26). Because it produces a noticeable anisotropy in the permeability, strength, and deformation properties of soil/rock masses, factors inherent in the nature of the materials and discontinuities may have an impact on engineering features of slopes (24). The lithology and slope of the ground determine the kind and intensity of landslides. It is well understood that lithological characteristics influence the physical properties of surface and subsurface materials, and therefore the danger of land sliding (27).

Pelitic vertisols are soils with high shrink-swell potential, which are characterized by a high clay content, cracks that open and close periodically and wedge-shaped aggregates and/or slickensides that occur at a specific depth (28). Chromic luvisols are dark reddish brown or reddish brown luvisols extracted from calcareous parent material. It's usually silty, with clay buildup (29).

The height above sea level is referred to as elevation. Within terrains, elevation is helpful for classifying local relief and locating places of greatest and lowest heights. It is one of the factors that causes landslides and erosion (11).

A slope is the rise or fall of the land surface. Slope angle is the most important relief characteristic that affects the mechanism and the intensity of the landslides. In general, if the slope is steeper it will be more susceptible to instability as compared to gentle slope. The gravity pull, which is the main driving force for instability, is directly proportional to the slope gradient. The nature and kind of pre-existing landslides are essential geomorphologic characteristics of slope instability because they influence the terrain's behavior (26). Landslides are more likely to occur on steeper slopes owing to gravity stress, as is widely known (30). Gravity is recognized to be the most prevalent factor that

causes movement on slopes. According to prior research, the majority of recorded debris/earth slides/flows and rockslides occurred in locations with slope angles of 15 to 45 degrees (3).

Aspect is the directional slope of the ground surface. It refers to the slope orientation, which is measured in degrees from 0 to 360 degrees. It is a significant factor in landslide studies because it regulates the slope's exposure to sunshine, wind direction, rainfall (degree of saturation), and discontinuity conditions. In the preparation of landslide susceptibility maps, aspect is also a significant component. Exposure to sunshine, drying winds, rainfall (degree of saturation), and discontinuities are all factors that might influence the incidence of landslides (31).

The curvature of topographic contours or the curvature of a line created by the intersection of an imaginary horizontal plane with the ground surface is known as plan curvature. Positive plan curvature (convex) indicates flow divergence, while negative plan curvature (concave) indicates flow concentration. Concave outward plan curvatures are known as hollows, convex outward plan curvatures are known as noses, and straight contours are known as planar regions. Water flow is concentrated in concave plan terrains, while it diverges in convex plan terrains. Converging or diverging flow and soil-water content are thus influenced by plan curvature. Slope forms control the distribution of water (surface/subsurface) within a slope, making it more susceptible to landslides. Concave plan terrains encourage concentrated water flow, whereas convex plan terrains encourage flow divergence. As a result, plan curvature controls converging/diverging flow and soil-water content (3).

The slope's proximity to the stream course is an important determinant of the area's landscape evolution as well as an indicator of landslides and other erosional issues. Since rivers erode the slope foundation and saturate the underwater portion of the slope forming material, they have a high chance of causing landslides. In landslide sensitivity studies, this parameter is considered one of the causal factors. Rivers incising the various rocks generally have a big effect in changing the terrain. The slope's closeness to the stream course is an essential component that influences the area's landscape evolution and serves as a predictor of landslides and related erosional issues. Landslides are more likely to occur in rivers with multiple drainage networks because they erode the slope base and saturate the submerged part of the slope forming material. The distance from drainage axis was considered while evaluating the influence of drainage on landslide incidence. Previous studies have shown that being adjacent to a stream has a significant impact on the occurrence of landslides, as extensive gully erosion is frequently the source of mass wasting (30) .

2.4 Statistical analysis review

In order to prepare the landslide susceptibility map quantitatively, the frequency ratio method was implemented using GIS techniques. Frequency ratio methods are based on the observed associations between the distribution of landslides and each landslide-related factor, to expose the correlation between landslide locations and the factors in the study area (11).

Landslide susceptibility analysis methods for various maps were used, according to (25),

Table 1. Different methods used for landslide susceptibility maps

no	Methods	Characteristics
1	Landslide distribution analysis	Analyze distribution and classification of landslide
2	Landslide activity analysis	Analyze temporal changes in landslide pattern
3	Landslide density analysis	Calculate landslide density in terrain units or as isopleths map
4	Geomorphologic analysis	Use in-field expert opinion in zonation
5	Qualitative map combination	Use expert-based weight values of parameter maps
6	Bivariate statistical analysis	Calculate importance of contributing factor
7	Multivariate statistical analysis	Calculate prediction formula from data matrix
8	Safety factor analysis	Apply slope stability model
9	Score method	Apply score table

Frequency ratio (FR) provides the probabilities of presence and absence of an event for individual conditioning factors by generating weights based on the ratio of areas which experienced landslides in the past to the total study area (32). The frequency ratio (FR), as a leading probability model, is based on the observed spatial relationships between landslide causal factors and landslide occurrences. Consequently, the FR can be used to quantitatively assess landslide susceptibility (33).

The FR method follows the principle of conditional probability, in which if the ratio is greater, the stronger the relationship between landslides and factor classes and vice versa. The frequency ratio was then summed to produce the final landslide susceptibility index (LSI) (34).

The ratio of percent domain of the class to percentage of total landslide in that class may be represented as the frequency ratio of each class inside a given factor. Each predictive component is repeatedly superimposed on the landslide inventory, and frequency ratio values for each class are calculated. The FR technique is based on the conditional probability concept, which states that the higher the ratio, the stronger the link between landslides and factor classes, and vice versa. The final landslide susceptibility index was calculated by adding the frequency ratios (LSI) (10).

CHAPTER THREE
MATERIAL AND RESEARCH METHODOLOGY

3.1 Introduction

This chapter describes the approaches and techniques used to collect data and investigate the research problem. It include description of the Study area, Study area weather condition, research design, study period, sample size, study variables, data collection processes, data analysis, data quality control (validity and reliability), ethical consideration and plan for dissemination.

3.2 Study area

The study was conducted in the Northern South Nations Nationalities and Peoples' Region (SNNPR) on Zabidar Mountain, approximately 127Km from Addis Ababa. Zabidar Mountain is located in central Ethiopia. It is the highest point in the Gurage zone and the entire Southern Nations, Nationalities and Peoples' Region. This mountain has an elevation of 3,719m above sea level. The proposed study area has a perimeter of 17.5km, an area of 17.9Km^2 and a 13.9km highway road through it. The study area is located in between six kebeles (Adeyo, Gugiso and Ageta) from Silt'e zone and (Mirab meskan, Aborat and Wurib) from the Gurage zone. Geographically found between latitude of $8^O 05'00"N$-$8^O 06'08"N$ and longitude of $38^O14'46"E$- $38^O17'26"E$ with an elevation of 2,221 to 3,364.9m above sea level as shown with elevation profile below.
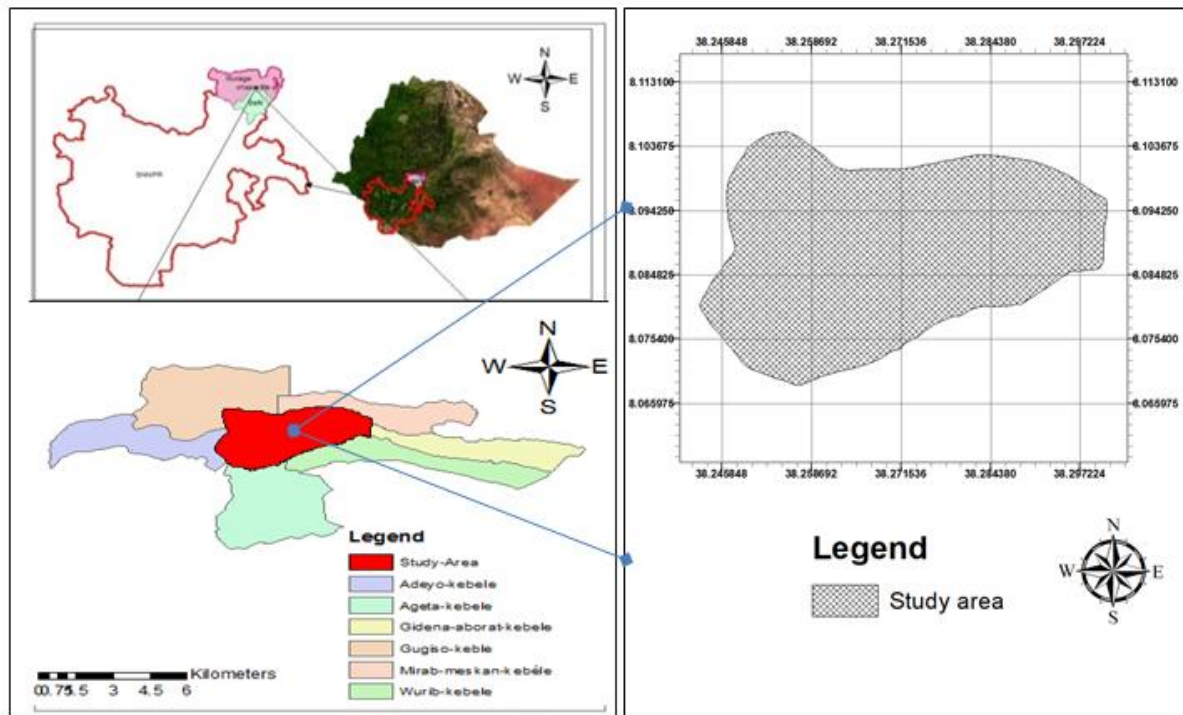
Figure 3. Geographical location of the study area
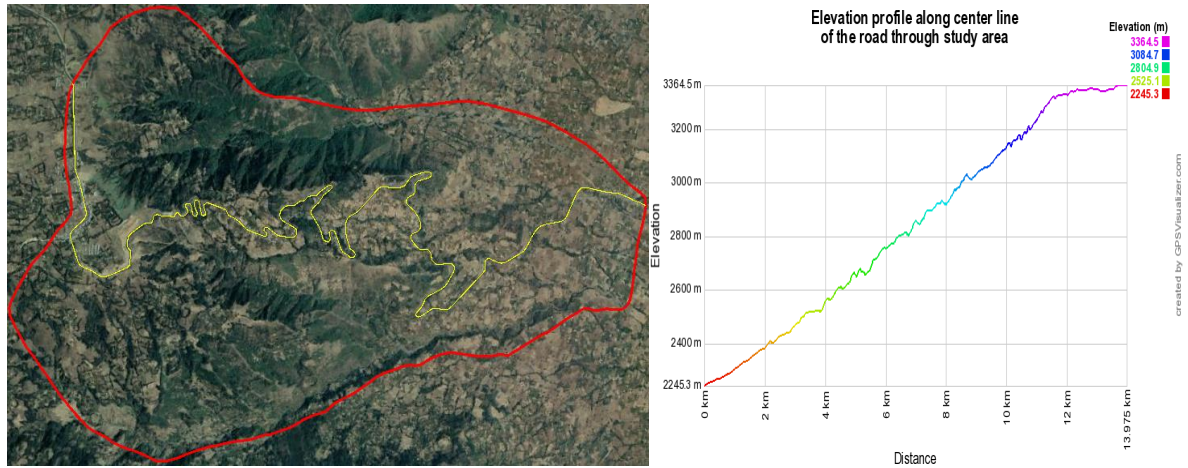
Figure 4. General elevation profile of study area (along center of road)

3.3. Study area weather condition

According to world weather conditions from https://www.worldweatheronline.com/lang/ru/agena-15day-weather-chart/et.aspx; the study area weather conditions are analyzed and estimated from Agena station. According to the data obtained from worldweatheronline, the average temperature, average rainfall and average snowfall for 15 days starting from 2009 G.C are shown below. As it is clearly seen from each of the graphs, the average low temperature and average high temperature for June, July, August and September are high and low respectively. While in the case of average rainfall and average snowfall for June, July, August and September are very high as compared to other months. In Ethiopia, these months (June, July, and August) are known as summer or kiremt season. From this information, it is highly estimated that the season when landslides will potentially occur in the area.
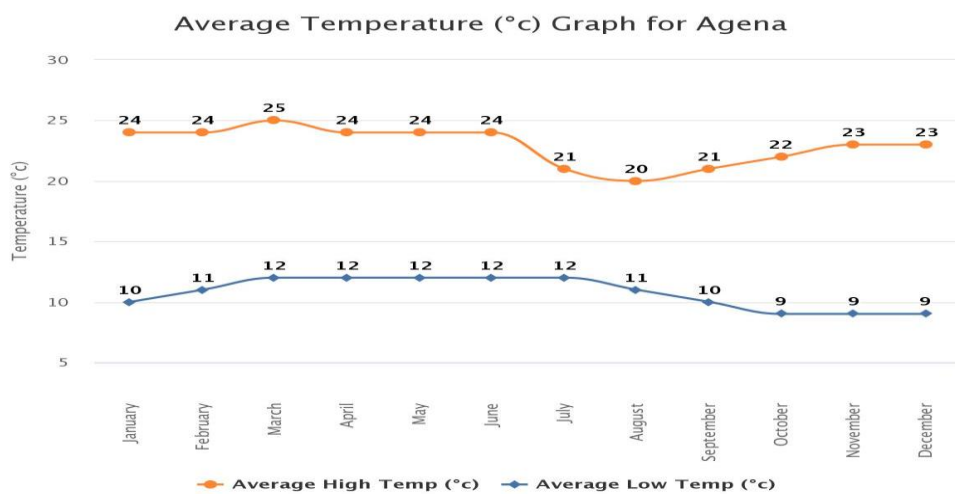
Figure 5. Average Temperature of the study area
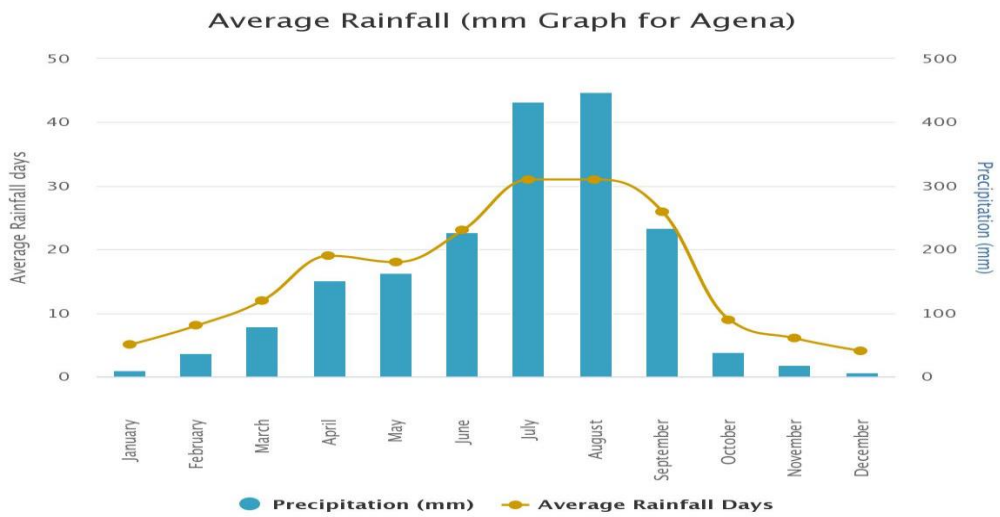
Figure 6. Average Rainfall of the study area
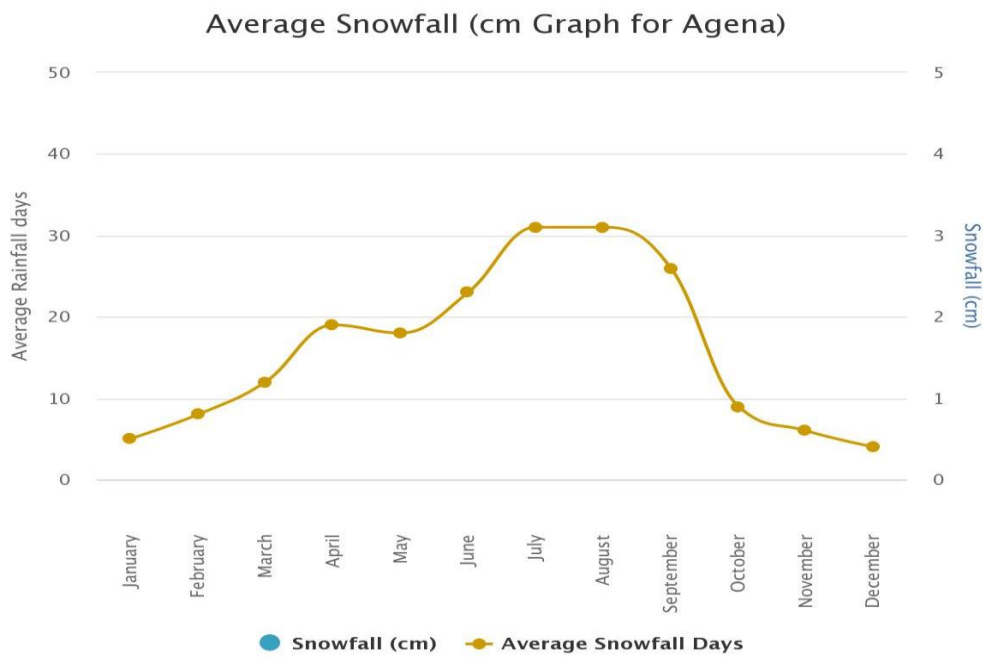
Figure 7. Average Snowfall of the study area

3.4 Study period

The research began in may, 2020 and ended in January, 2022

3.5 Research Design
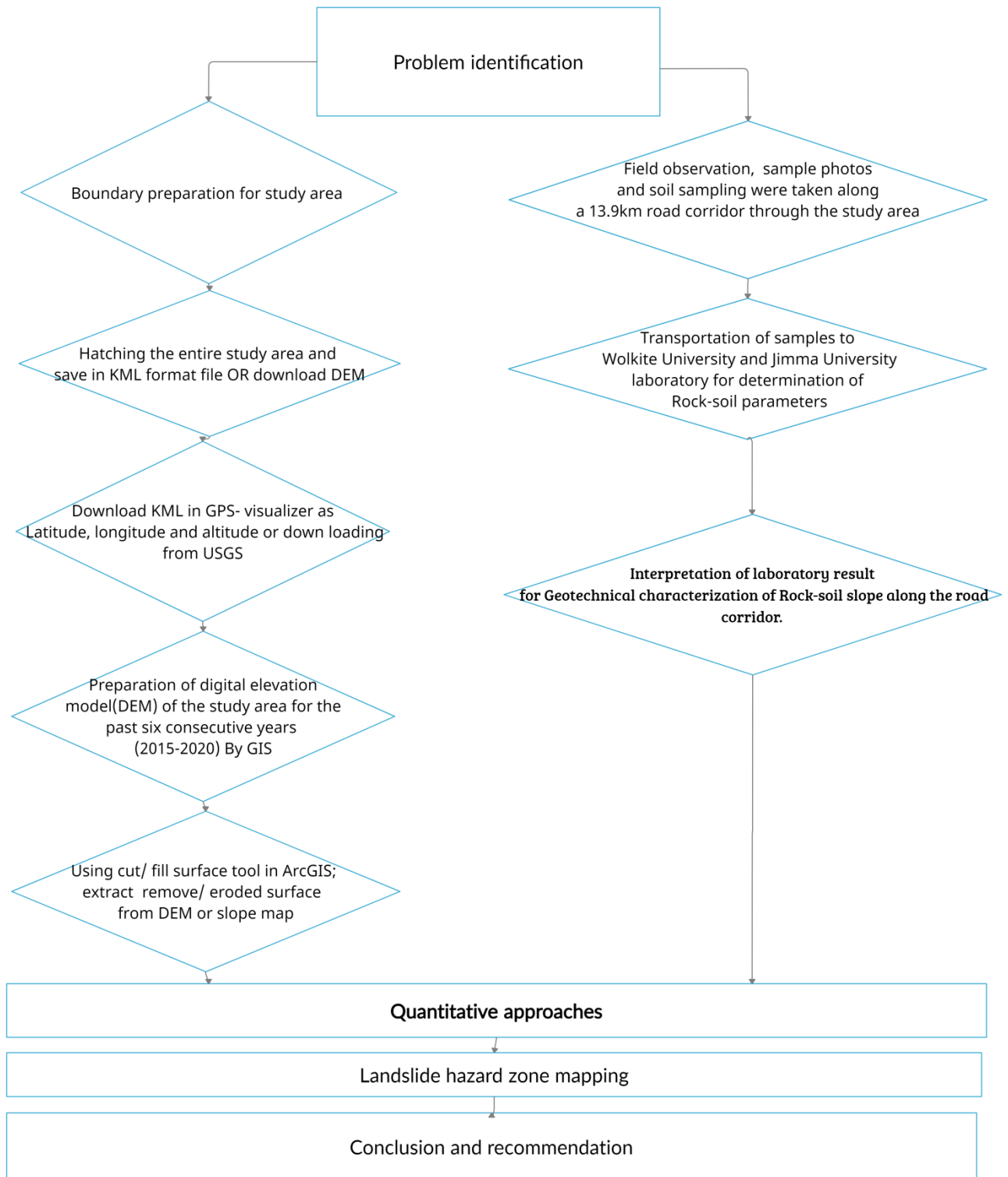
Figure 8. Flowchart for landslide susceptible Landslide zone map

3.6 Sample Size

After landslide hazard zone map development and field visit, the location of weathered rock masses and soil slope failures, insitu measurement of failure angle along the road (as shown on Figure 9) and samples for laboratory tests were taken from each point and transported to Wolkite University and Jimma University soil laboratory. Direct shear test for shear strength parameters (C,Φ) using ASTM standard (D-3080) for four points (2,3,4,5), sieve analysis using ASTM standard (D422-63) and angle of repose for each selected points were determined and interpreted. Field unconfined compressive strength of weathered rock mass was also tested at four points (2,3,4,5) and numerical analysis of rock masses and soil slope stability along the road corridor was done by the limit equilibrium method.
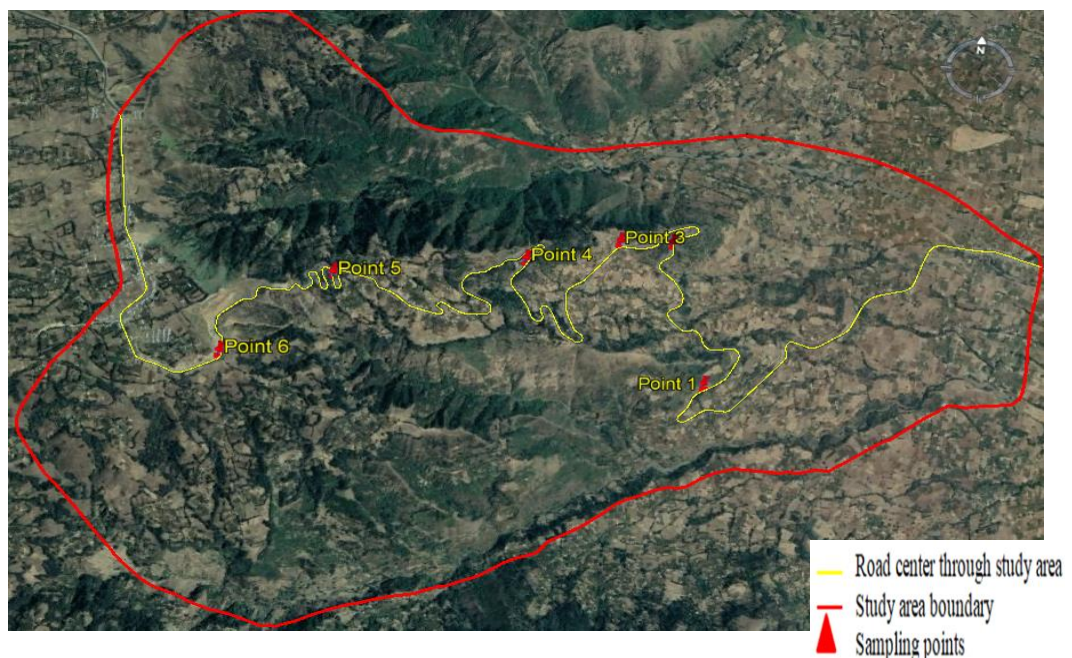
Figure 9. location map for Sampling

3.7 Study variables

In this study, there were two types of variables that were taken into consideration. They are dependent and independent variables. The dependent variables are all landslide and slope failures in the entire study area. The independent variables are all causative factors, such as lithology/soil mass, elevation, slope, aspect, curvature, and distance to stream, and triggering factors for landslide and slope failure occurrence in the study area.

3.8 Softwares Applied in the study

In general, to achieve this study, programs like Google Earth pro, Gps-visualizer and software like GIS, Rocscience(Slide), MS word, MS excel were used. Google Earth Pro is a free application that allows you to see, evaluate, overlay, and create geographical data. It may also be used to examine its ultra-high-resolution satellite images, upload and download geospatial data in its native interoperable file format (KML), and locate places. GPS Visualizer is a free online program that downloads survey data from Google Earth into the latitude, longitude, and altitude coordinate systems and generates maps from GPS data, simple coordinates, or street addresses. A Geographic Information System (GIS) combines map visual components and features with the ability to correlate these features' attributes to databases. This connection allows GIS to find, display, analyze, and model information. Rocscience (Slide) is a software used for limit equilibrium slope stability program for evaluating the safety factor or probability of failure. MS Excel is a spreadsheet programme that allows you to save a huge quantity of data or information in a structured tabular style with numerical and alphabetical values. MS Word is a word processing programme which can be used to write letters, essays, notes, and other documents.

3.9 Data collection process

In order to achieve the objective of this study, all pertinent data required for susceptibility of landslide mapping for the entire study area and for rock-soil slope stability evaluation along the road in the study area were collected from primary and secondary sources. For data collection and process; different activities were carried out. These activities were classified into three phases: pre-field work, field work and post field work. Each of the three steps comprises different activities.

3.9.1 Pre-field work

At this stage, the available information about the study area was compiled by reviewing literature or available information from different sources, both published and unpublished, to get some information to begin the study. Sufficient secondary data such as geological data, satellite images, and meteorological data were collected. By using Google earth pro and Gps-Visualizer programs or downloading from appropriate sites, survey data of the study area was prepared.

Using GIS (Geographical Information System) or downloading original 30x30m pixel size digital elevation model from ASTER (Advanced Spaceborne Thermal Emission and Reflection Radiometer), GDEM (Global digital elevation model), and USGS (United States Geological Survey); or manually by hatching on google earth pro and downloading survey data in latitude, longitude and altitude format. From these data causative factors like lithology, elevation, slope, aspect, curvature, and distance from stream/river maps of the study area were developed by processing in required

pixel size (resampling) for the previous six years. Finally, using GIS cut/fill raster surface tool, either from digital elevation models (DEM) or Slope map; lossed, gained and unchanged surface in each causative factors class for each year were developed. Since the study is targeted at landslides, only lost surface was considered and extracted for each of the last 6 years. In each causative factor class in the excel sheet that shows the number of lossed/eroded pixel numbers for each of the last 6 years (2015- 2020) were tabulated.

3.9.2 Field work

In the field, the ground verification of potential landslides, general layout of the study area, identification of mode and condition of landslides, measurement of depth, width and length of some past (older) landslides were done for validation. Some of the visible geological outcrops and the topographic condition, condition of geotechnical works, photographs of important features of the area, visual identification of rock and soil profiles along the road corridor throughout the study area, geometry of slope failure along road corridor, rebound test for compressive strength of rocks, location of samples to be taken and sampling were made for determination of the geotechnical properties.
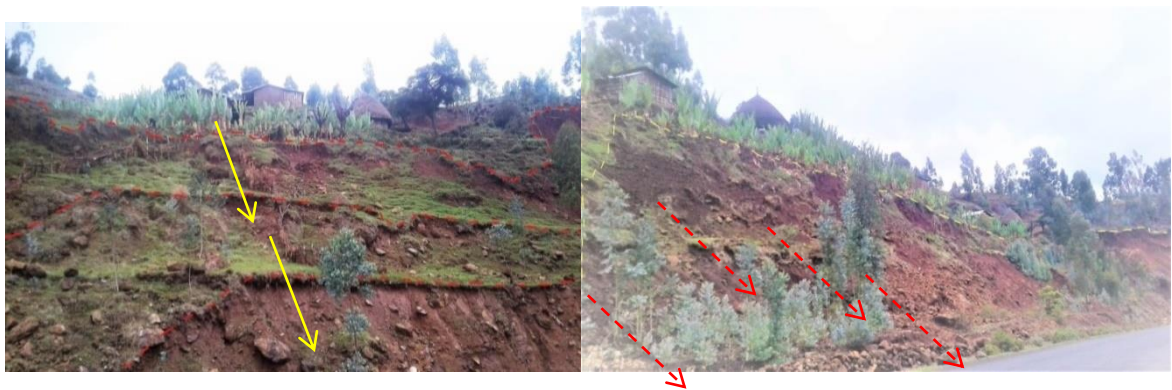
Figure 10. Sample photo that shows failure slope by human activity

Figure 11. Sample photo that shows failure Rock-soil slope along road corridor

Figure 12. Sample photo that shows flooding risk local residents

3.9.3 Post field work

The densities of landslide occurrences within each causative factor map class were obtained in the stage of pre-field and field work. Areas which are susceptible to landslides were identified by a bivariate statistical approach (Calculate importance of contributing factor) through frequency ratio (FR).

In the laboratory, limited geotechnical properties were determined, specifically particle size analysis, angle of repose and Direct shear test for shear strength parameters (C,Φ). The samples for sieve analysis and angle of repose were tested in Wolkite University's soil mechanics laboratory and Direct shear test were conducted in Jimma University's soil mechanics laboratory.

3.10 Geology

Geology is the study of the occurrence and change of rock on the Earth's surface over time. Since various rock types have differing resistance to weathering and soil erosion, geology has a big impact on the occurrence of landslides. The geological map of the study area has been updated from the Ethiopian Geological Survey's 1973 Geological Map (GSE,2011).As shown in the map below, the geological composition of the study area is alkaline, Trachyte, tractry basalt, and per alkaline rhyolite with subordinate alkaline basalt.
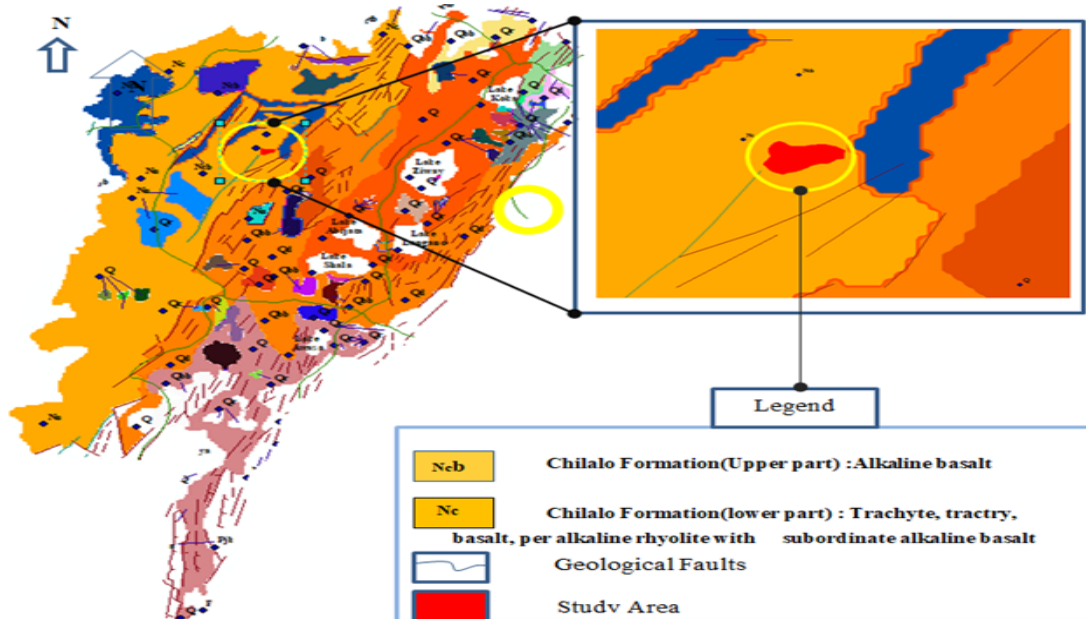
Figure 13.Geological map of the study area

3.11 Ethical consideration

After Jimma University wrote an official letter and sent it to the appropriate local authorities and other organizations, demanding that data and samples be taken and relevant tests be conducted, the necessary data was gathered. Prior to data collection and analysis, the study's objective was made clear to the organization and the concerned local communities.

3.12 Data quality control (validity and reliability)

The data's accuracy was ensured by a cross-check with real field measurement (validity) data, as well as close attention paid to data collection and documentation.

3.13 Plan for dissemination

The thesis mainly focuses on Jimma University's academic purposes. For this analysis, random surface elevation points of the study area were prepared by downloading DEM (digital elevation maps) from known sites and processed as required pixel sizes. This approach tends to simplify data collection methods by avoiding errors in manually recording the number of landslides, avoiding errors in measuring the area and amount of landslides, and reducing the number of labour forces and resources needed. Finally, a landslide hazard zone map was prepared for the entire study area. The findings were presented to Jimma Institute of Technology's Civil Engineering Department and Geotechnical Engineering Stream, as well as Jimma University's Technology Library and other relevant governmental and non-governmental organizations.

CHAPTER FOUR
RESULT AND DISCUSSION

4.1 Landslide causative factors

Using the frequency ratio (FR) model, this study investigated the relationship between six causative factors and the occurrence of landslides. In order to know landslide hazard-prone areas and prepare a landslide susceptibility map, it's important to assess the impact of causative factors on the spatial distribution of landslides.

4.1.1 Lithology/ Soil mass Map

The current research area's lithological map was collected from the Ethiopian Geological Survey 1973 report (GSE,2011). The study area has three types of soil mass. According to the data from the map, Pelitic vertisols, Stone crust, and Chromic luvisols are the three types of lithology/soil masses that cover the study area. In this study, Pelitic vertisols occupy 87.7 percent of the study area, Stone surface accounts for 12.2 percent, and Chromic luvisols account for 0.1 percent.
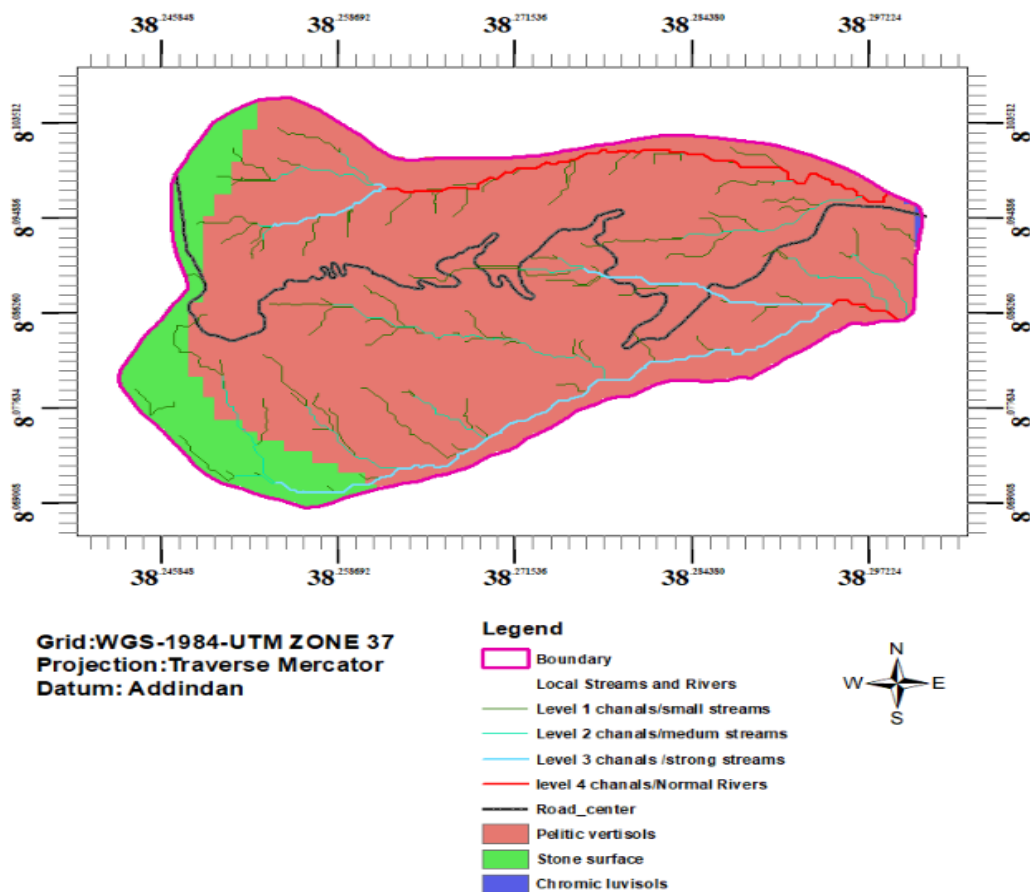
Figure 14. Lithological map /soil mass of the study area.

4.1.2 Elevation map

A digital elevation model (DEM) was created for this study over the last six years (2015-2020). The elevation maps for all years were classified into five subclasses: 2221-2450 meters, 2450–2670 meters, 2670-2900 meters, 2900-3100 meters, and 3100-3370 meters above sea level.

Elevation map for the past six years
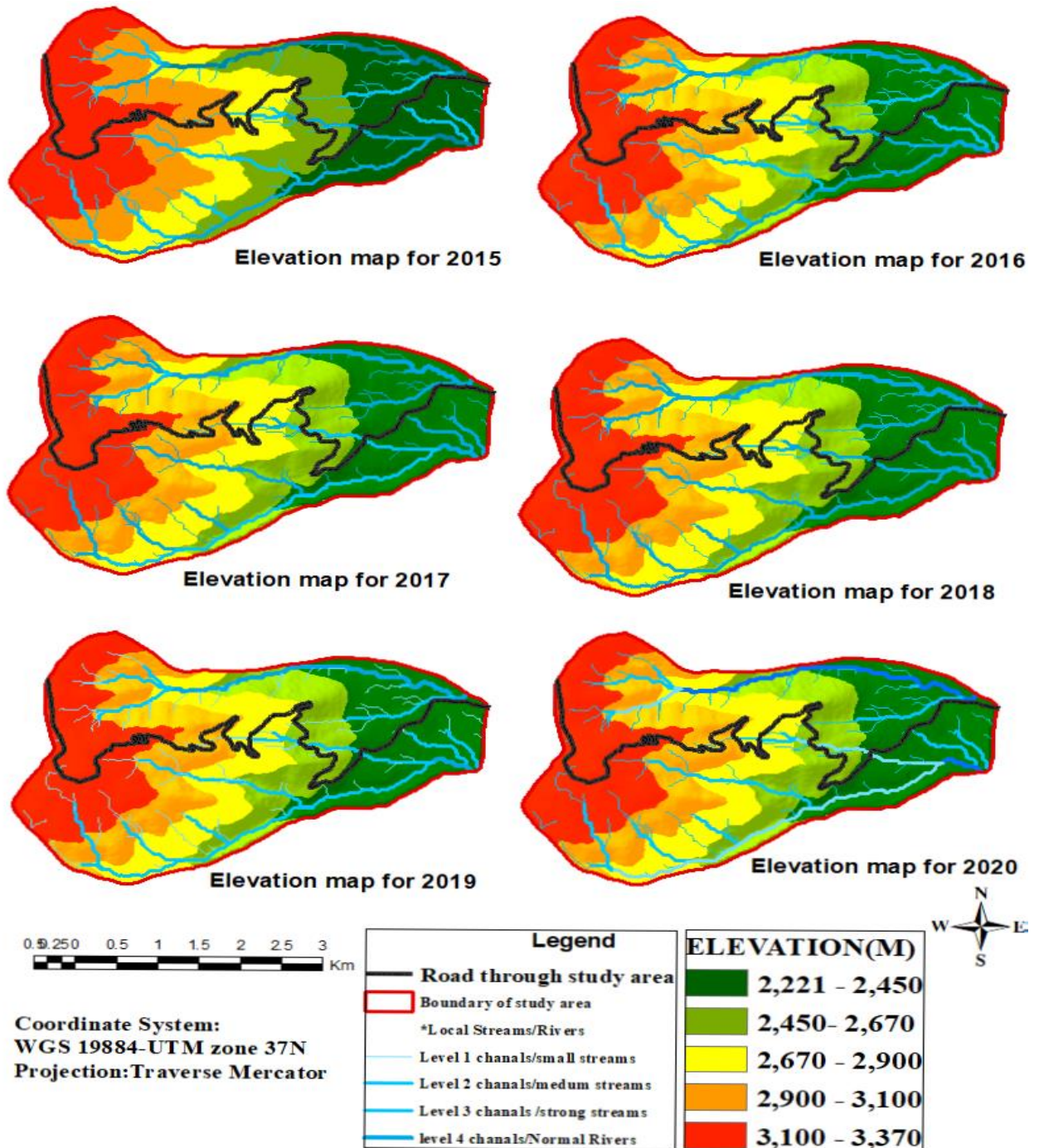
Figure 15. Elevation map of the study area.

4.1.3 Slope Map

The slope for the present study area for each of the past six years was extracted from the digital elevation model (DEM). A slope category (subclass) map was created for four categories for the current study: (i) 0–5%, (ii) 5–25%, (iii) 25–50%, and (iv) 50–100%, as shown in the figure below.

Slope map for the past six years
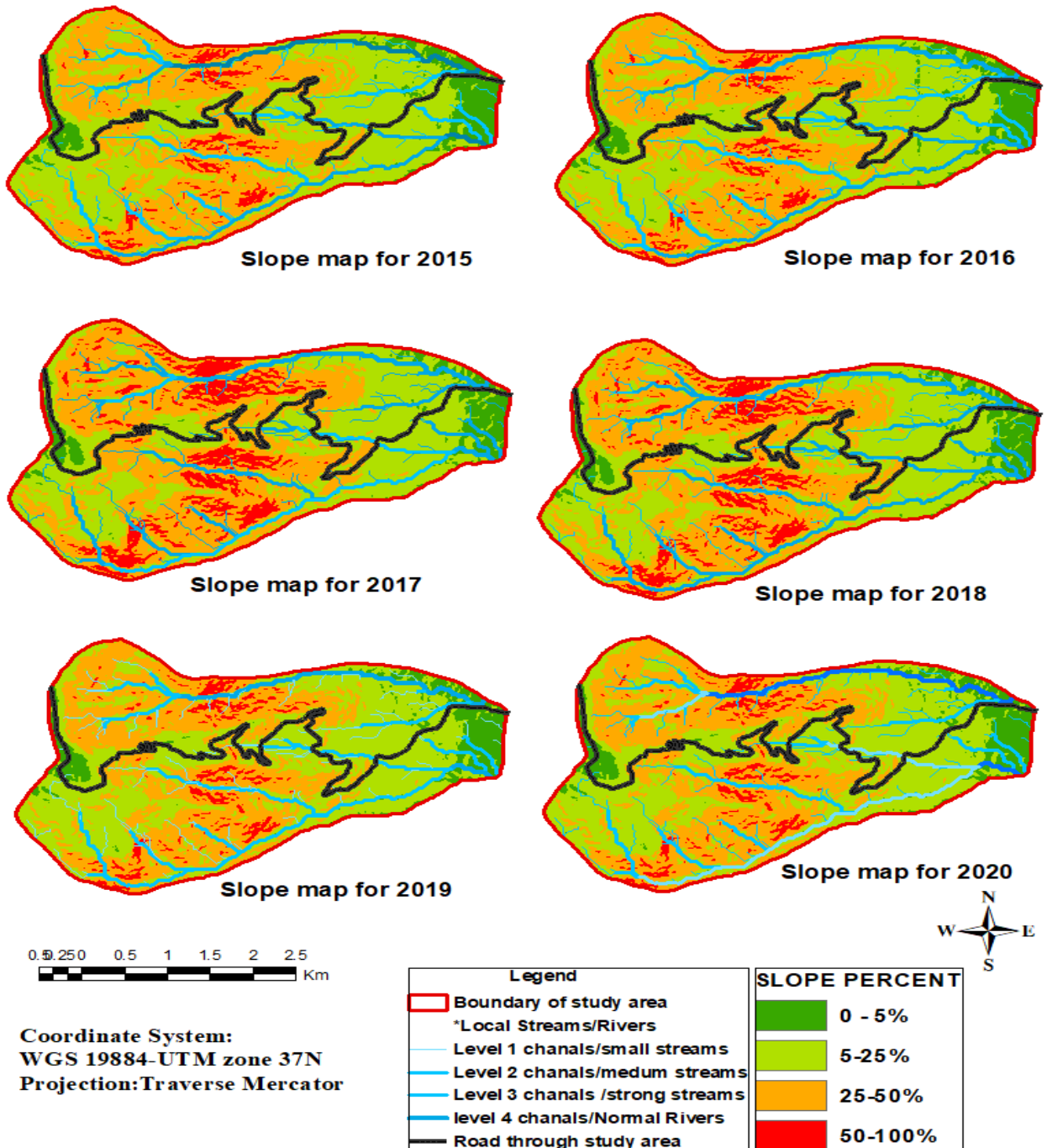
Figure 16. Slope map of the study area.

4.1.4 Aspect Map

For this study, the slope aspect was derived from the DEM data and it was divided into nine categories: flat (1), northeast (22.5–67.5), east (67.5–112.5), southeast (112.5–157.5), south (157.5–202.5), southwest (202.5–247.5), west (247.5–292.5) and northwest (292.5–337.5) (Fig. 14).

Aspect map for the past six years
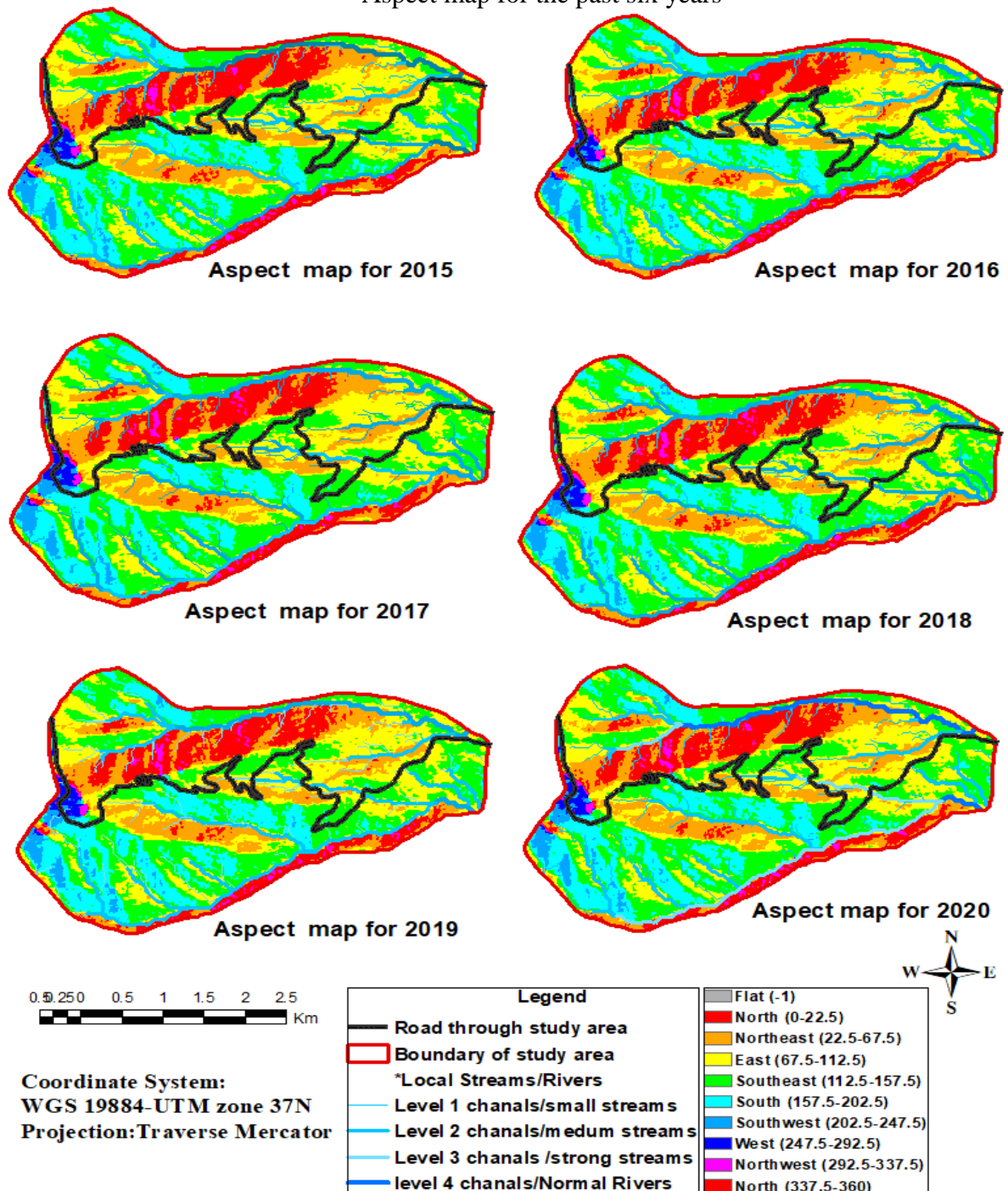
Figure 17. Aspect map of the study area.

25

4.1.5 Plan Curvature Map

The plan curvature for the present study area for each of the past six years was developed from the digital elevation model (DEM). A Plan curvature subclass map was prepared for three categories: (a) Concave, (b) Flat and (c) Convex as shown below

Curvature map for the past six years
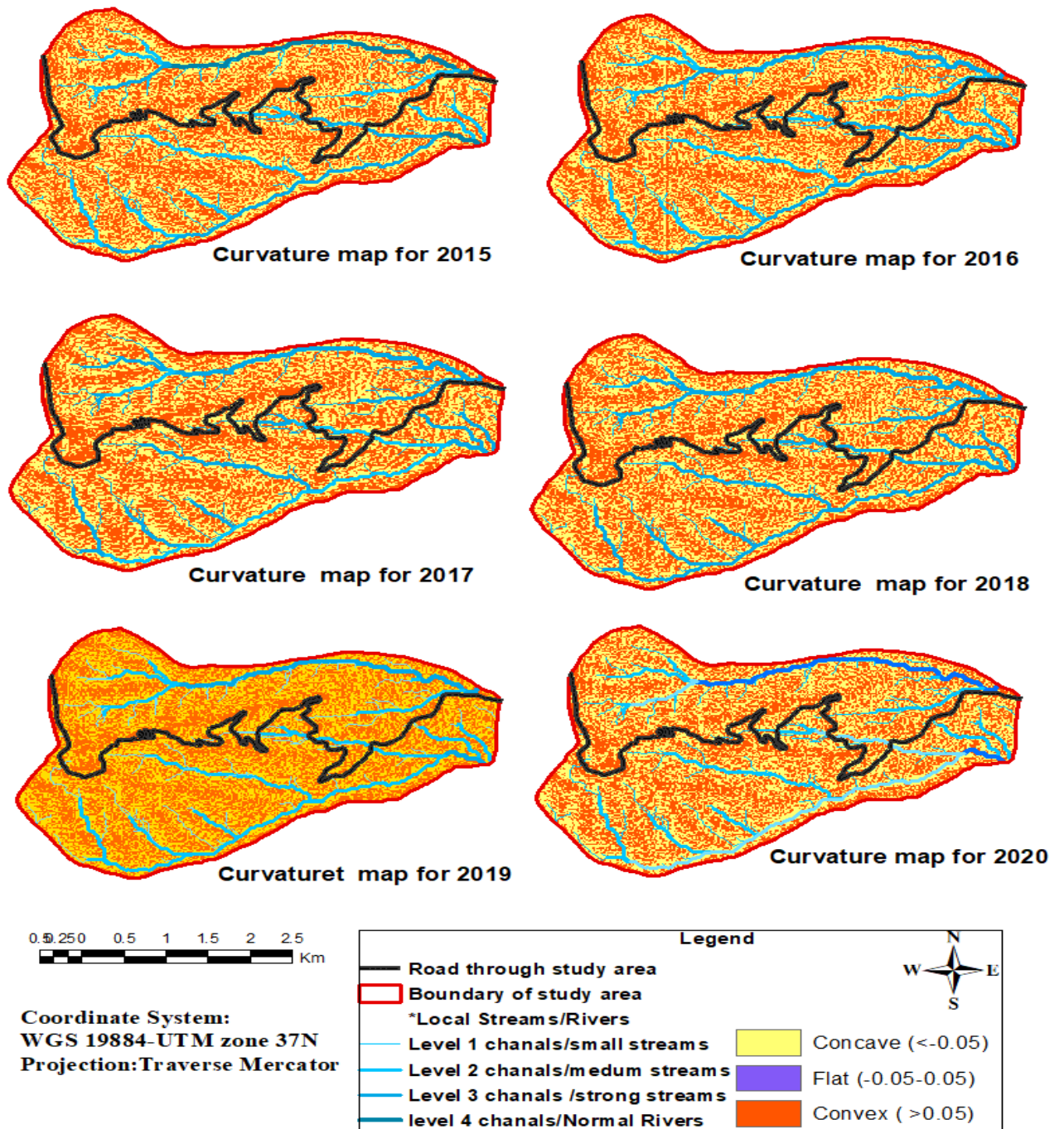
Figure 18. Curvature map of the study area.

4.1.6 Distance from Stream/River map

As a result, five subclasses were defined for this analysis based on their respective distances. 0-5 metres, 5-10 metres, 10-15 metres, 15-20 metres, 20-25 metres, and 25-35 metres from the stream's centre.
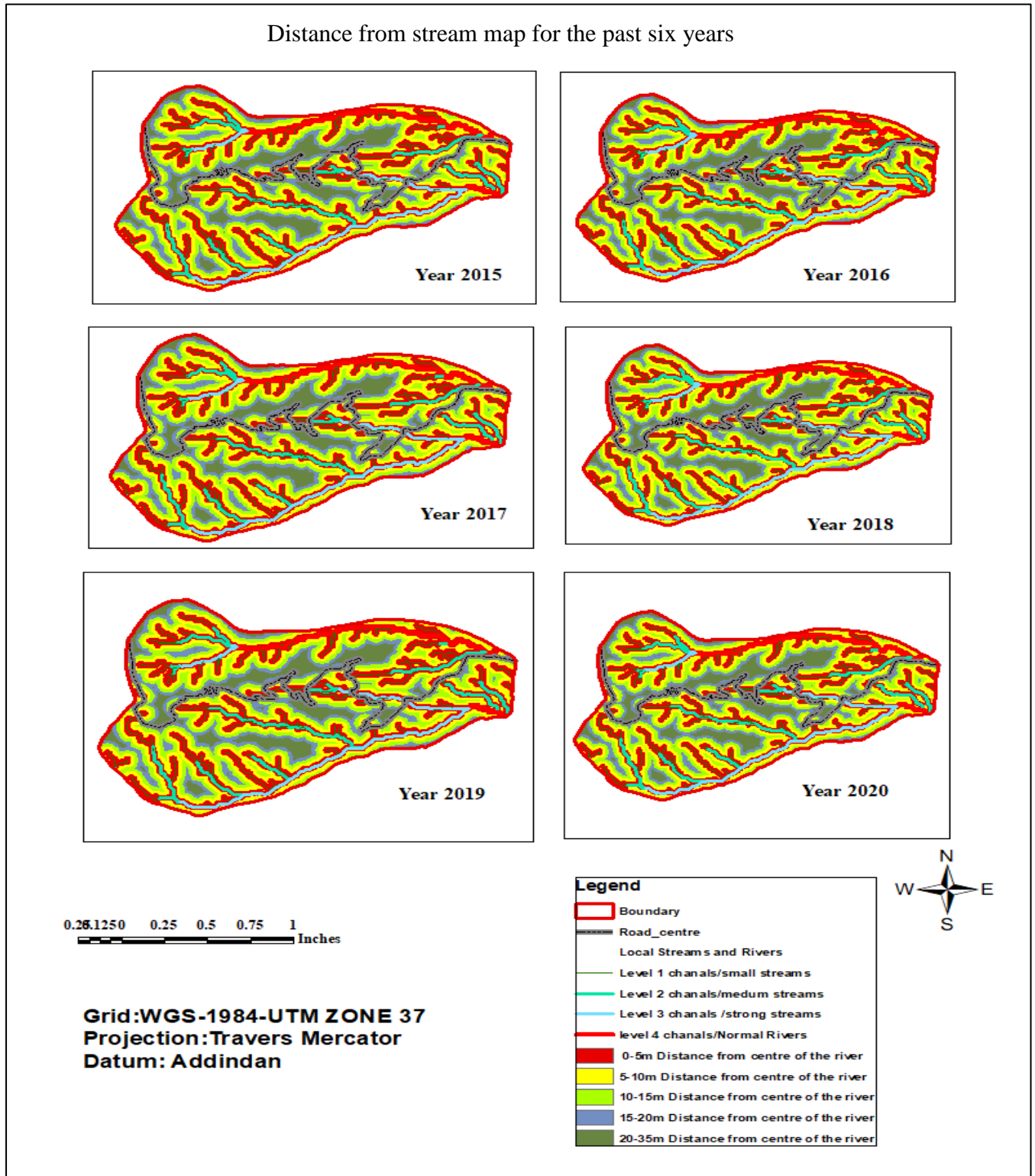
Figure 19. Distance from streams/river map of the study area

4.2 Data analysis

4.2.1 Extraction of eroded/ removed surface

The cut/fill spatial analyst tool in GIS-10.3.1 allows us to generate a map centered on two input surfaces (before and after), showing the areas and amounts of surface material that have been changed by the addition or removal of surface material. For this study, the two consecutive years' DEM (Digital elevation model) or Slope map was used as an input. After running cut/fill processing, the output results are lost, unchanged, and gained. Since the aim of this research is to evaluate landslides, only the loss surface pixel number in each causative factor is calculated and counted.
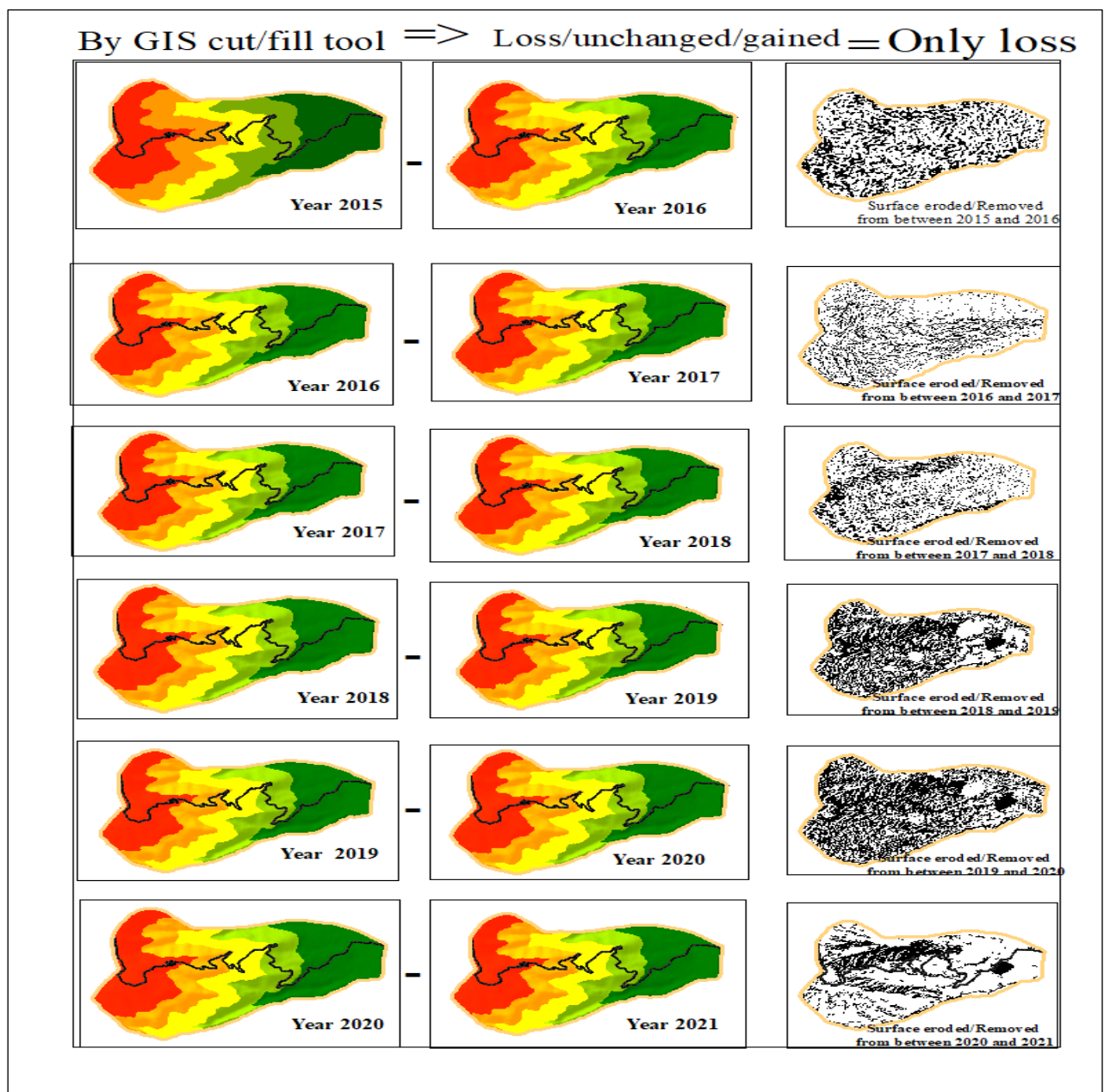
Figure 20. Map that show elevation difference in for past six consecutive years of the study area

Table 2. lossed surface pixel number for each of the past six years in each causative factor subclasses

Using Elevation map						
Year	Causative factor Elevation subclasses	Number of removed pixels		Year	Causative factor Elevation subclasses	Number of removed pixels
2015	2221-2450	5583		2018	2221-2450	6012
	2450-2670	4474			2450-2670	6222
	2670-2900	4334			2670-2900	7226
	2900-3100	5028			2900-3100	7847
	3100-3370	6356			3100-3370	10342
	Total	25775			Total	37649
2016	2221-2450	2823		2019	2221-2450	7404
	2450-2670	2086			2450-2670	6540
	2670-2900	2677			2670-2900	7530
	2900-3100	3807			2900-3100	8237
	3100-3370	4090			3100-3370	10582
	Total	15483			Total	40293
2017	2221-2450	3357		2020	2221-2450	2437
	2450-2670	3265			2450-2670	3172
	2670-2900	3847			2670-2900	4067
	2900-3100	4722			2900-3100	4646
	3100-3370	5972			3100-3370	5554
	Total	21163			Total	19876

After determining the number of eroded pixel numbers (15.4x15.4m size), they were projected or overlayed techniques were applied with each causative factor subclass (lithology/soil mass, elevation, slope, aspect, plan curvature, and distance from stream) in each of the previous six years (2015-2020) using the zonal statistics tool in GIS.

4.2.1.1 On lithology/soil mass map

Since each class of materials has different shear strength and permeability characteristics, lithology is one of the most important limiting parameters in slope stability. Different rock types have different

compositions and structures, which can either help or hurt the slope material's resistance. In comparison to the softer/weaker rock units, the stronger rock units have greater resistance to the pushing forces. As a result, the number of lost surface pixels in each elevation or slope map subclasses were determined using GIS software and tabulated in excel sheet for the previous six consecutive years.

Overlay on Lithology map for the past six years
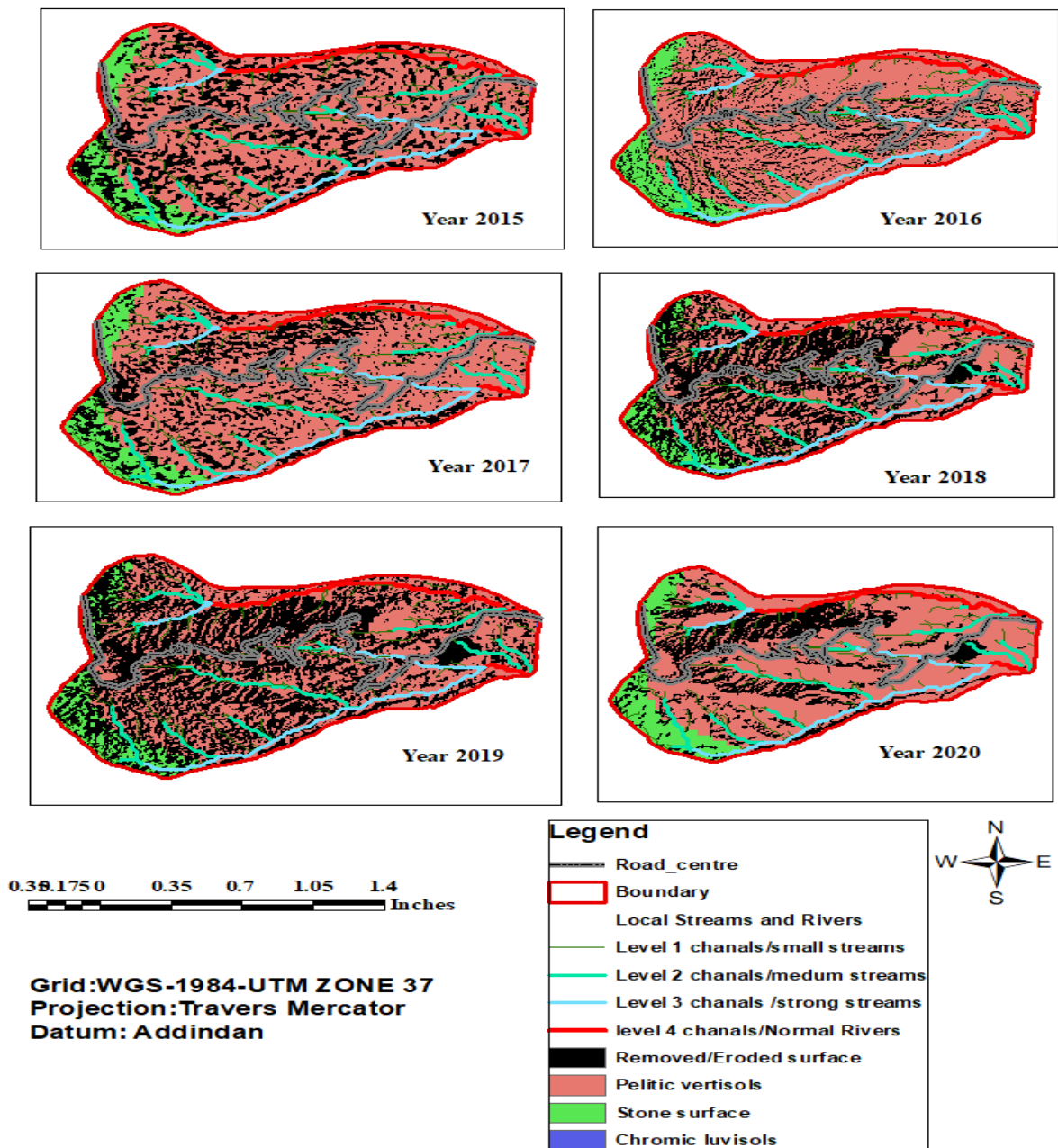
Figure 21. Mapping the lost/eroded surfaces on lithological map for the past six years

Table 3. Eroded/removed surface (in percent) on each lithology/soil mass subclasses

Year	Causative factor subclasses	Sub class pixels number	Eroded surface pixel number	Eroded/ removed surface in percent
2015	a. Pelitic vertisols	66605	22467	87
	b. Stone surface	8378	3308	13
	c. Chromic luvisols	70	3	0
	Total	75053	25778	
2016	a. Pelitic vertisols	66605	13662	88
	b. Stone surface	8378	1802	12
	c. Chromic luvisols	70	16	0
	Total	75053	15480	
2017	a. Pelitic vertisols	66605	18322	87
	b. Stone surface	8378	2837	13
	c. Chromic luvisols	70	2	0
	Total	75053	21161	
2018	a. Pelitic vertisols	66605	32768	87
	b. Stone surface	8378	4855	13
	c. Chromic luvisols	70	21	0
	Total	75053	37644	
2019	a. Pelitic vertisols	66605	35281	88
	b. Stone surface	8378	4982	12
	c. Chromic luvisols	70	30	0
	Total	75053	40293	
2020	a. Pelitic vertisols	66605	18109	91
	b. Stone surface	8378	1756	9
	c. Chromic luvisols	70	9	0
	Total	75053	19874	
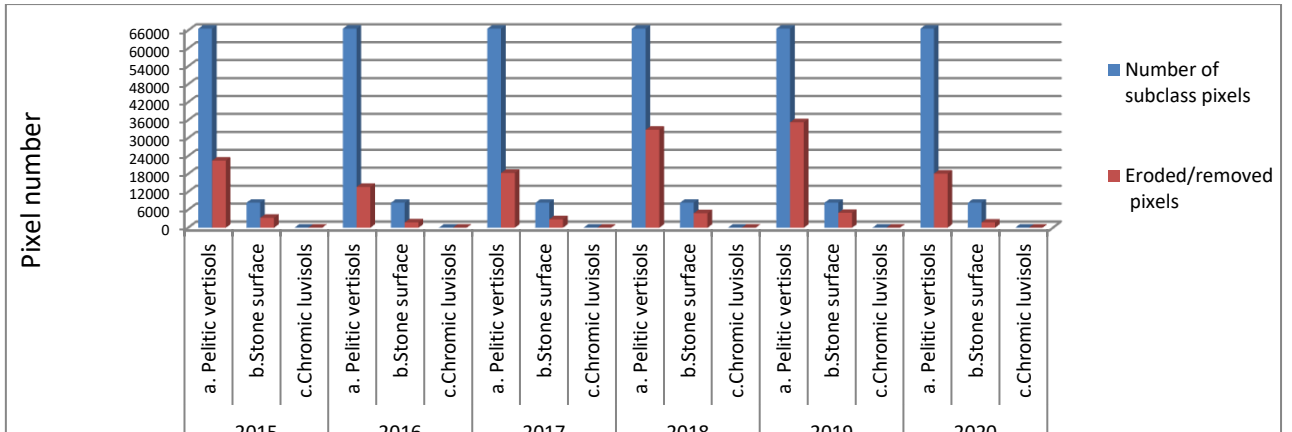
Figure 22. Bar chart of eroded/removed pixel numbers in each classes in each six years.

4.2.1.2 On elevation map

Changes in elevation affect the geomorphology, vegetation, and rate of erosion in a given region, altering landslide susceptibility. As a result, the number of missing surface pixels in each elevation map subclass was determined and tabulated using GIS software for the previous consecutive six years.

Overlay on Elevation map for the past six years
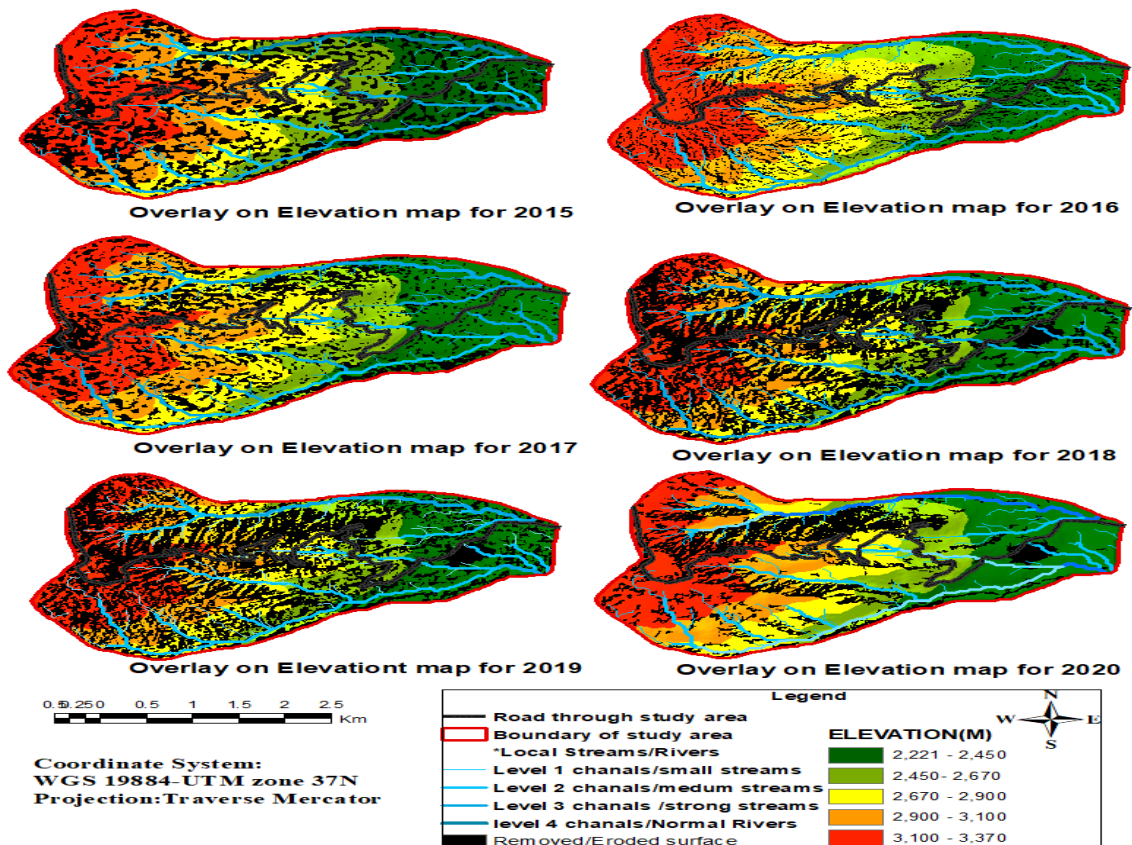
Figure 23. Mapping the lost/eroded surfaces on elevation map for the past six years.

Table 4. lossed surface pixel number on elevation map for the past six years.

Year	Causative factor subclasses	Sub class pixels number	Removed pixel number	Removed surface percent	Year	Causative factor subclasses	Sub class pixels number	Removed pixel number	Removed surface percent
2015	2221-2450	18087	5583	22	2018	2221-2450	18087	6012	16
	2450-2670	12521	4474	17		2450-2670	12521	6222	17
	2670-2900	12884	4334	17		2670-2900	12884	7226	19
	2900-3100	14482	5028	20		2900-3100	14482	7847	21
	3100-3370	17078	6356	25		3100-3370	17079	10342	27
	Total	75052	25775			Total	75053	37649	
2016	2221-2450	18087	2823	18	2019	2221-2450	18087	7404	18
	2450-2670	12521	2086	13		2450-2670	12521	6540	16
	2670-2900	12884	2677	17		2670-2900	12884	7530	19
	2900-3100	14482	3807	25		2900-3100	14482	8237	20
	3100-3370	17078	4090	26		3100-3370	17078	10582	26
	Total	75052	15483			Total	75052	40293	
2017	2221-2450	18087	3357	16	2020	2221-2450	18087	2437	12
	2450-2670	12521	3265	15		2450-2670	12521	3172	16
	2670-2900	12884	3847	18		2670-2900	12884	4067	20
	2900-3100	14482	4722	22		2900-3100	14482	4646	23
	3100-3370	17078	5972	28		3100-3370	17078	5554	28
	Total	75052	21163			Total	75052	19876	

4.2.1.3 On slope map

According to the reviewed literature, slope is a critical parameter for landslide study because it has a clear relationship with the frequency of landslides. As a consequence, it's commonly used in landslide susceptibility mapping. As a result, in each slope map subclasses, the amount of removed/eroded surface pixels was calculated and tabulated using GIS tools for each of the previous six years.

Overlay on Slope map for the past six years
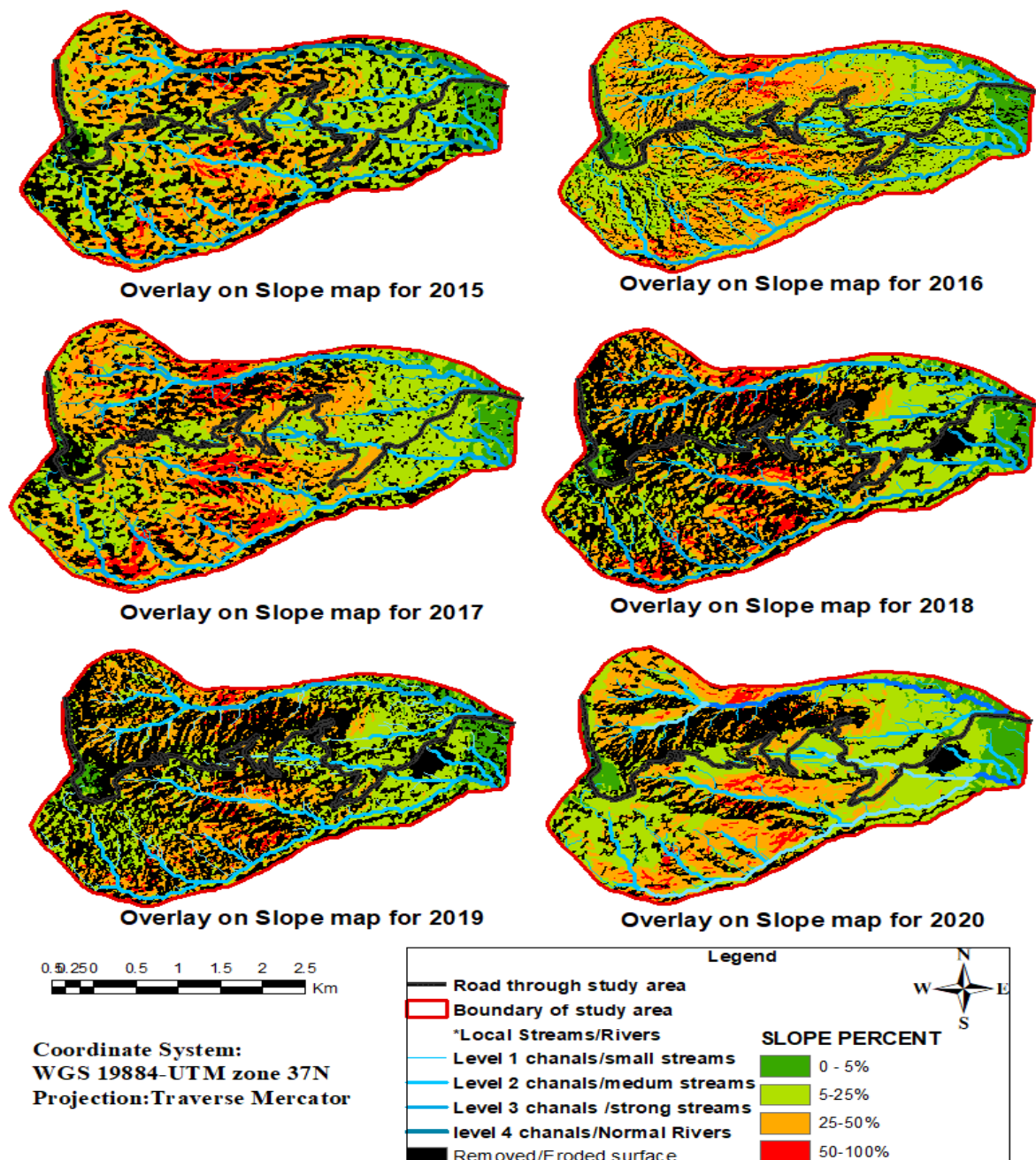
Figure 24 Mapping the lost/eroded surfaces on slope map for the past six years.

Table 5. lossed surface pixel number on slope map for the past six years.

Year	Causative factor subclasses	Sub class pixels number	Removed surface pixel number	Eroded surface percent		Year	Causative factor subclasses	Sub class pixels number	Removed surface pixel number	Eroded/removed surface percent
2015	0-5%	6478	2066	8		2018	0-5%	5361	1916	5
	5-25%	38546	13354	52			5-25%	34124	15954	42
	25-50%	27050	9242	36			25-50%	29313	16410	44
	50-100%	2976	1114	4			50-100%	6254	3367	9
	Total	75050	25776				Total	75052	37647	
2016	0-5%	6620	949	6		2019	0-5%	6507	2831	7
	5-25%	38761	8097	52			5-25%	38667	20124	50
	25-50%	26972	5884	38			25-50%	26705	15509	38
	50-100%	2702	553	4			50-100%	3174	1828	5
	Total	75055	15483				Total	75053	40292	
2017	0-5%	5052	1189	6		2020	0-5%	6507	715	4
	5-25%	32715	8475	40			5-25%	38667	9076	46
	25-50%	30153	9006	43			25-50%	26705	8943	45
	50-100%	7133	2494	12			50-100%	3172	1142	6
	Total	75053	21164				Total	75051	19876	
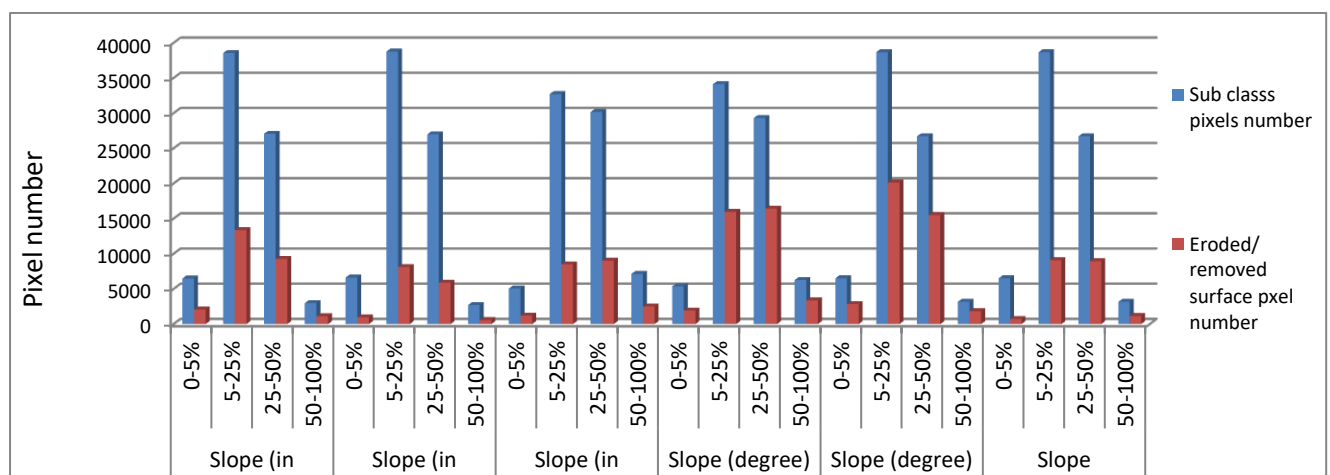
Figure 25. Bar chart of lost/eroded pixel in each subclasses on slope map for the past six years.

4.2.1.4 On Aspect map

In landslide studies, this aspect is significant since it influences the slope's exposure to sunshine, wind speed, rainfall (degree of saturation), and discontinuity conditions. As a result, all eroded/removed surface pixel numbers in the elevation or slope map were counted in each aspect subclass and tabulated.

Overlay on Aspect map for the past six years
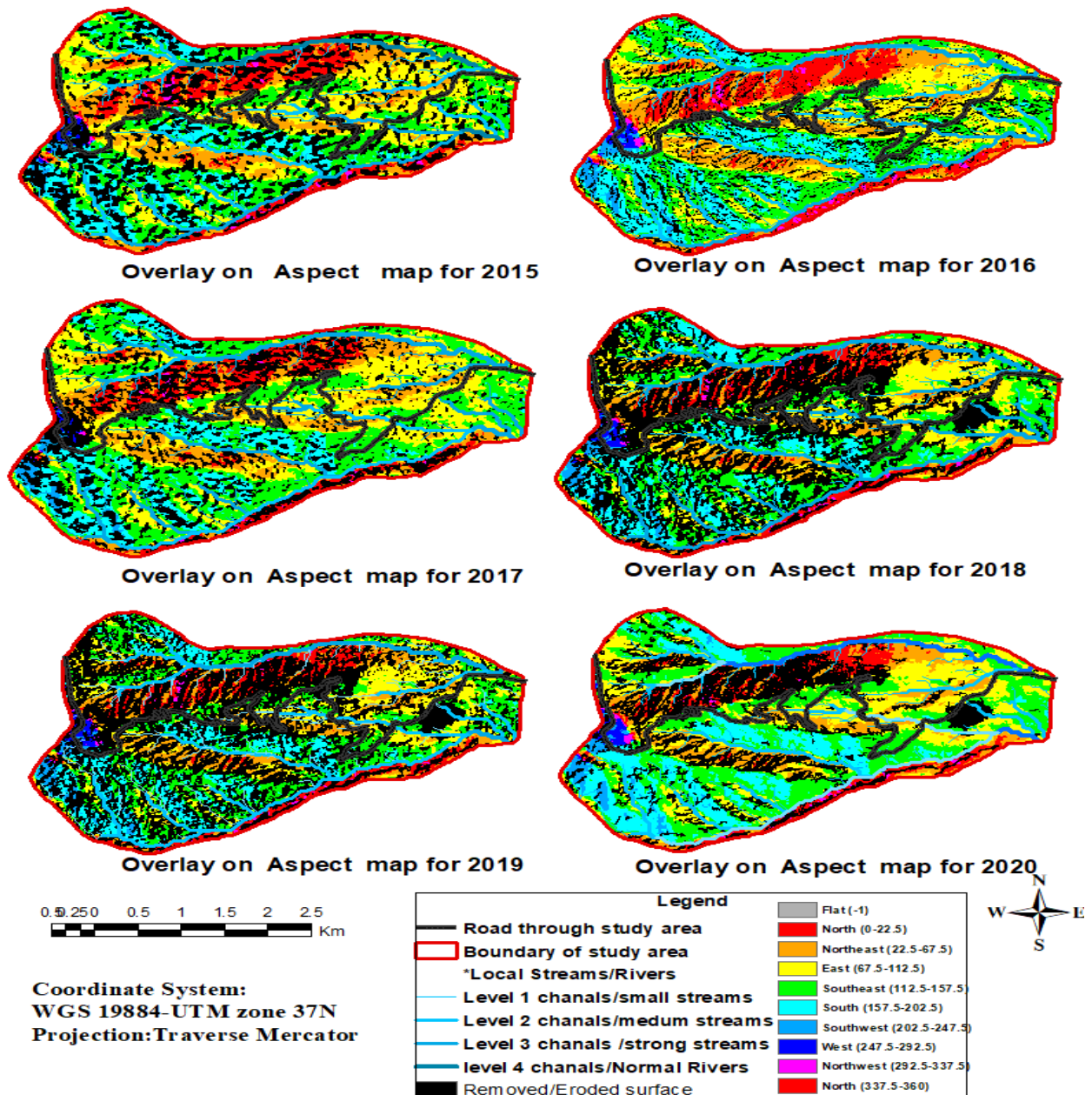
Figure 26. Mapping the lost/eroded surfaces on aspect map for the past six years.

Table 6. lossed surface pixel number on aspect map for the past six years.

year	causative factor subclasses	sub class pixels number	Removed surface pixel number	Removed surface percent	year	causative factor subclasses	sub class pixels number	Removed surface pixel number	Removed surface percent
2015	FLAT	5604	2323	9	2018	FLAT	5547	3424	9
	N	12314	3294	13		N	12254	6806	18
	NE	18085	4193	16		NE	18298	8818	23
	E	22287	7396	29		E	22200	10079	27
	SE	10714	5125	20		SE	10691	5036	13
	S	1581	1142	4		S	1630	818	2
	SW	740	474	2		SW	719	358	1
	W	793	385	1		W	743	459	1
	NW	2935	1444	6		NW	2972	1850	5
2016	FLAT	5649	762	5	2019	FLAT	5399	3274	8
	N	12319	2651	17		N	12336	7146	18
	NE	18085	3515	23		NE	18158	9513	24
	E	22210	4774	31		E	22183	11170	28
	SE	10852	2718	18		SE	10741	5416	13
	S	1560	411	3		S	1622	873	2
	SW	702	156	1		SW	758	380	1
	W	750	108	1		W	795	499	1
	NW	2926	389	3		NW	3062	2021	5
2017	FLAT	5593	2927	14	2020	FLAT	5664	3377	17
	N	12302	3899	18		N	12321	5211	26
	NE	18290	2711	13		NE	18075	4164	21
	E	22252	3901	18		E	22349	3310	17
	SE	10662	3870	18		SE	10676	996	5
	S	1570	897	4		S	1614	321	2
	SW	742	615	3		SW	698	184	1
	W	701	491	2		W	778	429	2
	NW	2939	1854	9		NW	2877	1881	9
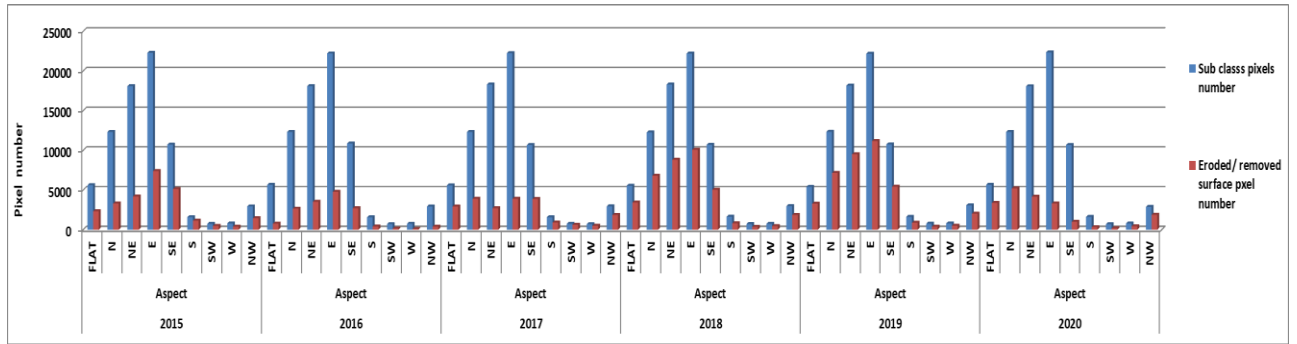
Figure 27. Bar chart of lost/eroded pixels in each subclasses on aspect map for the past six years.

4.2.1.5 On plan curvature map

Hollows are concave outward plan curvatures, noses are convex outward plan curvatures, and straight contours are known as planar areas. To know the frequency of landslide occurrence, all eroded/removed surface pixel numbers counted in each plan curvature subclass and tabulated.

Overlay on Curvature map for the past six years
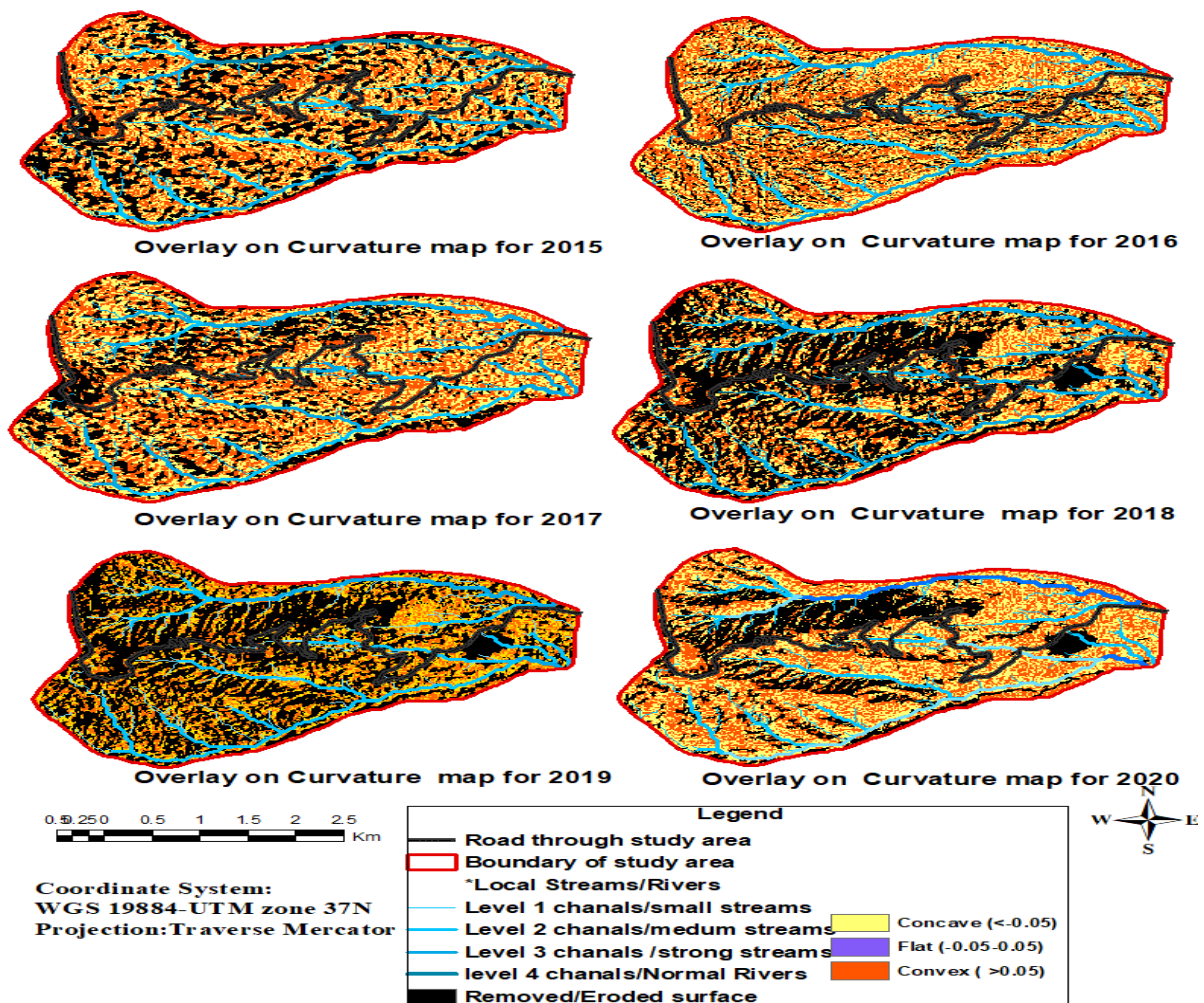
Figure 28. Mapping the lost/eroded surfaces on curvature map for the past six years.

Table 7. lossed surface pixel number on Curvature map for the past six years.

year	Causative factor subclasses	class pixels	landslide pixels	percentage of landslide pixels	year	Causative factor subclasses	class pixels	Landslide pixels	percentage of landslide pixels
2015	a. Concave	37599	13116	51	2018	a. Concave	37488	17910	48
	b. Flat	64	3	0		b. Flat	5	2	0
	c. Convex	37393	12657	49		c. Convex	37559	19736	52
	Total	75056	25776			Total	75052	37648	
2016	a. Concave	37802	7636	49	2019	a. Concave	37455	19296	48
	b. Flat	6	2	0		b. Flat	13	3	0
	c. Convex	37246	7846	51		c. Convex	37584	20993	52
	Total	75054	15484			Total	75052	40292	
2017	a. Concave	37570	10231	48	2020	a. Concave	37631	9214	46
	b. Flat	17	4	0		b. Flat	11	8	0
	c. Convex	37466	10933	52		c. Convex	37411	10654	54
	Total	75053	21168			Total	75053	19876	
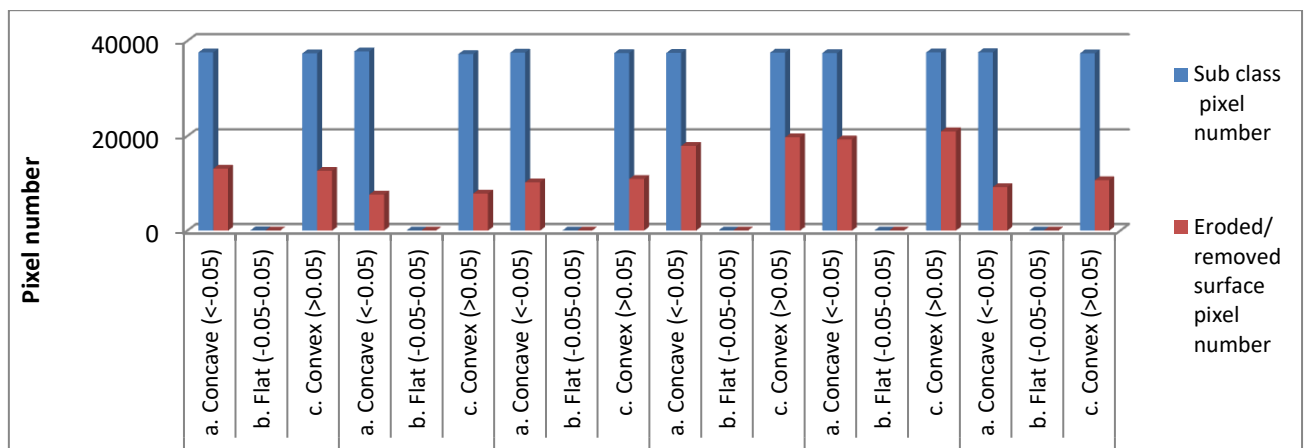
Figure 29. Bar chart of lost/eroded pixel in each subclasses on curvature map for six years

4.2.1.6 Distance from Stream/River map

Rivers with many drainage networks are more likely to cause landslides when they erode the slope foundation and saturate the submerged portion of the slope-forming soil. In this study, the number of lost parts or surfaces were counted and tabulated for each distance subclass for each year.

Overlay on distance from stream map of study
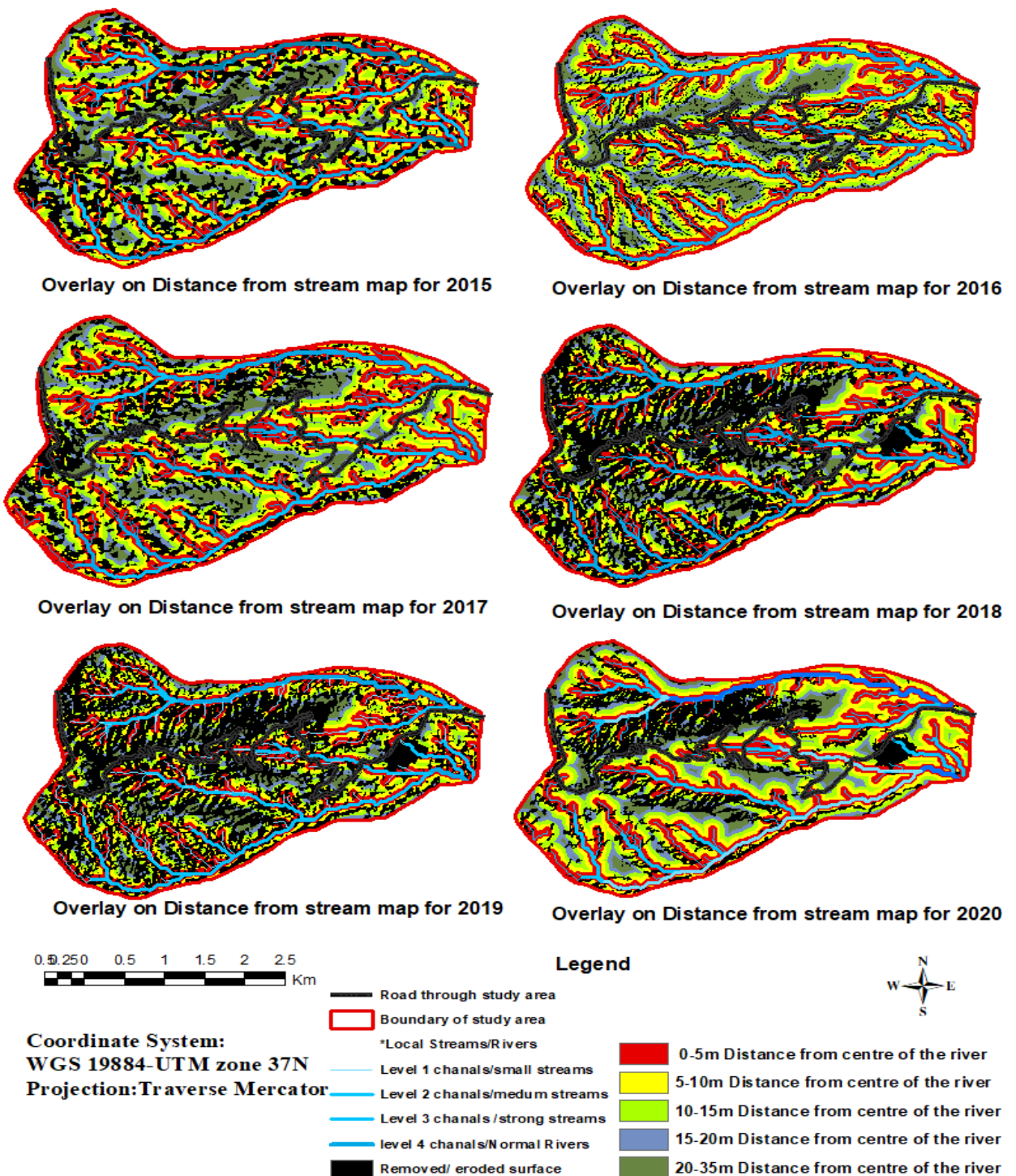
Figure 30. Mapping the lost/eroded surfaces on distance from the river map for the past six years.

Table 8. lossed surface pixel number on distance from streams/rivers map for the past six years.

Year	Causative factor subclasses	Sub class pixels number	Eroded surface pixel number	Eroded/removed surface percent	Year	Causative factor subclasses	Sub class pixels number	Eroded surface pixel number	Eroded/removed surface percent
2015	0-5m	23722	7001.4	27	2018	0-5m	23724	12179	32
	5-10m	18303	5936.4	23		5-10m	18303	9519	25
	10-15m	14572	6072.4	24		10-15m	14574	7182	19
	15-20m	10014	3739.4	15		15-20m	10014	4710	13
	20-35m	8439	3026.4	12		20-35m	8439	4057	11
2016	0-5m	23724	5884	38	2019	0-5m	23724	10785	27
	5-10m	18303	4501	29		5-10m	18302	9995	25
	10-15m	14574	3391	22		10-15m	14573	6976	17
	15-20m	10013	1112	7		15-20m	10015	5886	15
	20-35m	8439	594	4		20-35m	8441	6653	17
2017	0-5m	23724	5082	24	2020	0-5m	23724	4760	24
	5-10m	18302	5142	24		5-10m	18304	4560	23
	10-15m	14574	4253	20		10-15m	14573	4351	22
	15-20m	10012	3269	15		15-20m	10015	3367	17
	20-35m	8439	3420	16		20-35m	8440	2838	14
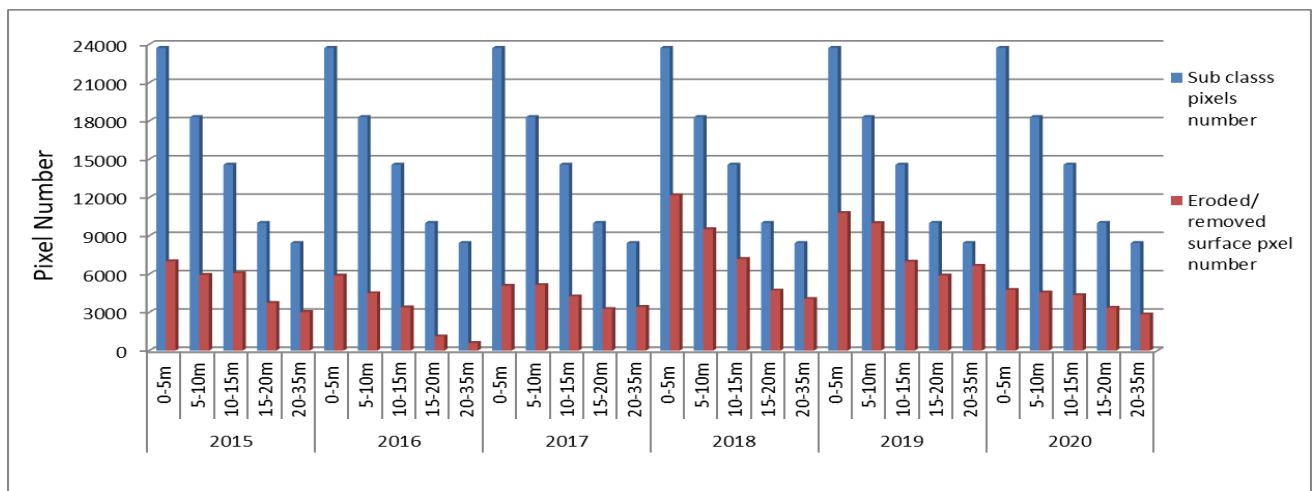
Figure 31. Bar chart of lost/eroded pixel in each subclasses on distance from stream map

The percentage distribution of landslide/removed surface in corresponding subclasses of various causative factors for each of the past six consecutive years are shown below.

Year 2015 — Percent

Causative factors	Percentage of eroded/slided surface
Lithology	
a. Pelitic vertisols	87
	13
c.Chromic luvisols	0
Elevation (m)	
	22
2450-2670	17
	17
2900-3100	20
	25
Slope (percent)	
0-5%	8
	52
25-50%	36
	4
Aspect	
FLAT	9
	13
NE	16
	29
SE	20
	4
SW	2
	1
NW	6
Curvature	
	51
b. Flat (-0.05-0.05)	0
	49
Distance from river(M)	
a. 0-5	27
	23
c.10-15	24
	15
e.20-35	12

Year 2016 — Percent

Causative foactors	Percentage of eroded/slided surface
Lithology	
a. Pelitic vertisols	88
b.Stone surface	12
c.Chromic luvisols	0
Elevation (m)	
2221-2450	18
2450-2670	13
2670-2900	17
2900-3100	25
3100-3370	26
Slope (percent)	
0-5%	6
5-25%	52
25-50%	38
50-100%	4
Aspect	
FLAT	5
N	17
NE	23
E	31
SE	18
S	3
SW	1
W	1
NW	3
Curvature	
a. Concave (<-0.05)	49
b. Flat (-0.05-0.05)	0
c. Convex (>0.05)	51
Distance from river(M)	
a. 0-5	38
b.5-10	29
c.10-15	22
d.15-20	7
e.20-35	4

Year 2017 — Percentage

Causative factors	Percentage of eroded/slided...
Lithology	
a. Pelitic vertisols	87
	13
c.Chromic luvisols	0
Elevation (m)	
	16
2450-2670	15
	18
2900-3100	22
	28
Slope (Percent)	
0-5%	6
	40
25-50%	43
	12
Aspect	
FLAT	14
	18
NE	13
	18
SE	18
	4
SW	3
	2
NW	9
Curvature	
	48
b. Flat (-0.05-0.05)	0
	52
Distance from river(M)	
a. 0-5	24
	24
c.10-15	20
	15
e.20-35	16

Year 2018 — Percentage

Causative factors	percentage of eroded/slided surface
Lithology	
a. Pelitic vertisols	87
	13
c.Chromic luvisols	0
Elevation (m)	
	16
2450-2670	17
	19
2900-3100	21
	27
Slope (Percent)	
0-5%	5
	42
25-50%	44
	9
Aspect	
FLAT	9
	18
NE	23
	27
SE	13
	2
SW	1
	1
NW	5
Curvature	
	48
b. Flat (-0.05-0.05)	0
	52
Distance from river(M)	
a. 0-5	32
	25
c.10-15	19
	13
e.20-35	11

Figure 32. Bar chart that shows distribution of lossed/eroded surface for the past six years.

After all of the eroded or removed surfaces' pixel number in each causative factor class was counted for each six past consecutive years of the study area, based on the ideology of "soil erosion initiates landslides" (19); statistical hazard model through frequency ratio (FR) were tabulated.

$$Fri, j'' = \frac{ni,j/Ni,j}{nT/NT} \quad \ldots\ldots\ldots\ldots\ldots\ldots. (1*)$$ where, ni, j =The number pixels of lossed/eroded land surface in j^{th} subclass of the factor i during rainy season

Ni, j = The number of pixels in the corresponding subclass

nT =The total number pixels of lossed/eroded land surface and

NT =The total number of pixel number under investigation.

As indicated in the appendix from table 1A to 6A; the landslide inventory were repeatedly overlaid with each predictive factor, and frequency ratio values of each class get calculated summarized as follow.

Table 9. Frequency ratio of eroded/removed surface on each causative factors for past six years.

No.	causative factors	causative factor subclasses	Frequency (FR)					
			Year					
			2015	2016	2017	2018	2019	2020
1	Lithology	a. Pelitic vertisols	1.0	1.0	1.0	1.0	1.0	1.0
		b. Stone surface	1.1	1.0	1.2	1.2	1.1	0.8
		c. Chromic luvisols	0.1	1.1	0.1	0.6	0.8	0.5
2	Elevation (m)	2221-2450	0.9	0.8	0.7	0.7	0.8	0.5
		2450-2670	1.0	0.8	0.9	1.0	1.0	1.0
		2670-2900	1.0	1.0	1.1	1.1	1.1	1.2
		2900-3100	1.0	1.3	1.2	1.1	1.1	1.2
		3100-3370	1.1	1.2	1.2	1.2	1.2	1.2
3	Slope (percent)	0-5%	0.9	0.7	0.8	0.7	0.8	0.4
		5-25%	1.0	1.0	0.9	0.9	1.0	0.9
		25-50%	1.0	1.1	1.1	1.1	1.1	1.3
		50-100ᴼ%	1.1	1.0	1.2	1.1	1.1	1.4
4	Aspect	FLAT	1.2	0.7	1.9	1.2	1.1	2.3
		N	0.8	1.0	1.1	1.1	1.1	1.6
		NE	0.7	0.9	0.5	1.0	1.0	0.9
		E	1.0	1.0	0.6	0.9	0.9	0.6
		SE	1.4	1.2	1.3	0.9	0.9	0.4
		S	2.1	1.3	2.0	1.0	1.0	0.8
		SW	1.9	1.1	2.9	1.0	0.9	1.0
		W	1.4	0.7	2.5	1.2	1.2	2.1
		NW	1.4	0.6	2.2	1.2	1.2	2.5
5	Plan Curvature	a. Concave (<-0.05)	1.0	1.0	1.0	1.0	1.0	0.9
		b. Flat (-0.05-0.05)	0.1	1.6	0.8	0.8	0.4	2.7
		c. Convex (>0.05)	1.0	1.0	1.0	1.0	1.0	1.1
6	Distance from Stream/river(M)	a. 0-5	0.9	1.2	0.8	1.0	0.8	0.8
		b.5-10	0.9	1.2	1.0	1.0	1.0	0.9
		c.10-15	1.2	1.1	1.0	1.0	0.9	1.1
		d.15-20	1.1	0.5	1.2	0.9	1.1	1.3
		e.20-35	1.0	0.3	1.4	1.0	1.5	1.3
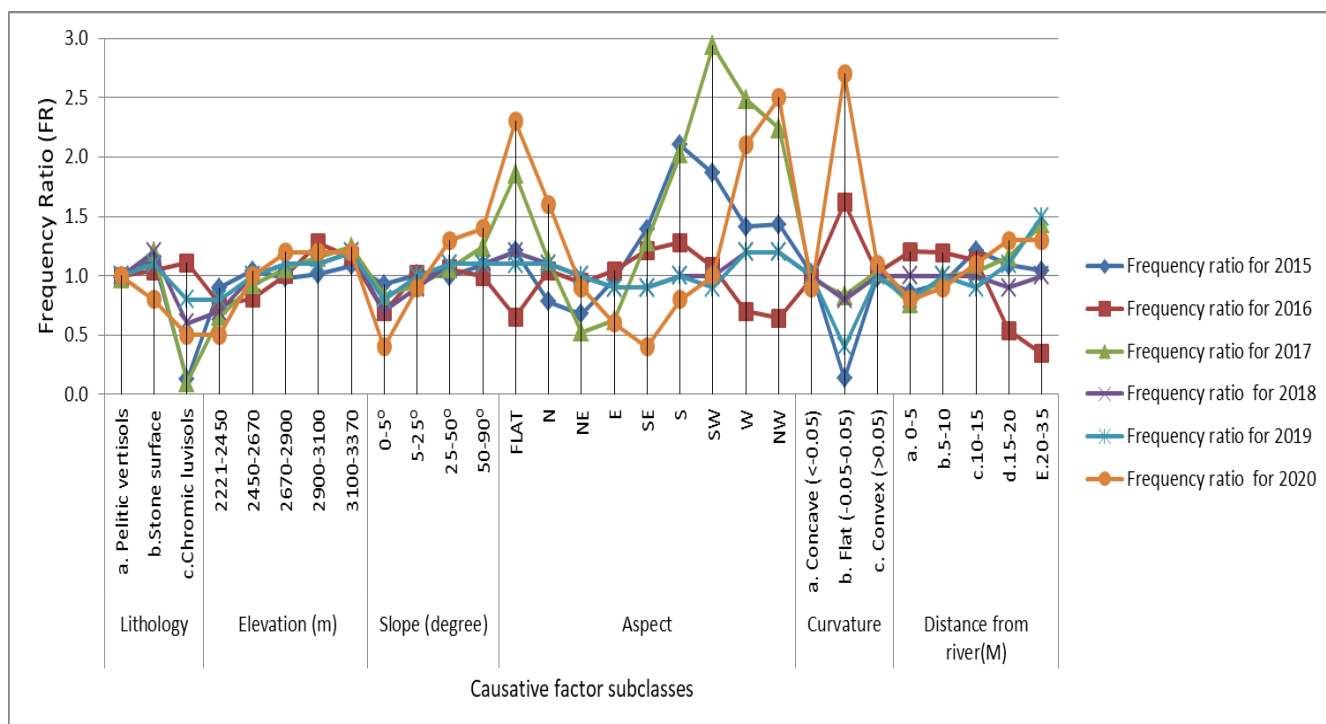
Figure 33. line chart that shows frequency ratio of lossed/eroded surface for the past six years.

The FR method follows the principle of conditional probability, in which if the ratio is greater, the stronger the relationship between landslides and factor classes and vice versa. From this frequency analysis, it is observed that the stronger the relationship of landslide/removed surfaces and causative factor subclasses for each of the past consecutive six years were identified.

Table 10. Landslide frequency ratio of eroded surface on each causative factors for past six years.

Years					
2015	2016	2017	2018	2019	2020
Dominant landslide causative factors					
-S (To south direction)	-On flat surface	-SW (To south west direction)	-Stone surface -On 3100-3370m -On flat surface -W (To west direction) -NW (To North west direction)	-In 20-35m from river	-On flat surface

Finally, the landslide Susceptibility index (LSI) for each of six past years causative factors were created by summing the FR values of each subclasses in the conventional FR method.

$$\text{LSI}=FR_{li} + FR_{el} + FR_{sl} + FR_{as} + FR_{cu} + FR_{dr} \quad \ldots\ldots\ldots\ldots\ldots(2^*) \quad \text{where},$$

LSI = landslide Susceptibility index, FR_{li} = frequency ratio value of lithology

FR_{el} = frequency ratio value of elevation, FR_{sl} = frequency ratio value of slope

FR_{as} = frequency ratio value of aspect, FR_{cu} = frequency ratio value of curvature,

FR_{dr} = frequency ratio value of distance from stream/ river

Table 11. Landslide susceptibility index of each causative factors for past six years.

No.	Causative factors	years					
		2015	2016	2017	2018	2019	2020
		landslide Susceptibility index (LSI)					
1	Lithology	2.3	3.1	2.3	2.7	2.9	2.3
2	Elevation	5	5	5	5.1	5	5.1
3	Slope	4	3.8	4.1	3.9	3.9	3.9
4	Aspect	11.8	8.6	15.1	9.6	9.4	11.9
5	Plan curvature	2.1	3.6	2.8	2.8	2.4	4.7
6	Distance from Stream/River	5.1	4.4	8.2	4.9	10.2	14.9
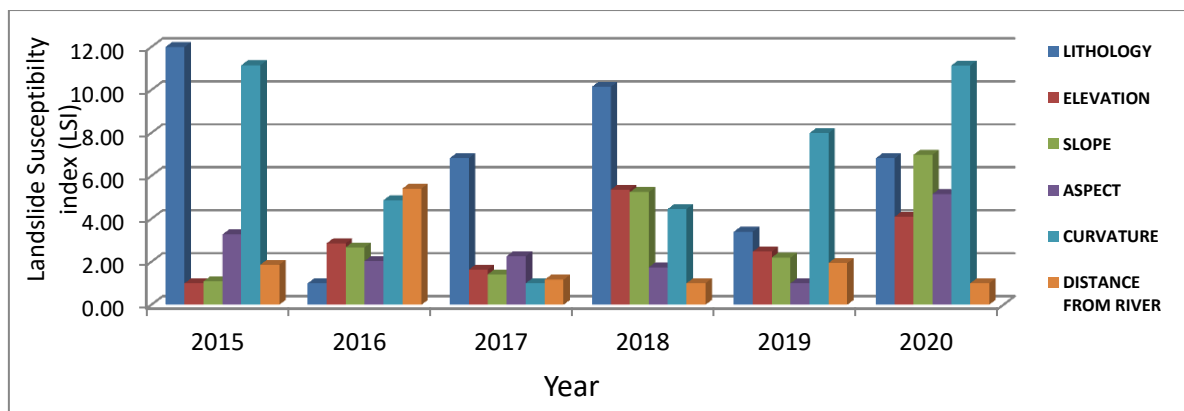
Figure 34. Bar chart of landslide susceptibility index of the study area for the past six years.

Landslide susceptibility index (LSI) indicate the degree of susceptibility of the area for landslide occurrence. The higher the value of landslide susceptibility index (LSI), the higher the probability of landslide occurrence, but the lower the landslide susceptibility index (LSI) value indicate the lower the probability of landslide occurrence. Based on the value of LSI for each causative factors subclasses in each years, the following hierarchal rank of causative factors were developed for each years.

Table 12. Hierarchal rank of causative factors for landslide occurrence each of the past six years.

Rank	2015	2016	2017	2018	2019	2020
	Landslide susceptibility index order (LSI)					
1st	Aspect	Aspect	Aspect	Aspect	Distance from Stream	Distance from Stream
2nd	Distance from Stream	Elevation	Distance from Stream	Elevation	Aspect	Aspect
3rd	Elevation	Distance from Stream	Elevation	Distance from Stream	Elevation	Elevation
4th	Slope	Slope	Slope	Slope	Slope	Plan curvature
5th	Lithology	Plan curvature	Plan curvature	Plan curvature	Lithology	Slope
6th	Plan curvature	Lithology	Lithology	Lithology	Plan curvature	Lithology

4.3 Landslide susceptibility mapping analyses

The frequency ratio approach was used in this work to conduct landslide susceptibility studies. After the frequency ratio for all considered causative factor subclasses for all the past six consecutive years were calculated, further analysis between all six causative factors and landslides was made to deduce correlation ratings. The governing parameters were rated using a GIS-based statistical and likelihood approach, and then a customized raster calculation was used to develop the landslide hazard zone maps for each of the past six years.

During the present study six causative factors namely; lithology/soil mass, Elevation, slope, aspect, Plan curvature, and distance from river were considered. It was assumed that these causative factors were probably responsible for landslides in the area. The probability method attempt was made to establish a spatial relationship between these factors and the landslides/erosion occurred in the study area for all the past consecutive six years. By using statistical approach, in addition to frequency ratio (FR) different parameters such as frequency rate (RF), frequency rate in percentage (RF%) and Probability ratio(PR) was tabulated by excel sheet.

$$\text{Frequency rate } (RF) = \frac{frequency\ ratio\ (FR)}{\sum_{n=1}^{\infty} frequency\ ratio\ (FR)}$$

$$\text{Frequency rate } (RF\%) = \frac{frequency\ ratio\ (FR)}{\sum_{n=1}^{\infty} frequency\ ratio\ (FR)} * 100$$

INT(RF)= Integer value of rate of frequency(RF) Without including any decimal value of rate of frequency(RF)

$$Probabilty\ ratio(PR) = \frac{Max\ RF - Min\ RF}{MININUM\ OF(Max\ RF - Min\ RF)}$$

Where, Min RF= Minimum frequency rate and

Max RF=Maximum frequency rate

Table 13. Probability ratio of eroded/removed surface on each causative factors for year 2015.

No.	Causative factors	Causative factor subclass	Frequency(FR)	Frequency rate (RF)	frequency rate RF(%)	INT(RF)	Min RF	Max RF	Max RF-Min RF(a)	MIN(Max RF-Min RF)(b)	Probability ratio PR=a/b
					Year 2015						
1	Lithology	a. Pelitic vertisols	1.0	0.435	43.5	43					
		b. Stone surface	1.1	0.509	50.9	50					
		c. Chromic luvisols	0.1	0.055	5.5	5					
		Total	2.3	1.000			0.06	0.51	0.454	0.037	12.31
2	Elevation (m)	2221-2450	0.9	0.179	17.9	17					
		2450-2670	1.0	0.208	20.8	20					
		2670-2900	1.0	0.195	19.5	19					
		2900-3100	1.0	0.202	20.2	20					
		3100-3370	1.1	0.216	21.6	21					
		Total	5.0	1.000			0.18	0.22	0.037	0.037	1
3	Slope (percent)	0-5%	0.9	0.231	23.1	23					
		5-25%	1.0	0.251	25.1	25					
		25-50%	1.0	0.247	24.7	24					
		50-90⁰%	1.1	0.271	27.1	27					
		Total	4.0	1.000			0.23	0.27	0.040	0.04	1.09
4	Aspect	FLAT	1.2	0.102	10.2	10					
		N	0.8	0.066	6.6	6					
		NE	0.7	0.057	5.7	5					
		E	1.0	0.082	8.2	8					
		SE	1.4	0.118	11.8	11					
		S	2.1	0.178	17.8	17					

No	Causative factors	Causative factor subclass	Frequency(FR)	Frequency rate(RF)	Frequency rate RF(%)	INT(RF)	Min RF	Max RF	Max RF-Min RF(a)	MIN(Max RF Min RF)(b)	PR=a/b
		SW	1.9	0.158	15.8	15					
		W	1.4	0.119	11.9	11					
		NW	1.4	0.121	12.1	12					
		Total	11.8	1.000			0.06	0.18	0.121	0.04	3.27
5	Plan Curvature	a. Concave	1.0	0.475	47.5	47					
		b. Flat	0.1	0.064	6.4	6					
		c. Convex	1.0	0.461	46.1	46					
		Total	2.1	1.000			0.06	0.48	0.411	0.04	11.2
6	Distance from river(M)	a. 0-5	0.9	0.167	16.7	16					
		b.5-10	0.9	0.183	18.3	18					
		c.10-15	1.2	0.236	23.6	23					
		d.15-20	1.1	0.211	21.1	21					
		e.20-35	1.0	0.203	20.3	20					
		Total	5.1	1.000			0.17	0.24	0.069	0.04	1.86

Table 14. Probability ratio of eroded/removed surface on each causative factors for year 2016

No	Causative factors	Causative factor subclass	Frequency(FR)	Frequency rate(RF)	Frequency rate RF(%)	INT(RF)	Min RF	Max RF	Max RF-Min RF(a)	MIN(Max RF Min RF)(b)	PR=a/b
											Year 2016
1	Lithology	a. Pelitic vertisols	1.0	0.316	31.6	31					
		b. Stone surface	1.0	0.332	33.2	33					
		c. Chromic luvisols	1.1		35.2	35					
		Total	3.1				0.316	0.35	0.04	0.04	1
2	Elevation (m)	2221-2450	0.8	0.151	15.1	15					
		2450-2670	0.8	0.161	16.1	16					
		2670-2900	1.0	0.201	20.1	20					
		2900-3100	1.3	0.255	25.5	25					
		3100-3370	1.2	0.232	23.2	23					
		Total	5.0				0.151	0.26	0.10	0.04	2.86

No	Factor	Class									
3	Slope (degree)	0-5%	0.7	0.185	18.5	18					
		5-25%	1.0	0.270	27.0	26					
		25-50%	1.1	0.281	28.1	28					
		50-100%	1.0	0.264	26.4	26					
		Total	3.8				0.185	0.28	0.10	0.04	2.67
4	Aspect	FLAT	0.7	0.076	7.6	7					
		N	1.0	0.121	12.1	12					
		NE	0.9	0.110	11.0	10					
		E	1.0	0.121	12.1	12					
		SE	1.2	0.141	14.1	14					
		S	1.3	0.149	14.9	14					
		SW	1.1	0.125	12.5	12					
		W	0.7	0.081	8.1	8					
		NW	0.6	0.075	7.5	7					
		Total	8.6				0.075	0.15	0.07	0.04	2.04
5	Plan Curvature	a. Concave	1.0	0.271	27.1	27					
		b. Flat	1.6	0.447	44.7	44					
		c. Convex	1.0	0.282	28.2	28					
		Total	3.6				0.271	0.45	0.18	0.04	4.87
6	Distance from river(m)	a. 0-5	1.2	0.273	27.3	27					
		b.5-10	1.2	0.271	27.1	27					
		c.10-15	1.1	0.256	25.6	25					
		d.15-20	0.5	0.122	12.2	12					
		e.20-35	0.3	0.078	7.8	7					
		Total	4.4				0.078	0.27	0.20	0.04	5.41

Table 15. Probability ratio of eroded/removed surface on each causative factors for year 2017.

No.	Causative factors	Causative factor subclass	Frequency (FR)	Frequency rate(RF)	frequency rate RF(%)	INT(RF)	Min RF	Max RF	Max RF-Min RF (a)	MIN(Max RF-Min RF)(b)	PR=a/b
1	Lithology	a. Pelitic vertisols	1.0	0.428	42.8	42					
		b. Stone surface	1.2	0.527	52.7	52					
		c. Chromic luvisols	0.1	0.044	4.4	4					
		Total	2.3				0.044	0.527	0.483	0.071	6.83
	Elevation (m)	2221-2450	0.7	0.131	13.1	13					
		2450-2670	0.9	0.184	18.4	18					
		2670-2900	1.1	0.210	21.0	21					
		2900-3100	1.2	0.230	23.0	22					
		3100-3370	1.2	0.246	24.6	24					
		Total	5.0				0.131	0.246	0.115	0.071	1.63
3	Slope (degree)	0-5%	0.8	0.206	20.6	20					
		5-25%	0.9	0.227	22.7	22					
		25-50%	1.1	0.261	26.1	26					
		50-100%	1.2	0.306	30.6	30					
		Total	4.1				0.206	0.306	0.100	0.071	1.41
4	Aspect	FLAT	1.9	0.123	12.3	12					
		N	1.1	0.074	7.4	7					
		NE	0.5	0.035	3.5	3					
		E	0.6	0.041	4.1	4					
		SE	1.3	0.085	8.5	8					
		S	2.0	0.134	13.4	13					
		SW	2.9	0.195	19.5	19					
		W	2.5	0.164	16.4	16					
		NW	2.2	0.148	14.8	14					

No	Causative factors	Causative factor subclass	Frequency(FR)	Frequency rate(RF)	frequency rate RF(%)	INT(RF)	Min RF	Max RF	Max RF-Min RF(a)	MIN(Max RF-Min RF)(b)	PR=a/b
		Total	15.1				0.035	0.195	0.160	0.071	2.26
5	Curvature	a. Concave	1.0	0.341	34.1	34					
		b. Flat	0.8	0.294	29.4	29					
		c. Convex	1.0	0.365	36.5	36					
		Total	2.8				0.294	0.365	0.071	0.071	1
6	Distance from river(M)	a. 0-5	0.8	0.092	9.2	9					
		b.5-10	1.0	0.121	12.1	12					
		c.10-15	1.0	0.126	12.6	12					
		d.15-20	1.2	0.141	14.1	14					
		E.20-35	1.4	0.175	17.5	17					
		Total	8.2				0.092	0.175	0.082	0.071	1.17

Table 16. Probability ratio of eroded/removed surface on each causative factors for year 2018.

No.	Causative factors	Causative factor subclass	Frequency(FR)	Frequency rate(RF)	frequency rate RF(%)	INT(RF)	Min RF	Max RF	Max RF-Min RF(a)	MIN(Max RF-Min RF)(b)	PR=a/b
					Year 2018						
1	Lithology	a. Pelitic vertisols	1.0	0.359	35.9	35					
		b. Stone surface	1.2	0.42	42.3	42					
		c. Chromic luvisols	0.6	0.219	21.9	21					
		Total	2.7				0.22	0.42	0.2	0.02	10.6
2	Elevation (m)	2221-2450	0.7	0.131	13.1	13					
		2450-2670	1.0	0.196	19.6	19					
		2670-2900	1.1	0.221	22.1	22					
		2900-3100	1.1	0.214	21.4	21					
		3100-3370	1.2	0.239	23.9	23					
		Total	5.1				0.13	0.24	0.1	0.02	5.4
3	(degre	0-5%	0.7	0.186	18.6	18					
		5-25%	0.9	0.243	24.3	24					

		25-50%	1.1	0.291	29.1	29						
		50-100%	1.1	0.280	28.0	27						
		Total	3.8					0.19	0.29	0.1	0.02	5.2
4	Aspect	FLAT	1.2	0.128	12.8	12						
		N	1.1	0.115	11.5	11						
		NE	1.0	0.100	10.0	9						
		E	0.9	0.094	9.4	9						
		SE	0.9	0.098	9.8	9						
		S	1.0	0.104	10.4	10						
		SW	1.0	0.103	10.3	10						
		W	1.2	0.128	12.8	12						
		NW	1.2	0.129	12.9	12						
		Total	9.6					0.1	0.13	0.0	0.02	1.7
5	Curvature	a. Concave	1.0	0.340	34.0	34						
		b. Flat	0.8	0.285	28.5	28						
		c. Convex	1.0	0.374	37.4	37						
		Total	2.8					0.29	0.37	0.1	0.02	4.5
6	Distance from river(M)	a. 0-5	1.0	0.207	20.7	20						
		b.5-10	1.0	0.210	21.0	20						
		c.10-15	1.0	0.199	19.9	19						
		d.15-20	0.9	0.190	19.0	18						
		e.20-35	1.0	0.194	19.4	19						
		Total	4.9					0.19	0.21	0.0	0.02	1

Table 17. Probability ratio of eroded/removed surface on each causative factors for year 2019

No.	Causative factors	Causative factor subclass	Frequency (FR)	Frequency rate(RF)	frequency rate RF(%)	INT(RF)	Min RF	Max RF	Max RF-Min RF (a)	MIN(Max RF-Min RF)(b)	PR=a/b
						Year 2019					
1	Lithology	a. Pelitic vertisols	1.0	0.341	34.1	34					
		b. Stone surface	1.1	0.383	38.3	38					
		c. Chromic luvisols	0.8	0.276	27.6	27					
		Total	2.9				0.28	0.38	0.107	0.03	3.4
2	Elevation (m)	2221-2450	0.8	0.151	15.1	15					
		2450-2670	1.0	0.193	19.3	19					
		2670-2900	1.1	0.216	21.6	21					
		2900-3100	1.1	0.210	21.0	21					
		3100-3370	1.2	0.229	22.9	22					
		Total	5.0				0.15	0.23	0.078	0.03	2.5
3	Slope (degree)	0-5%	0.8	0.206	20.6	20					
		5-25%	1.0	0.246	24.6	24					
		25-50%	1.1	0.275	27.5	27					
		50-100%	1.1	0.273	27.3	27					
		Total	3.9				0.21	0.28	0.069	0.03	2.2
4	Aspect	FLAT	1.1	0.120	12.0	12					
		N	1.1	0.115	11.5	11					
		NE	1.0	0.104	10.4	10					
		E	0.9	0.100	10.0	9					
		SE	0.9	0.100	10.0	9					
		S	1.0	0.107	10.7	10					
		SW	0.9	0.099	9.9	9					
		W	1.2	0.124	12.4	12					
		NW	1.2	0.131	13.1	13					
		Total	9.4				0.1	0.13	0.031	0.03	1.0

No	Causative factors	Causative factor subclass	Frequency (FR)	Frequency rate(RF)	frequency rate RF(%)	INT(RF)	Min RF	Max RF	Max RF-Min RF (a)	MIN(Max RF-Min RF)(b)	PR=a/b
5	Curvature	a. Concave	1.0	0.395	39.5	39					
		b. Flat	0.4	0.177	17.7	17					
		c. Convex	1.0	0.428	42.8	42					
		Total	2.4				0.2	0.4	0.251	0.0	8.0
6	Distance from river(m)	a. 0-5	0.8	0.083	8.3	8					
		b.5-10	1.0	0.100	10.0	9					
		c.10-15	0.9	0.088	8.8	8					
		d.15-20	1.1	0.108	10.8	10					
		e.20-35	1.5	0.144	14.4	14					
		Total	10.2				0.9	0.1	0.061	0.1	1.9

Table 18. Probability ratio of eroded/removed surface on each causative factors for year 2020

No	Causative factors	Causative factor subclass	Frequency (FR)	Frequency rate(RF)	frequency rate RF(%)	INT(RF)	Min RF	Max RF	Max RF-Min RF (a)	MIN(Max RF-Min RF)(b)	PR=a/b
					Year 2020						
1	Lithology	a. Pelitic vertisols	1.0	0.446	44.6	44					
		b. Stone surface	0.8	0.344	34.4	34					
		c. Chromic luvisols	0.5	0.211	21.1	21					
		Total	2.3				0.21	0.45	0.235	0.034	6.82
2	Elevation (m)	2221-2450	0.5	0.100	10.0	9					
		2450-2670	1.0	0.188	18.8	18					
		2670-2900	1.2	0.234	23.4	23					
		2900-3100	1.2	0.238	23.8	23					
		3100-3370	1.2	0.241	24.1	24					
		Total	5.1				0.10	0.24	0.141	0.034	4.09
3	Slope (degree)	0-5%	0.4	0.106	10.6	10					
		5-25%	0.9	0.226	22.6	22					
		25-50%	1.3	0.322	32.2	32					

No	Factor	Subclass									
		50-100%	1.4	0.346	34.6	34					
		Total	3.9				0.17	0.35	0.241	0.034	6.98
4	Aspect	FLAT	2.3	0.189	18.9	18					
		N	1.6	0.134	13.4	13					
		NE	0.9	0.073	7.3	7					
		E	0.6	0.047	4.7	4					
		SE	0.4	0.030	3.0	2					
		S	0.8	0.063	6.3	6					
		SW	1.0	0.083	8.3	8					
		W	2.1	0.175	17.5	17					
		NW	2.5	0.207	20.7	20					
		Total	11.9				0.03	0.21	0.177	0.034	5.15
5	Curvature	a. Concave	0.9	0.195	19.5	19					
		b. Flat	2.7	0.579	57.9	57					
		c. Convex	1.1	0.227	22.7	22					
		Total	4.7				0.2	0.58	0.384	0.034	11.1
6	Distance from river(m)	a. 0-5	0.8	0.051	5.1	5					
		b.5-10	0.9	0.063	6.3	6					
		c.10-15	1.1	0.076	7.6	7					
		d.15-20	1.3	0.085	8.5	8					
		e.20-35	1.3	0.09	8.5	8					
		Total	14.9				0.05	0.09	0.034	0.034	1

After all, required parameters for each causative factors' subclasses for each of the past six years, by using the raster calculator in ArcGIS landslide susceptibility maps for each of the past six years were established.

$$landslide\ hazard\ map(LHM)\ for\ year(ij) = \sum_{n=1}^{\infty}(\text{Causative factor map(ij)} * PR(ij))$$

LHZ (Year ij)=[Lithology map(ij)*PR(li)+Elevation map(ij)*PR(el)+Slope

map(ij)*PR(sl)+Aspect map(ij)*PR(as)+Plan curvature map(ij)*PR(cu)+ Distance from

river/stream map (ij)*PR(dr)]

Where,   PR(li)=Probability ratio for Lithology map, PR(el)= Probability ratio for Elevation map

PR(sl)= Probability ratio for Slope map, PR(as)= Probability ratio for Aspect map

PR(cu)= Probability ratio for Plan curvature map, PR(dr)= Probability ratio for Distance from river/stream map

Applying this statistical approach, landslide hazard maps for each year under consideration were prepared. Susceptibility to landslides is observed in the areas near rivers/streams, directional slopes to the north and south, and highly steep slope areas, as shown in each of the maps.

Hazard map for the past six years
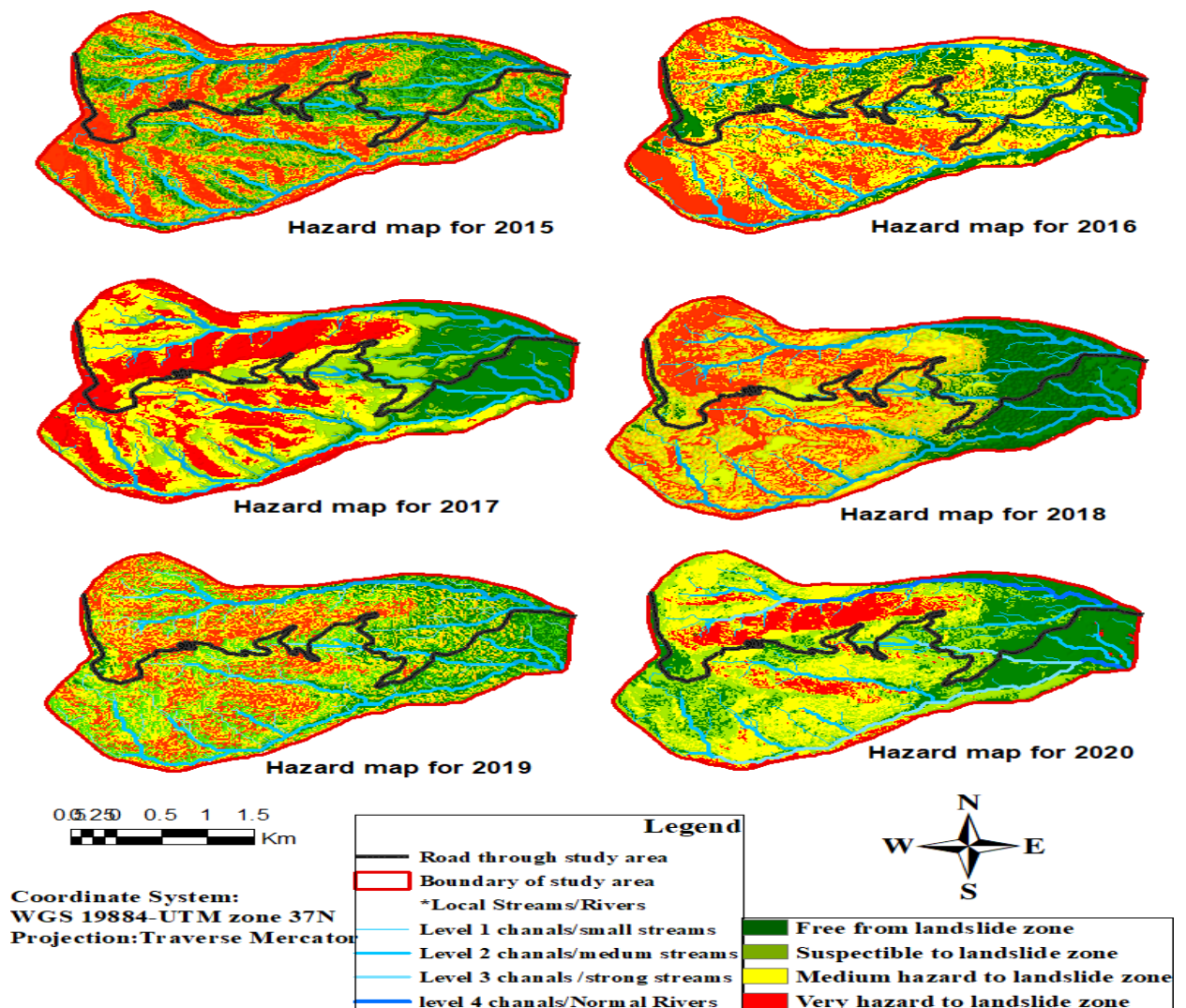
Figure 35. Maps that show landslide hazard zone classes distribution for the past six years.

The final landslide hazard zone of the study area was developed by using the average value of each year as follow.

Table 19. Average Probability ratio of eroded/removed surface on each causative factors for study area

No.	Causative factors	Causative factor subclass	Years — Integer (INT) 2015	2016	2017	2018	2019	2020	Average Integer(INT)		Years — Probability Ratio (PR) 2015	2016	2017	2018	2019	2020	Average Probability
1	Lithology	a. Pelitic vertisols	43	31	42	35	34	44	38								
		b. Stone surface	50	33	52	42	38	34	42								
		c. Chromic luvisols	5	35	4	21	27	21	17								
		Total									12.31	1	6.83	10.15	3.40	6.82	6.75
2	Elevation (m)	2221-2450	17	15	13	13	15	9	13								
		2450-2670	20	16	18	19	19	18	18								
		2670-2900	19	20	21	22	21	23	21								
		2900-3100	20	25	22	21	21	23	22								
		3100-3370	21	23	24	23	22	24	23								
		Total									1	2.86	1.63	5.36	2.47	4.09	2.90
3	Slope (percent)	0-5%	23	18	20	18	20	10	17								
		5-25%	25	26	22	24	24	22	23								
		25-50%	24	28	26	29	27	32	28								
		50-90°%	27	26	30	27	27	34	28								
		Total									1.09	2.67	1.41	5.24	2.19	6.98	3.26
4	Aspect	FLAT	10	7	12	12	12	18	11								
		N	6	12	7	11	11	13	10								
		NE	5	10	3	9	10	7	7								
		E	8	12	4	9	9	4	7								
		SE	11	14	8	9	9	2	8								

#	Factor	Class															
		S	17	14	13	10	10	6	11								
		SW	15	12	19	10	9	8	12								
		W	11	8	16	12	12	17	12								
		NW	12	7	14	12	13	20	12								
		Total									3.27	2.03	2.26	1.74	1.00	5.15	2.58
5	Plan Curvature	a. Concave	47	27	34	34	39	19	32								
		b. Flat	6	44	29	28	17	57	32								
		c. Convex	46	28	36	37	42	22	34								
		Total									11.15	4.87	1	4.45	7.99	11.14	6.77
6	Distance from river(M)	a. 0-5	16	27	9	20	8	5	16								
		b.5-10	18	27	12	20	9	6	17								
		c.10-15	23	25	12	19	8	7	17								
		d.15-20	21	12	14	18	10	8	15								
		e.20-35	20	7	17	19	14	8	15								
		Total									1.86	5.41	1.17	1	1.94	1	2.06

Accordingly, the following average landslide hazard zone map groups were established based on the statistical analysis approach: free from landslide zone, susceptible to landslide zone, low to landslide zone, and very hazard to landslide zone.
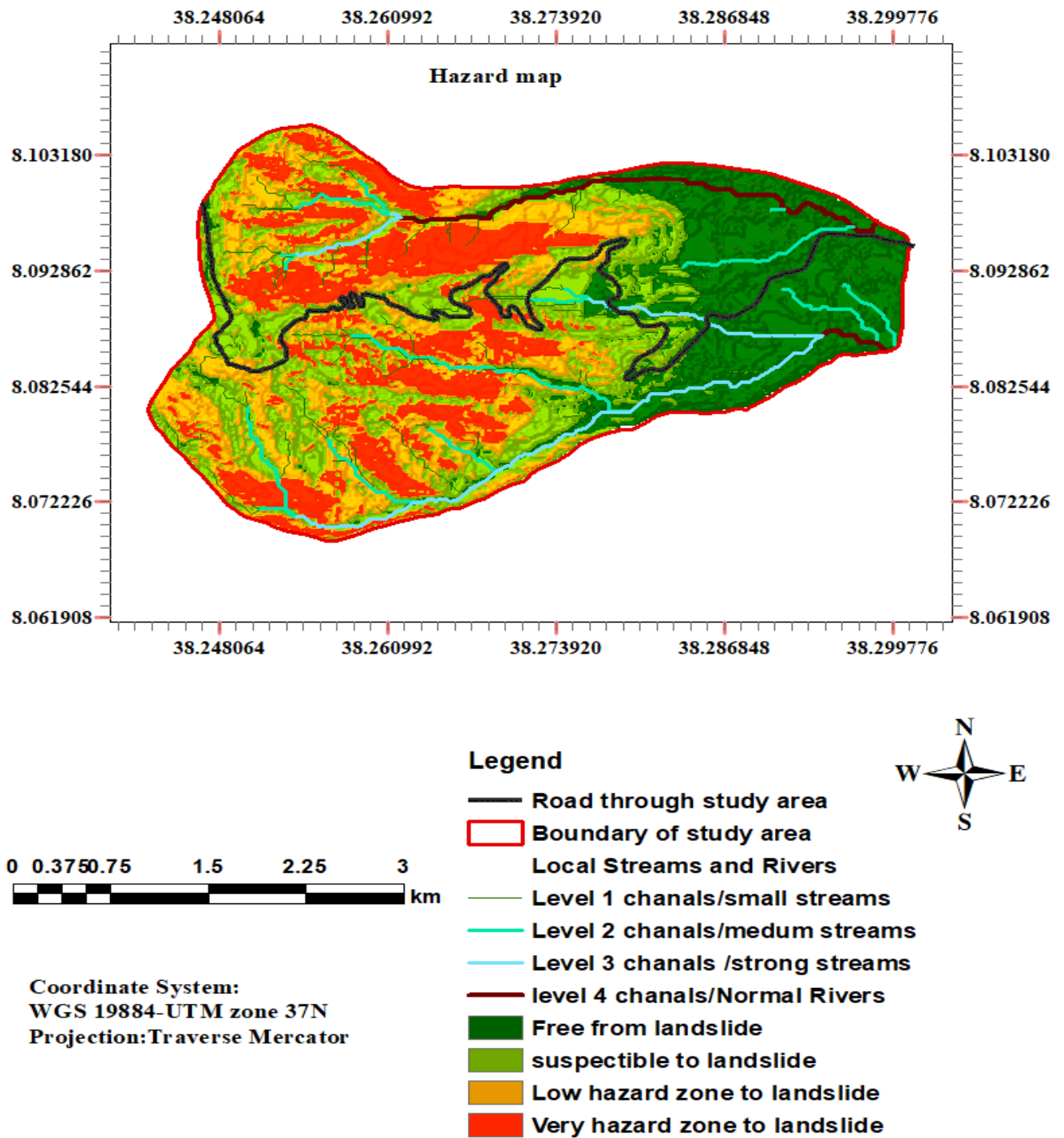
Figure 36. Maps of average/ generalized landslide hazard zone classes distribution.

In general, from the landslide hazard map built, out of a total of 17.9 km2, 27 percent (4.8 km2) of free from landslide zone, 29 percent (5.2 km2) susceptible to landslide zone, 23 percent (4.1 km2) low to landslide zone, and 21 percent (3.8 km2) of really hazard to landslide zone.
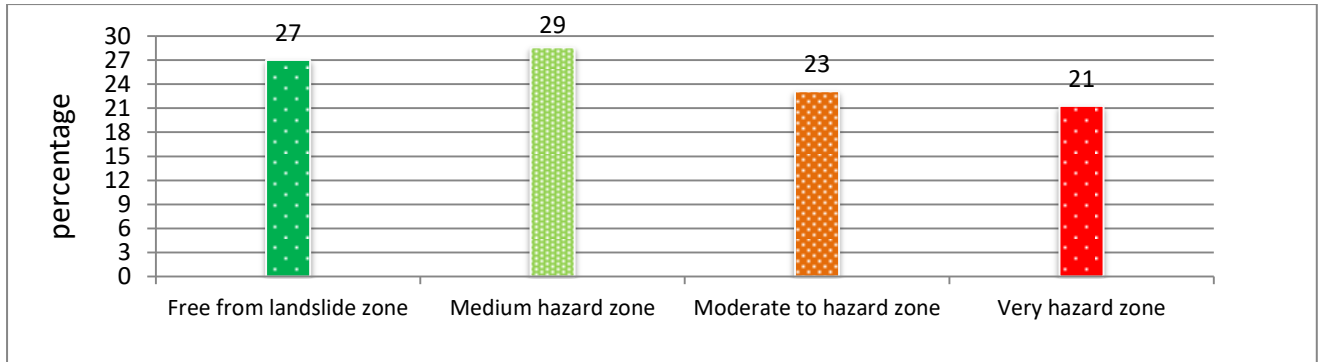
Figure 37. Bar chart of distribution/coverage of landslide hazard classes in the study area.

Based on the hazard map developed, geotechnical characterization of rock-soil slope failure along road corridor were studied. To do this on some selected points sieve analysis, angle of repose and direct shear for soil part were conducted in soil laboratory and unconfined compressive strength for weathered rock mass were done in field and interpreted.

Figure 38. Sample photos that shows weathered rock-soil slope failure along road corridor

Using ASTM standard (D422-63); the following sieve analysis for six points along the road corridor and the slope failure angle in the field were done. Based on the analysis; the amount of soil mass fractions (gradation) were categorized and presented as follows.
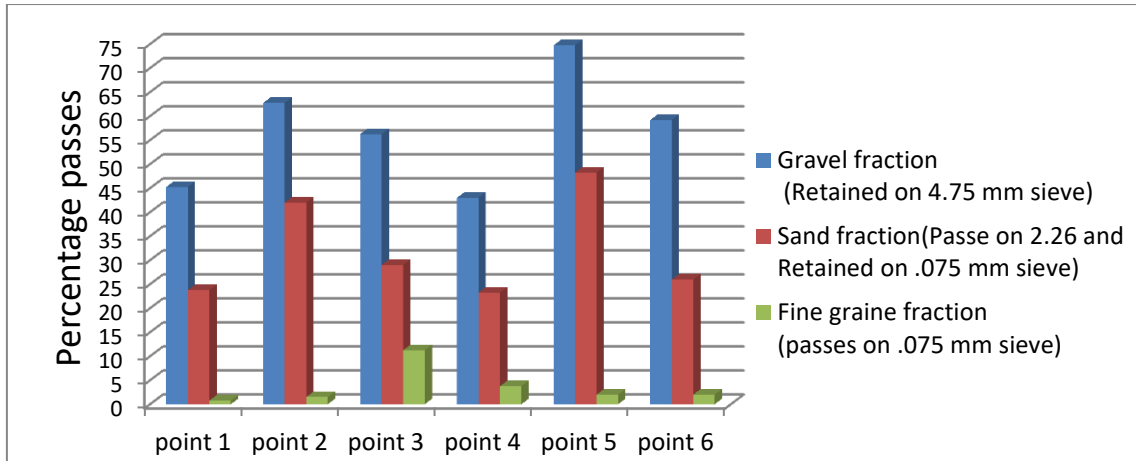
Figure 39. Bar chart that shows rock-soil fraction along road corridor for selected points

The slope failure angle in the field and angle of repose in the laboratory were also conducted and compared.

Figure 40. photo taken during determination of angle of repose in the laboratory.
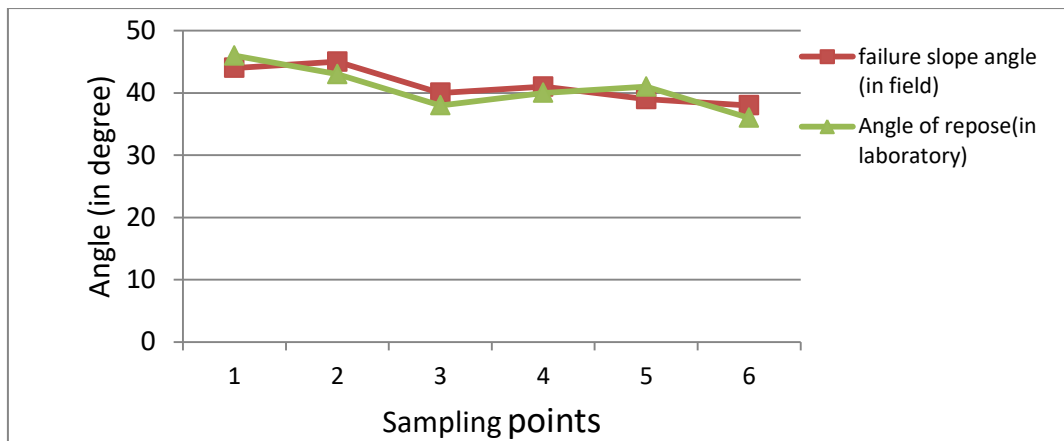
Figure 41. Curve of weathered rock-soil slope failure angle with angle of repose along road.

As observed from the total point results, nearly 67% of the angle of repose measured values in the laboratory are smaller than the failure slope angle measured in the field. This shows that there is a

probable continuous decreasing of field slope angle until the minimum slope angle is maintained and the soil is stable by its own weight.

The direct shear tests for determination of shear strength parameters for four points along the road corridor were conducted as follow.

Table 20. Table for direct shear test results for shear strength parameters

Point	Unit weight (γ in KN/m^3)	Angle of internal friction (φ in ^{o})	Cohesive force (C in KN/m$^{2)}$)
2	17.5	32	28
3	18	30	68
4	17	31	14
5	18	30	68

Shear stress Vs Normal stress Curve for point 2

$y = 0.62x + 28.06$
$R^2 = 0.99$

Shear stress Vs Normal stress Curve for point 3&5

$y = 0.58x + 67.58$
$R^2 = 1.00$
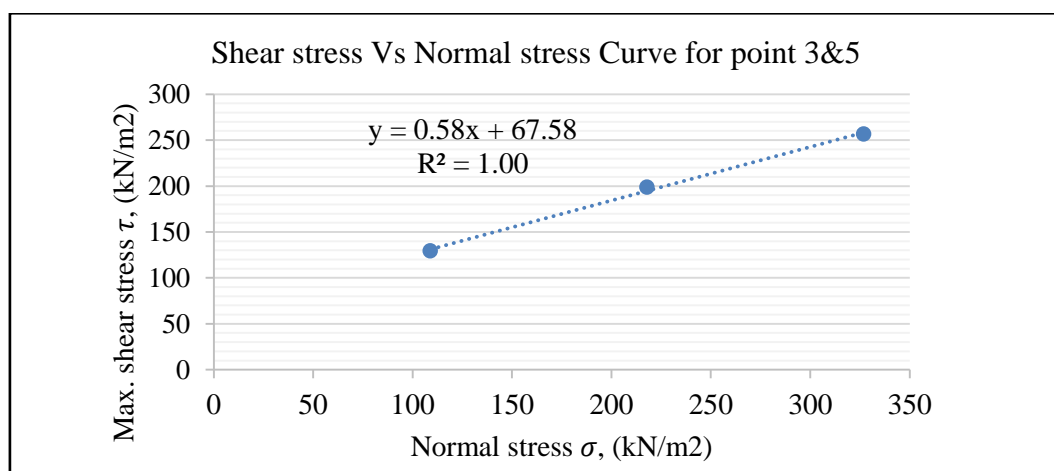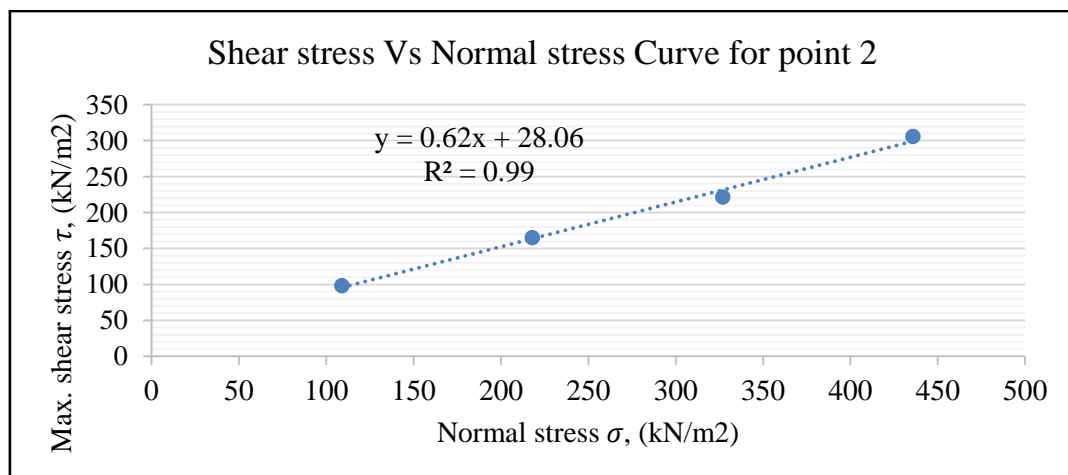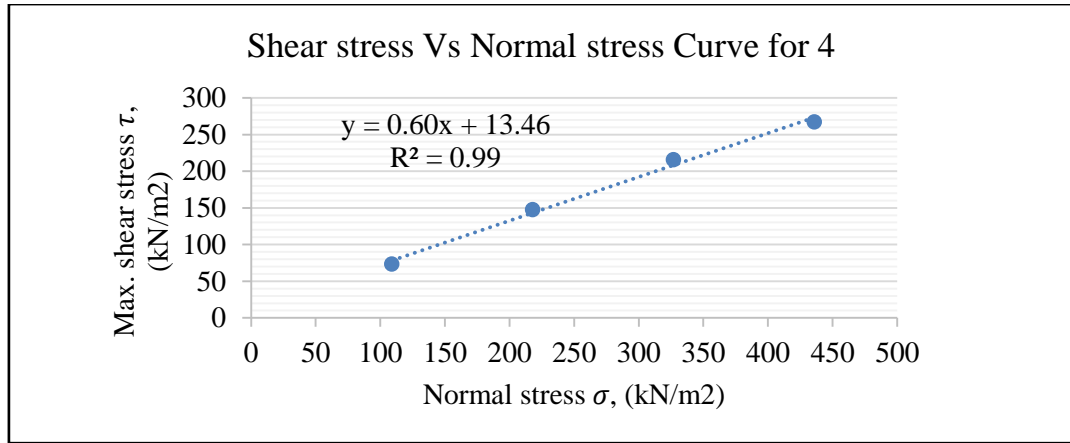
Figure 42. Curves of direct shear test results for selected points

In addition to sieve analysis (gradation), angle of repose and direct shear, Unconfined Compressive Strength (UCS), which is related to the uniaxial compressive strength of weathered rock slopes along the road corridor, was determined. For this work, the Schmidt hammer (also known as the rebound or impact hammer) test was applied to determine the strength of rock in terms of surface rebound hardness from center of failure points to outside.
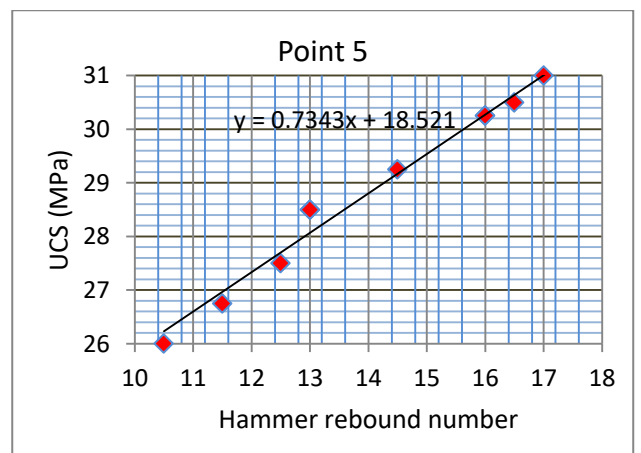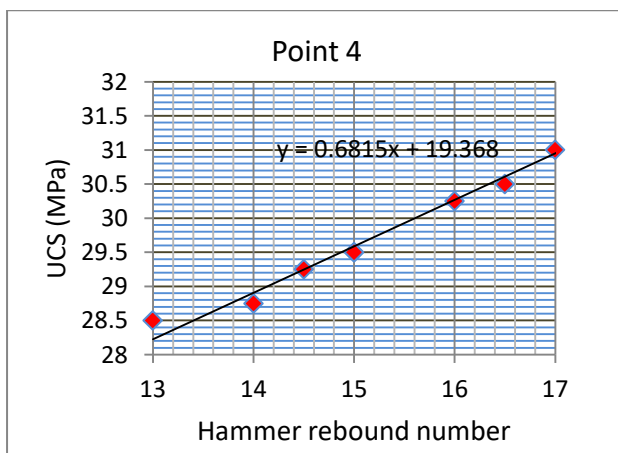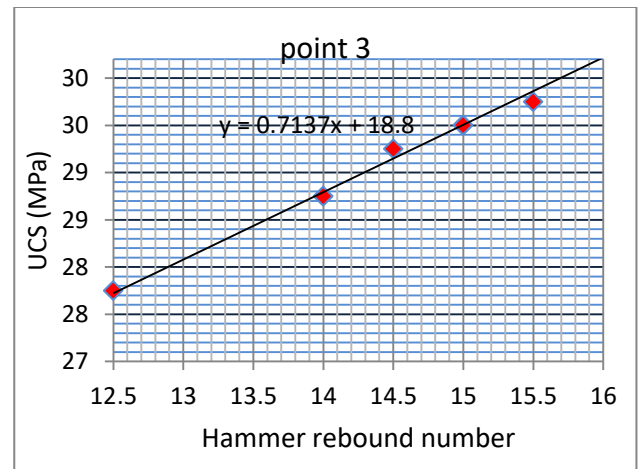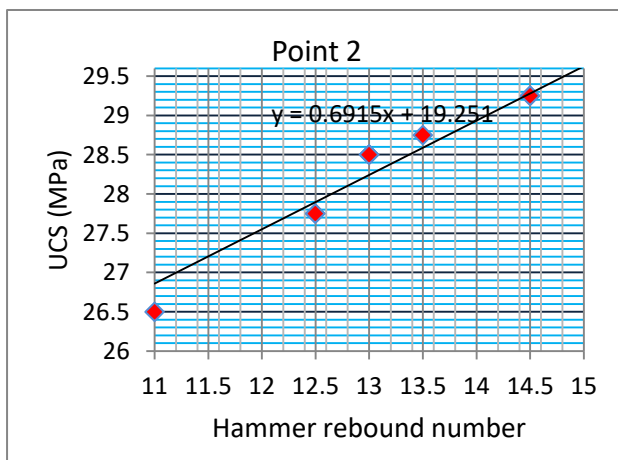
Figure 43. Curves of unconfined compressive strength of weathered rock slope failure

The unconfined compressive strength of weathered rock near the failure point is smaller than the values obtained far from the failure points. It has also been observed in the field that water flows through the thin permeable zones (joints) more through the failed weathered rock-soil slope zone than through the unfailed weathered rock-soil slope zone, producing pore-water pressures and seepage forces during rainstorms and decreasing the shear strength of materials. Using Rocscience software (Slide), and general Hoek Brown of strength type, characterization of rock mass properties, and the geological strength index (GSI) value of all four points were described as follows and its slope stability analysis by the limit equilibrium method was determined.

Table 21. Geological strength index (GSI) value of rock mass of selected points
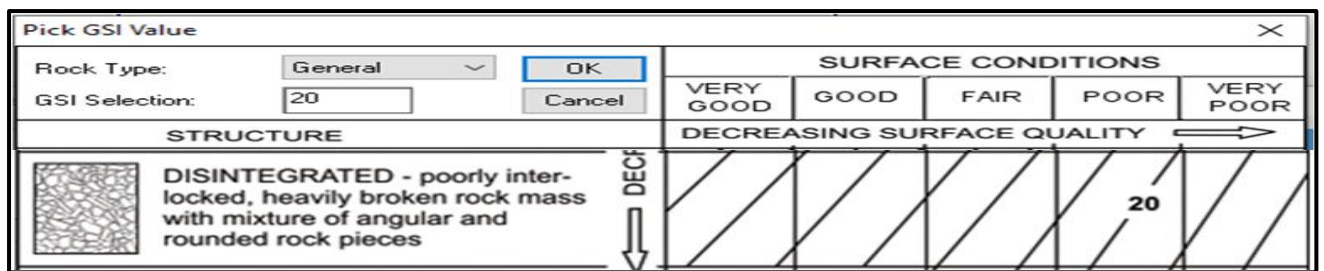
point	Structure	Geological strength index (GSI) value.	Intact rock constant (mi)	UCS(intact) In KN/m^2	Unit weight In KN/m^3
2	Disintegrated-poorly interlocked, heavily broken rock mass with mixture of angular and rounded rock pieces	20	10	28562.5	21
3	Disintegrated-poorly interlocked, heavily broken rock mass with mixture of angular and rounded rock pieces	20	10	29437.5	22
4	Disintegrated-poorly interlocked, heavily broken rock mass with mixture of angular and rounded rock pieces	20	10	29562.5	22
5	Disintegrated-poorly interlocked, heavily broken rock mass with mixture of angular and rounded rock pieces	20	10	27812.5	21

The General Hoek Brown technique, which is a commonly used method of rock mass slope stability analysis, was used with Rocscience software (Slide) for the 2D limit equilibrium method of rock slope stability analysis for points 2,3,4 and 5. Even though a very thin layer of soil was found, it was assumed to be a homogeneous weathered rock mass at full depth for this work, and the usual practices of Bishop simplified, Janbu simplified, and Ordinary/Fellenius were used as factor of safety determination methods.
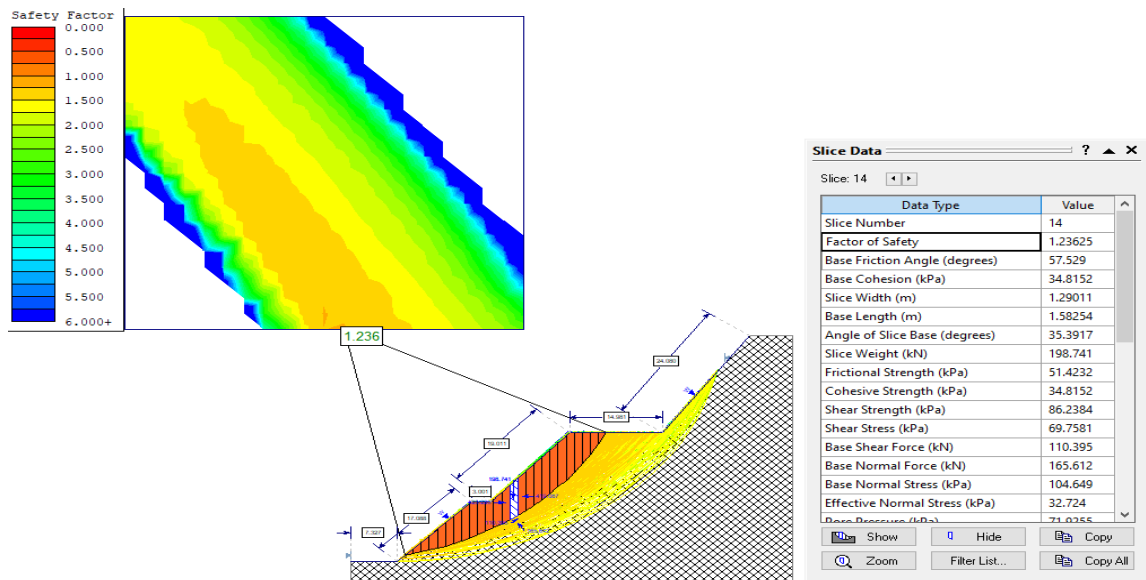
A. Bishop simplified method of limit equilibrium analysis for point 2
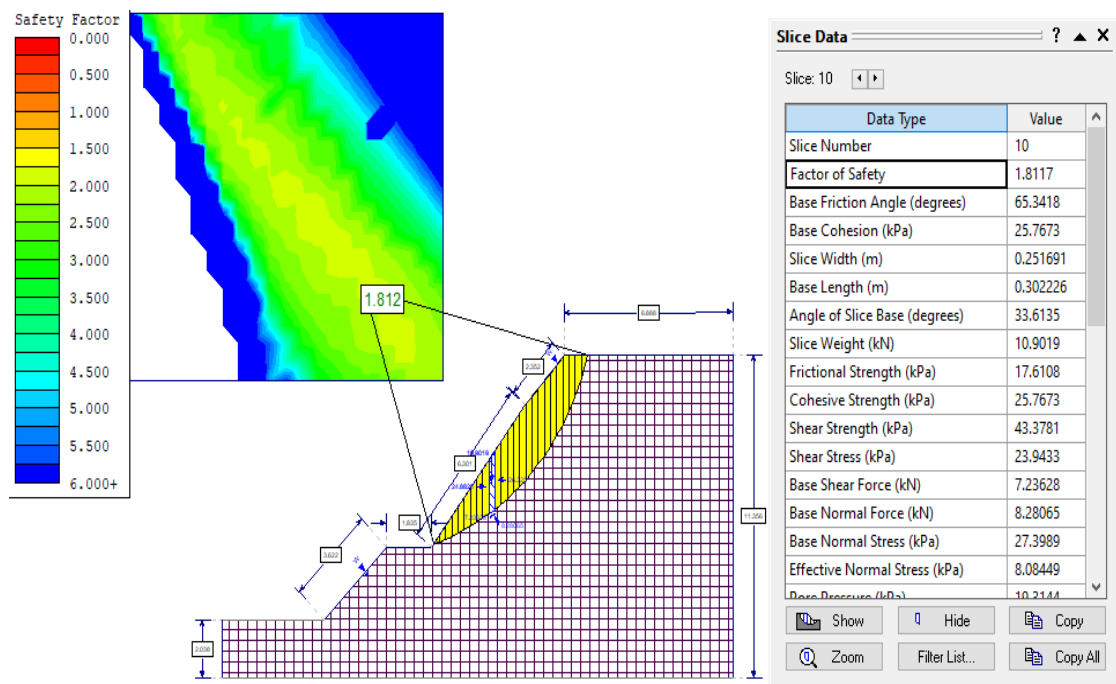
B. Bishop simplified method of limit equilibrium analysis for point 3
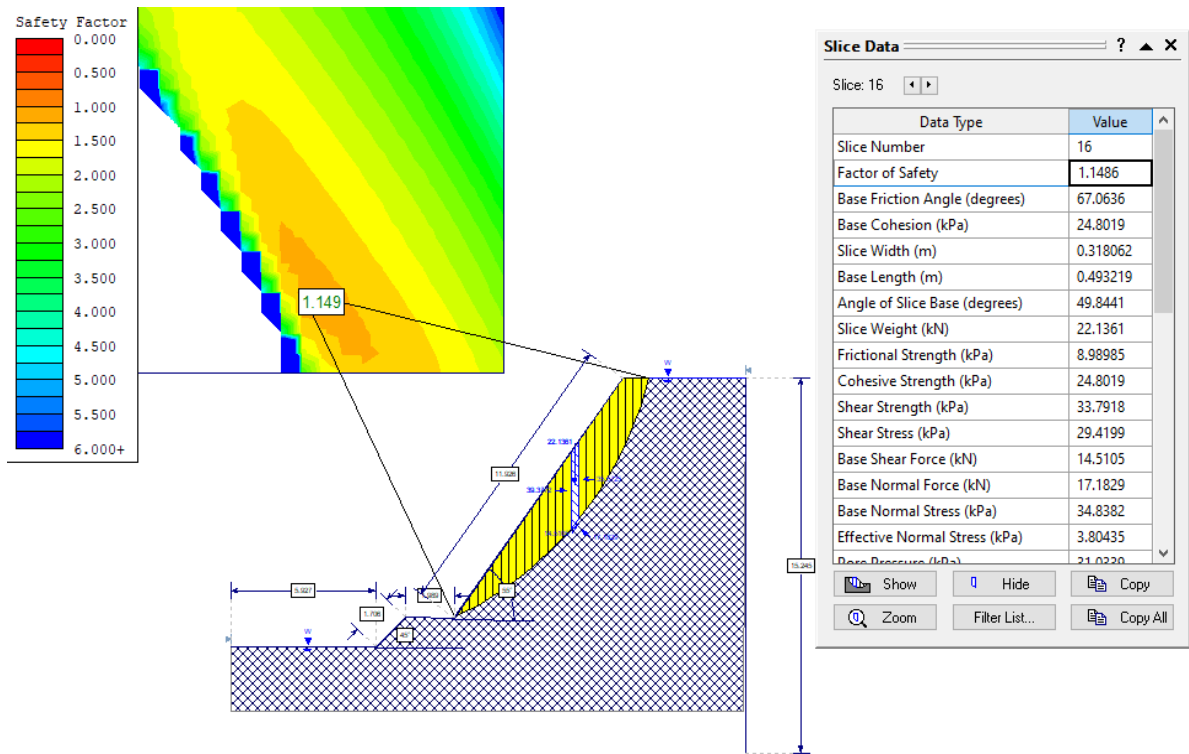
C. Bishop simplified method of limit equilibrium analysis for point 4
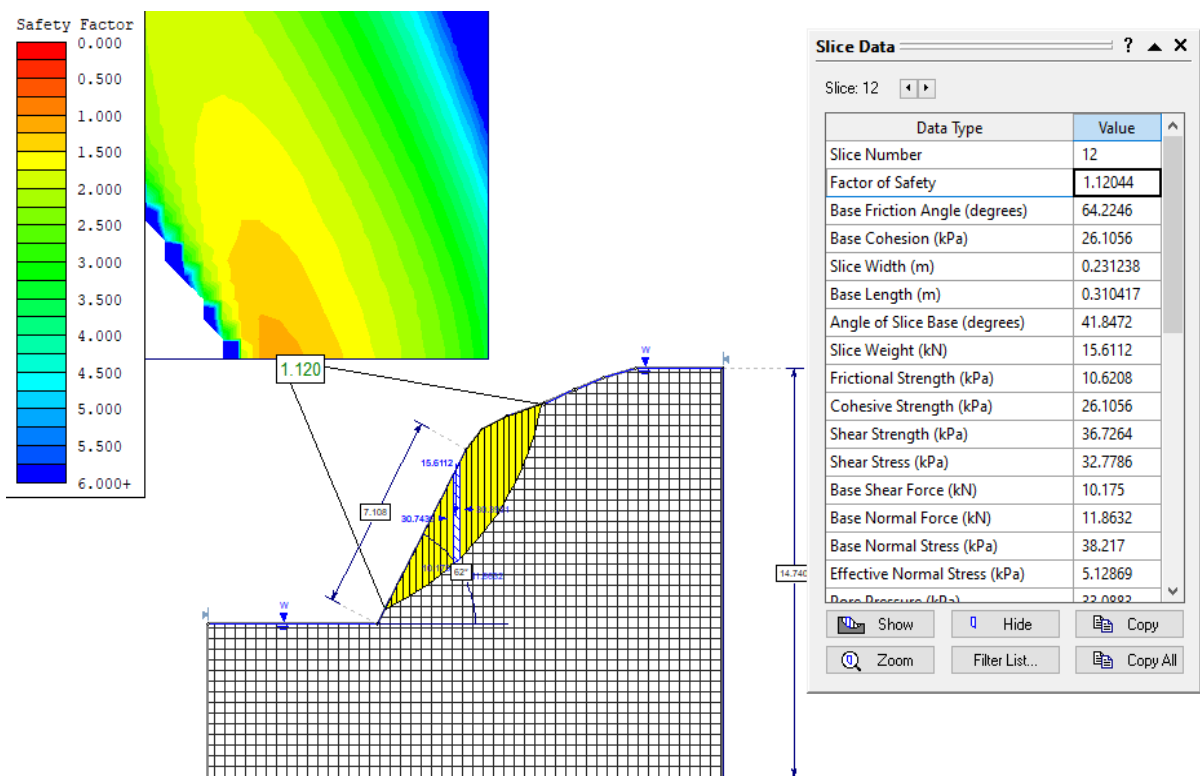
D. Bishop simplified method of limit equilibrium analysis for point 5

Figure 44. Limit equilibrium method analysis of weathered rock slope along road

Table 22. Factor of safety (FS) based on the methods

Failure points	Factor of safety(FS) based on the methods		
	Bishop simplified	Janbu simplified	Ordinary/Fellenius
Point 2	1.236	1.093	1.473
Point 3	1.812	1.488	2.397
Point 4	1.149	0.892	1.985
Point 5	1.120	0.926	1.898
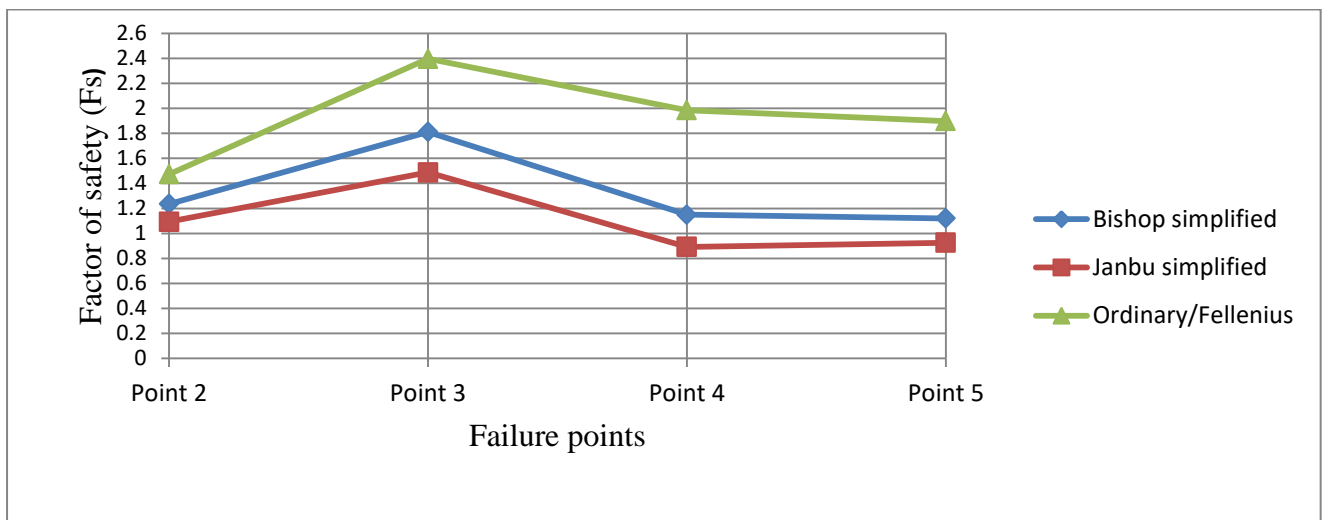
Figure 45. Curve of Factor of safety(FS) based on three methods

The result shows 80% is unstable slope by Bishop's and Janbu's simplified (factor of safety less than 1.5). Therefore, based on this result as evidence, it can be generalized that from landslide hazard zone map developed, more than 80% of very hazard zone to landslide subclass is unstable area. Therefore, all weathered rock-soil slope failure points along road corridor and all this subclass in entire study area need follow up and special treatment, such as by constructing retaining walls, gabions, grouting, planting, etc. In addition to slope treatment, awareness should be given for all societies who are living in this risky area.

During the research, it was assessed that there are approximately 1,432 households in the entire study area. Using overlay analysis of these households over the whole area map, it was discovered that 588 households live in the free from landslide zone, 555 households live in the susceptibility to landslide zone, 228 households live in the low landslide zone, and 61 households live in the extremely high

danger to landslide zone. Sample photos are taken from the study area which shows resident those are in high hazard to landslide area.

Figure 46. Sample photos that show risked residents in the hazard area.

According to information collected from societies in the study region, landslides have killed people and animals, as well as damaging houses, crops, and utilities including roads and power lines. Because of all of these reasons, any zone may be dangerous for future habitation or development. According to the study's results, the main causes of landslides in the current research area are linked to hydrology, geometry and gravity movement favored by the area's usual geological and geomorphological conditions. The landslides in the region were caused entirely by heavy rainfall during summer season.

As a result, urgent mitigation steps are expected in susceptible-hazard zone areas, or such zones must be avoided for human settlement or other planned construction projects unless land erosion management and landslide protection mechanisms are absolutely necessary.

Therefore, this area requires a detailed investigation to evaluate the causes, types and failure mechanisms of landslides and to prepare the landslide susceptibility maps. Therefore the following hazard zone map with current social settlement is developed.
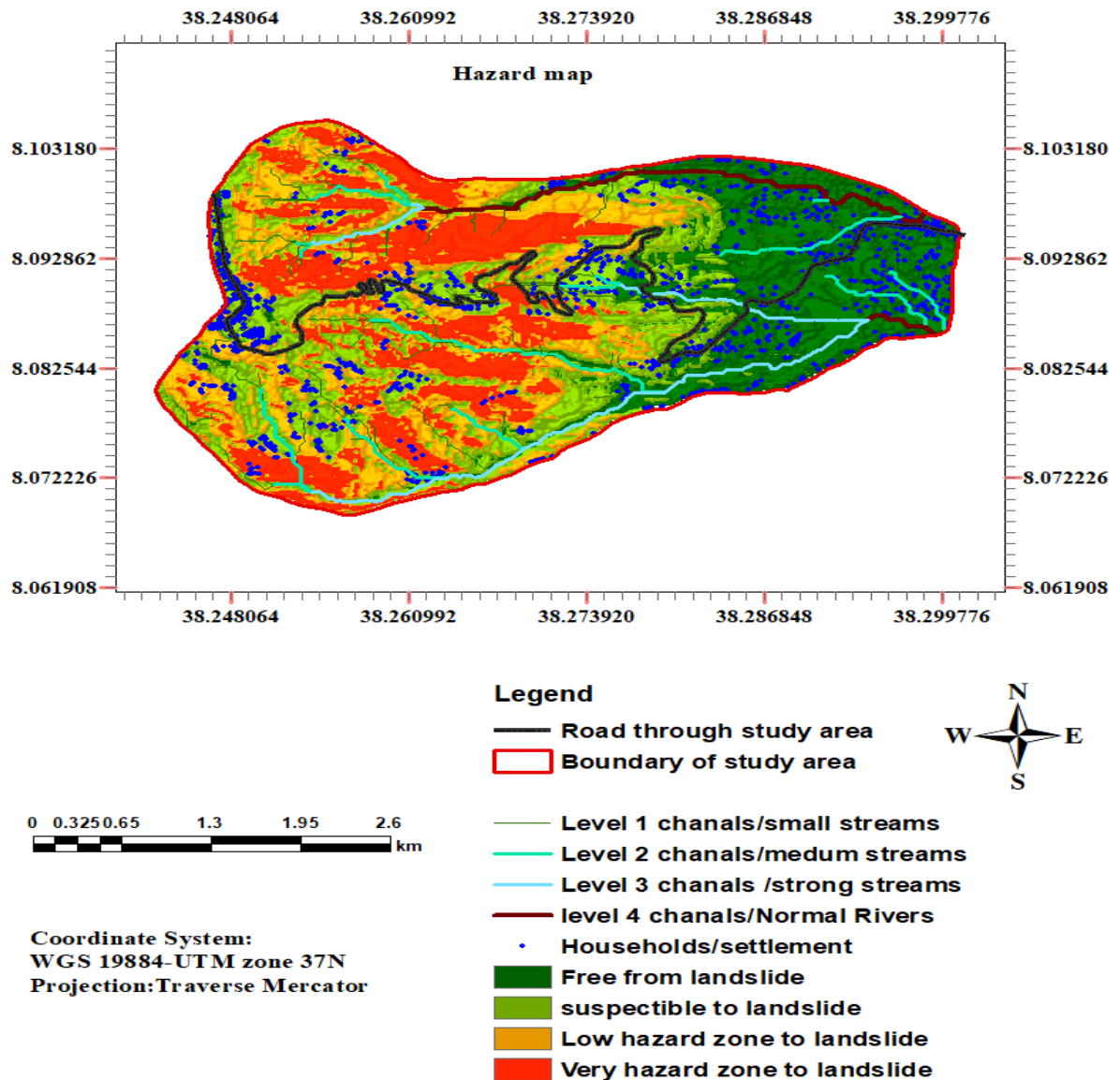
Figure 47. Maps of settlement of households distribution in landslide hazard zone classes

4.4 Validation of landslide hazard zone map

Few scholars argue for another different validation approach that compares current landslides to the landslide susceptibility map and applies the success-rate curve of the area under the curve (AUC) to qualitatively assess forecast accuracy. The success rate curve depicts how well the model and factors accurately forecast landslides. The number of landslides classified into each susceptibility class was obtained by an overlay analysis of landslides with the best landslide susceptibility map. If the number of landslides in the high and very high susceptibility classes is significant, the landslide susceptibility map can be trusted to predict future landslides. The success-rate curves were used to

calculate the forecast accuracy that was utilized to choose the best susceptibility map (37, 38). In this study, for all the past six years, an average total of 26707 removed/eroded pixels was calculated. From this 26707, 80% (21366 pixels) were used as training and (20%) as validation landslide. To validate the landslide hazard zone map, zonal overlay statistical analysis was applied. The success and predictive rate curves can be created for the FR model. The success rate curve is based on the comparison between the predictive model and the training landslide. The predictive rate curve is based on the comparison between the predicted map and the validation landslide. The developed curve shows a success rate of 89.58% and a predictive rate of 82.69% (Fig 49). In addition to this, a Google Earth image and a field visit (reconnaissance) were also used to confirm the final production of the landslide danger zone map. For example, all the six slope failure points along the road corridor shown in figure 38 in the study area are the best evidence for validation. As a result, approximately all of the previous landslide locations were in strong agreement with the landslide hazard zone map.

Table 23. Landslide susceptibility class and training landslide pixels of the FR model

No	Landslide susceptibility map classes	Map pixel number	Percentage of Map pixel number	80% of training landslide pixel (average for all six years)	20% of landslide pixel for validation	Percentage of training landslide	Cumulative of FR Success rate (A UC=89.58%)	Predicted percentage	Cumulative of FR Predicted rate (AUC=82.69%)
		0	0	0	0	0	0	0	0
1	Free from landslide zone	20276	27	2350	2718	11	45.65	18	36.49
2	Susceptible to landslide zone	21451	29	3632	4036	17	76.94	26	62.53
3	Low to landslide zone	17350	23	7264	4209	34	89.58	27	82.69
4	Hazard to landslide zone	15975	21	8119	4521	38	100	29	100
	Total	75052	100	21366	15484	100		100	
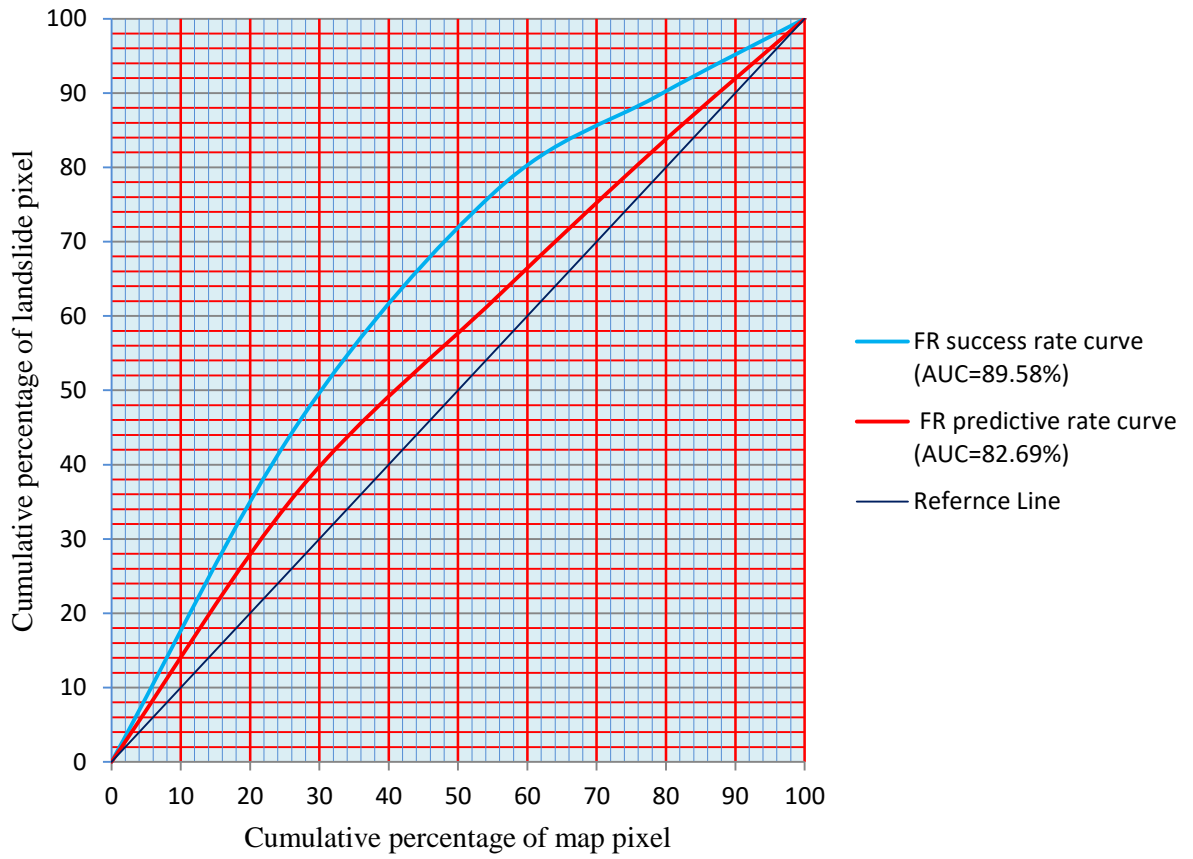
Figure 48. Success and Predictive rate curves of FR

Conclusion

Landslides are one of the world's most common natural problems, especially in mountainous terrain, where they have resulted in substantial injury and loss of life, as well as property and infrastructure damage. Ethiopia is one of the experienced countries in which rainfall-induced landslides of various forms and sizes often occur on hilly and mountainous terrains. As a result, if an appropriate landslide hazard map (LSM) is produced for the region, these landslide concerns may be handled.

The current research was carried out in the Gurage zone along the Zabidar mountain road corridor. According to the study's results, the main triggering factors of landslides in the current research area are linked to hydrology, geometry, human activity, geological and geomorphological conditions and gravitational force. The primary goal of this research was to assess landslide risk and create a landslide hazard zonation map for the study area by GIS. The aim of this analysis was to determine the relationship between different causative factors and past landslides, as well as their possible contribution to future landslides in the area. Lithology, elevation, slope, aspect, Plan curvature, and distance to streams were all considered as causative factors in this study. The spatial relationship between causative factors and landslide frequency was derived using the probability approach as part of the methodology used. In this analysis, the governing parameters were rated using a GIS-based statistical and frequency ratio approach, and the landslide hazard map was created using a customized raster calculation. The map created showed that 27 percent (4.8 km2) of the study area is no landslide or free from landslide, 29 percent (5.2 km2) shows susceptible to landslide zone, 23 percent (4.1 km2) low-risk landslide zone and 21 percent (3.8 km2) of the area is in a high-risk landslide zone. To know the accuracy of GIS result, laboratory tests such as sieve analysis, angle of repose and direct shear tests for determination of shear strength parameters were conducted for geotechnical characterization of some selected points. Rocscience(slide) software was used for numerical analysis of rock-soil slope stability along the road corridor by the limit equilibrium method. General Hoek Brown method as Strength type of the rock mass and Bishop's simplified, Janbu's simplified and Ordinary/Fellenius method for determination of factor of safety were applied. Out of five selected points for slope stability analysis, 80% is unstable slope by Bishop's simplified and Janbu's simplified method (factor of safety less than 1.5). Therefore we are confident to conclude that working with GIS software for landslide assessment /slope failure analysis can safe times, resources, labor forces, cover wide area and provide accurate results.

The landslide hazard assessment showed in free landslide zone 588, in susceptible to landslide zone 555, in a low-risk landslide zone 228 and in a high-risk landslide zone 61 households are living.

Recommendation

- Only a few causative variables were included in this study: lithology, elevation, slope, aspect, plan curvature, and distance to nearby streams. To obtain more practical outcomes, additional landslide causative factors such as land use/land cover, distance to faults, and other prone factors should be considered.

- Evaluation of the impact and speed of rock/soil weathering is needed.

- Only a small number of samples and tests were taken along the road for this study. But extensive tests through entire study area for geotechnical characterization and for advanced constitutive models of rock-soil slope stability analysis is recommended.

- In addition to 2D limit equilibrium method of slope stability analysis, 3D finite element method (FEM) of slope stability or entire area analysis is highly recommended.

- During the rainy season, vulnerable residents should be given priority in order to save their lives and property, based on the landslide danger zones (very hazard, low hazard, susceptible, and free from hazard zones).

- Landslides found in the research region ranges from no movement types (creep) to travel a great distance downslope, causing damage to inhabitants' lives, homes, properties, and utilities. As a result, diverting debris paths away from residential areas, afforestation, rather than deforestation, is strongly encouraged.

- Landslide detector like Slope inclinometers/slope indicators, Real time monitoring etc. should be installed.

- Along road corridor such as additional retaining wall, gabions, grouting and other rock-soil slope failure mitigation initiatives is essential to safe infrastructure from damage.

- Additional study should be done, specially on the effect of fresh rock weathering on the stability of cut or fill slopes along road corridors.

- This method of landslide hazard zone mapping should be widely applied in all susceptible landslide areas.

References

1. Lynn M. Highland, United States Geological Survey, and Peter Bobrowsky, Geological Survey of Canada. Lynn M. Highland, United States Geological Survey, and Peter Bobrowsky, Geological Survey of Canada .

2. Dai F, Lee CF. Landslides on Natural Terrain. Mred. 2002 Feb;22(1):40–7.

3. Woldearegay K. Review of the occurrences and influencing factors of landslides in the highlands of Ethiopia: With implications for infrastructural development. Momona Ethiopian Journal of Science. 2013 .

4. Landslide Modeling and Susceptibility Mapping of Giri River Watershed, Himachal Pradesh (India) | Semantic Scholar.

5. Wubalem A, Meten M. Landslide susceptibility mapping using information value and logistic regression models in Goncha Siso Eneses area, northwestern Ethiopia. SN Appl Sci. 2020 .

6. Spatial mapping of landslides by using arcgis and google earth: a case study of chure region in kanchanpur district, far-western nepal. 2013.

7. Hong H, Xu C, Bui DT. Landslide Susceptibility Assessment at the Xiushui Area (China) Using Frequency Ratio Model. Procedia Earth and Planetary Science. 2015.

8. Section1.pdf [Internet]. [cited 2021 May 8].

9. Woldearegay K, Schubert W, Klima K, Mogessie A. Landslide hazards mitigation strategies in the northern highlands of Ethiopia. Landslide Risk Management. 2005;25–37.

10. Zhou S, Chen G, Fang L, Nie Y. GIS-Based Integration of Subjective and Objective Weighting Methods for Regional Landslides Susceptibility Mapping. Sustainability. 2016 .

11. Yalcin A, Reis S, Aydinoglu AC, Yomralioglu T. A GIS-based comparative study of frequency ratio, analytical hierarchy process, bivariate statistics and logistics regression methods for landslide susceptibility mapping in Trabzon, NE Turkey. CATENA. 2011 Jun;85(3):274–87.

12. Landslide Susceptibility Assessment Using Frequency Ratio Technique with Iterative Random Sampling [Internet]. [cited 2020 Jun 27].

13. Oh H-J, Lee S, Hong S-M. Landslide Susceptibility Assessment Using Frequency Ratio Technique with Iterative Random Sampling. Journal of Sensors. 2017 Sep 6;2017:.

14. Van Westen CJ, Rengers N, Terlien MTJ, Soeters R. Prediction of the occurrence of slope instability phenomenal through GIS-based hazard zonation. Geol Rundsch.

15. Hungr O, Leroueil S, Picarelli L. The Varnes classification of landslide types, an update. Landslides. 2014 Apr 1.

16. U.S. Department of the Interior U.S. Geological Survey [Internet]. [cited 2021 May 7].

17. Types of Slope Failures [Internet]. The Constructor. 2018 [cited 2020 Jun 27].

18. Niroumand H, Kassim KA, Ghafooripour A, Nazir R, Far SYZ. Investigation of Slope Failures in Soil Mechanics. 17:18.

19. Sumudu Senanayake 1 , Biswajeet Pradhan 1,2,* , Alfredo Huete 1 and Jane Brennan 1 - Google Search [Internet]. [cited 2020 Jun 19].

20. U.S. Department of the Interior U.S. Geological Survey [Internet]. [cited 2021 May 8].

21. Basu A, Aydin A. A method for normalization of Schmidt hammer rebound values. International Journal of Rock Mechanics and Mining Sciences

22. Dongping D, Liang L, Wang J, Zhao L. Limit equilibrium method for rock slope stability analysis by using the Generalized Hoek–Brown criterion. International Journal of Rock Mechanics and Mining Sciences. 2016 Nov 30;89.

23. Varnes, 1978; WGS, 2017 - Google Search [Internet]. [cited 2020 Jun 23].

24. Woldearegay K. Review of the occurrences and influencing factors of landslides in the highlands of Ethiopia: With implications for infrastructural development. Momona Ethiopian Journal of Science. 2013 Feb 11;5:3.

25. Lee S, Min K. Statistical analysis of landslide susceptibility at Yongin, Korea. Env Geol. 2001 Aug 1;40(9):1095–113.

26. Kanungo DP, Arora MK, Sarkar S, Gupta RP. Landslide Susceptibility Zonation (LSZ) Mapping - A Review. :27.

27. Khan H, Shafique M, Khan MA, Bacha MA, Shah SU, Calligaris C. Landslide susceptibility assessment using Frequency Ratio, a case study of northern Pakistan. The Egyptian Journal of Remote Sensing and Space Science. 2019 Apr 1.

28. Heidari A, Roozitalab MH, Mermut AR. Diversity of clay minerals in the vertisols of three different climatic regions in western Iran. Journal of Agricultural Science and Technology. 2008 Jan 1.

29. 11259033_02.pdf [Internet]. [cited 2021 May 3].

30. Mersha T, Meten M. GIS-based landslide susceptibility mapping and assessment using bivariate statistical methods in Simada area, northwestern Ethiopia. Geoenviron Disasters. 2020 Dec.

31. Sivakami C. Landslide Susceptibility Zone using Frequency Ratio Model, Remote Sensing &GIS –A Case Study of Western Ghats, India (Part of Kodaikanal Taluk). 2014;9.

32. Lee S, Ab Talib J. Probabilistic landslide susceptibility and factor effect analysis. Environmental Geology. 2005 May 1.

33. Oh H-J, Lee S, Hong S-M. Landslide Susceptibility Assessment Using Frequency Ratio Technique with Iterative Random Sampling [Internet]. Vol. 2017, Journal of Sensors. Hindawi; 2017 [cited 2020 Jun 27].

34. Zhou S, Chen G, Fang L, Nie Y. GIS-based integration of subjective and objective weighting methods for regional landslides susceptibility mapping. Sustainability (Switzerland). 2016 Jan.

35. Effect of Landslide Factor Combinations on the Prediction Accuracy of Landslide Susceptibility Maps in the Blue Nile Gorge of Central Ethiopia | springerlink [Internet]. [cited 2020 Jun 18].

36. Hamza T. GIS based landslide hazard evaluation and zonation – A case from Jeldu District, Central Ethiopia. Journal of King Saud University - Science. 2017 Apr;29(2).

APPENDICES

Table 1A. Frequency ratio of eroded/removed surface on each causative factors for year 2015

No.	Causative factors	subclasses	Class pixels	% ge class pixels (a)	eroded/lossed pixels	%ge of erode/lossed pixels(b)	Frequency (FR) =b/a
		Year 2015					
1	Lithology	a. Pelitic vertisols	66605	88.7	22467	87.2	1.0
		b. Stone surface	8378	11.2	3308	12.8	1.1
		c. Chromic luvisols	70	0.1	3	0.0	0.1
		Total	75053	100.0	25778	100.0	2.3
2	Elevation (m)	2221-2450	18087	24.1	5583	21.7	0.9
		2450-2670	12521	16.7	4474	17.4	1.0
		2670-2900	12884	17.2	4334	16.8	1.0
		2900-3100	14482	19.3	5028	19.5	1.0
		3100-3370	17078	22.8	6356	24.7	1.1
		Total	75052	100.0	25775	100.0	5.0
3	Slope (percent)	0-5%	6478	8.6	2066	8.0	0.9
		5-25%	38546	51.4	13354	51.8	1.0
		25-50%	27050	36.0	9242	35.9	1.0
		50-100°%	2976	4.0	1114	4.3	1.1
		Total	75050	100.0	25776	100.0	4.0
4	Aspect	FLAT	5604	7.5	2323	9.0	1.2
		N	12314	16.4	3294	12.8	0.8
		NE	18085	24.1	4193	16.3	0.7
		E	22287	29.7	7396	28.7	1.0
		SE	10714	14.3	5125	19.9	1.4
		S	1581	2.1	1142	4.4	2.1
		SW	740	1.0	474	1.8	1.9
		W	793	1.1	385	1.5	1.4
		NW	2935	3.9	1444	5.6	1.4
		Total	75053	100.0	25776	100.0	11.8
5	Plan Curvature	a. Concave (<-0.05)	37599	50.1	13116	50.9	1.0

		b. Flat (-0.05-0.05)	64	0.1	3	0.0	0.1
		c. Convex (>0.05)	37393	49.8	12657	49.1	1.0
		Total	75056	100.0	25776	100.0	2.1
6	Distance from river(M)	a. 0-5	23722	31.6	7001.4	27.2	0.9
		b.5-10	18303	24.4	5936.4	23.0	0.9
		c.10-15	14572	19.4	6072.4	23.6	1.2
		d.15-20	10014	13.3	3739.4	14.5	1.1
		e.20-35	8439	11.2	3026.4	11.7	1.0
		Total	75050	100.0	25776	100.0	5.1

Table 1B. Frequency ratio of eroded/removed surface on each causative factors for year 2016

No.	Causative factors	Subclasses	Class pixels	%ge class pixels (a)	eroded/lossed pixels	%ge of erode/lossed pixels(b)	Frequency (FR) =b/a
				Year 2016			
1	Lithology	a. Pelitic vertisols	66605	88.7	13662	88.3	1.0
		b. Stone surface	8378	11.2	1802	11.6	1.0
		c. Chromic luvisols	70	0.1	16	0.1	1.1
		Total	75053	100.0	15480	100.0	3.1
2	Elevation (m)	2221-2450	18087	24.1	2823	18.2	0.8
		2450-2670	12521	16.7	2086	13.5	0.8
		2670-2900	12884	17.2	2677	17.3	1.0
		2900-3100	14482	19.3	3807	24.6	1.3

		3100-3370	17078	22.8	4090	26.4	1.2
		Total	75052	100.0	15483	100.0	5.0
3	Slope (percent)	0-5%	6620	8.8	949	6.1	0.7
		5-25%	38761	51.6	8097	52.3	1.0
		25-50%	26972	35.9	5884	38.0	1.1
		50-100%	2702	3.6	553	3.6	1.0
		Total	75055	100.0	15483	100.0	3.8
4	Aspect	FLAT	5649	7.5	762	4.9	0.7
		N	12319	16.4	2651	17.1	1.0
		NE	18085	24.1	3515	22.7	0.9
		E	22210	29.6	4774	30.8	1.0
		SE	10852	14.5	2718	17.6	1.2
		S	1560	2.1	411	2.7	1.3
		SW	702	0.9	156	1.0	1.1
		W	750	1.0	108	0.7	0.7
		NW	2926	3.9	389	2.5	0.6
		Total	75053	100.0	15484	100.0	8.6
5	Plan Curvature	a. Concave (<-0.05)	37802	50.4	7636	49.3	1.0

No.	Causative factors	subclasses	Class pixels	%ge class pixels (a)	eroded/lossed pixels	%ge of erode/lossed pixels(b)	Frequency (FR) =b/a
		b. Flat (-0.05-0.05)	6	0.0	2	0.0	1.6
		c. Convex (>0.05)	37246	49.6	7846	50.7	1.0
		Total	75054	100.0	15484	100.0	3.6
6	Distance from river(M)	a. 0-5	23724	31.6	5884	38.0	1.2
		b.5-10	18303	24.4	4501	29.1	1.2
		c.10-15	14574	19.4	3391	21.9	1.1
		d.15-20	10013	13.3	1112	7.2	0.5
		e.20-35	8439	11.2	594	3.8	0.3
		Total	75053	100.0	15482	100.0	4.4

Table 1C. Frequency ratio of eroded/removed surface on each causative factors for year 2017

No.	Causative factors	subclasses	Class pixels	% ge class pixels (a)	eroded/lossed pixels	%ge of erode/lossed pixels(b)	Frequency (FR) =b/a
				Year 2017			
1	Lithology	a. Pelitic vertisols	66605	88.7	18322	86.6	1.0
		b. Stone surface	8378	11.2	2837	13.4	1.2
		c. Chromic luvisols	70	0.1	2	0.0	0.1
		Total	75053	100.0	21161	100.0	2.3

		2221-2450	18087	24.1	3357	15.9	0.7
		2450-2670	12521	16.7	3265	15.4	0.9
2	Elevation (m)	2670-2900	12884	17.2	3847	18.2	1.1
		2900-3100	14482	19.3	4722	22.3	1.2
		3100-3370	17078	22.8	5972	28.2	1.2
		Total	75052	100.0	21163	100.0	5.0
3	Slope (percent)	0-5%	5052	6.7	1189	5.6	0.8
		5-25%	32715	43.6	8475	40.0	0.9
		25-50%	30153	40.2	9006	42.6	1.1
		50-100%	7133	9.5	2494	11.8	1.2
		Total	75053	100.0	21164	100.0	4.1
4	Aspect	FLAT	5593	7.5	2927	13.8	1.9
		N	12302	16.4	3899	18.4	1.1
		NE	18290	24.4	2711	12.8	0.5
		E	22252	29.6	3901	18.4	0.6
		SE	10662	14.2	3870	18.3	1.3
		S	1570	2.1	897	4.2	2.0

		SW	742	1.0	615	2.9	2.9
		W	701	0.9	491	2.3	2.5
		NW	2939	3.9	1854	8.8	2.2
		Total	75051	100.0	21165	100.0	15.1
5	Plan Curvature	a. Concave	37570	50.1	10231	48.3	1.0
		b. Flat	17	0.0	4	0.0	0.8
		c. Convex	37466	49.9	10933	51.6	1.0
		Total	75053	100.0	21168	100.0	2.8
6	Distance from river(M)	a. 0-5	23724	31.6	5082	24.0	0.8
		b.5-10	18302	24.4	5142	24.3	1.0
		c.10-15	14574	19.4	4253	20.1	1.0
		d.15-20	10012	13.3	3269	15.4	1.2
		E.20-35	8439	11.2	3420	16.2	1.4
		Total	75051	100.0	21166	100.0	8.2

Table 1D. Frequency ratio of eroded/removed surface on each causative factors for year 2018

No.	Causative factors	Subclasses	Class pixels	% ge class pixels (a)	eroded/lossed pixels	%ge of erode/lossed pixels(b)	Frequency (FR) =b/a
					Year 2018		
1	Lithology	a. Pelitic vertisols	66605	88.7	32768	87.0	1.0
		b. Stone surface	8378	11.2	4855	12.9	1.2
		c. Chromic luvisols	70	0.1	21	0.1	0.6
		Total	75053	100.0	37644	100.0	2.7
2	Elevation (m)	2221-2450	18087	24.1	6012	16.0	0.7
		2450-2670	12521	16.7	6222	16.5	1.0
		2670-2900	12884	17.2	7226	19.2	1.1
		2900-3100	14482	19.3	7847	20.8	1.1
		3100-3370	17079	22.8	10342	27.5	1.2
		Total	75053	100.0	37649	100.0	5.1
3	Slope (percent)	0-5%	5361	7.1	1916	5.1	0.7
		5-25%	34124	45.5	15954	42.4	0.9
		25-50%	29313	39.1	16410	43.6	1.1
		50-100%	6254	8.3	3367	8.9	1.1
		Total	75052	100.0	37647	100.0	3.8
4	Aspect	FLAT	5547	7.4	3424	9.1	1.2
		N	12254	16.3	6806	18.1	1.1
		NE	18298	24.4	8818	23.4	1.0
		E	22200	29.6	10079	26.8	0.9
		SE	10691	14.2	5036	13.4	0.9
		S	1630	2.2	818	2.2	1.0
		SW	719	1.0	358	1.0	1.0
		W	743	1.0	459	1.2	1.2
		NW	2972	4.0	1850	4.9	1.2
		Total	75054	100.0	37648	100.0	9.6
5	Plan Curvature	a. Concave (<-0.05)	37488	49.9	17910	47.6	1.0
		b. Flat (-0.05-0.05)	5	0.0	2	0.0	0.8
		c. Convex (>0.05)	37559	50.0	19736	52.4	1.0

		Total	75052	100.0	37648	100.0	2.8
6	Distance from river(M)	a. 0-5	23724	31.6	12179	32.4	1.0
		b.5-10	18303	24.4	9519	25.3	1.0
		c.10-15	14574	19.4	7182	19.1	1.0
		d.15-20	10014	13.3	4710	12.5	0.9
		e.20-35	8439	11.2	4057	10.8	1.0
		Total	75054	100.0	37647	100.0	4.9

Table 1E. Frequency ratio of eroded/removed surface on each causative factors for year 2019

No.	Causative factors	Subclasses	Year 2019				
			Class pixels	% ge class pixels (a)	eroded/lossed pixels	%ge of erode/lossed pixels(b)	Frequency (FR) =b/a
1	Lithology	a. Pelitic vertisols	66605	88.7	35281	87.6	1.0
		b. Stone surface	8378	11.2	4982	12.4	1.1
		c. Chromic luvisols	70	0.1	30	0.1	0.8
		Total	75053	100.0	40293	100.0	2.9
2	Elevation (m)	2221-2450	18087	24.1	7404	18.4	0.8
		2450-2670	12521	16.7	6540	16.2	1.0
		2670-2900	12884	17.2	7530	18.7	1.1
		2900-3100	14482	19.3	8237	20.4	1.1
		3100-3370	17078	22.8	10582	26.3	1.2
		Total	75052	100.0	40293	100.0	5.0
3	Slope (degree)	0-5°	6507	8.7	2831	7.0	0.8
		5-25°	38667	51.5	20124	49.9	1.0
		25-50°	26705	35.6	15509	38.5	1.1
		50-90°	3174	4.2	1828	4.5	1.1
		Total	75053	100.0	40292	100.0	3.9
4	Aspect	FLAT	5399	7.2	3274	8.1	1.1
		N	12336	16.4	7146	17.7	1.1
		NE	18158	24.2	9513	23.6	1.0

		Subclass	Class pixels	%	Eroded	%	FR
		E	22183	29.6	11170	27.7	0.9
		SE	10741	14.3	5416	13.4	0.9
		S	1622	2.2	873	2.2	1.0
		SW	758	1.0	380	0.9	0.9
		W	795	1.1	499	1.2	1.2
		NW	3062	4.1	2021	5.0	1.2
		Total	75054	100.0	40292	100.0	9.4
5	Plan Curvature	a. Concave (<-0.05)	37455	49.9	19296	47.9	1.0
		b. Flat (-0.05-0.05)	13	0.0	3	0.0	0.4
		c. Convex (>0.05)	37584	50.1	20993	52.1	1.0
		Total	75052	100.0	40292	100.0	2.4
6	Distance from river(M)	a. 0-5	23724	31.6	10785	26.8	0.8
		b.5-10	18302	24.4	9995	24.8	1.0
		c.10-15	14573	19.4	6976	17.3	0.9
		d.15-20	10015	13.3	5886	14.6	1.1
		e.20-35	8441	11.2	6653	16.5	1.5
		Total	75055	100.0	40295	100.0	10.2

Table 1F. Frequency ratio of eroded/removed surface on each causative factors for year 2020

			Year 2020					
	Causative factors	Subclasses	Class pixels	% ge class pixels (a)	eroded/loss ed pixels	%ge of erode/losse d pixels(b)	Frequency (FR) =b/a
1	Lithology	a. Pelitic vertisols	66605	88.7	18109	91.1	1.0
		b. Stone surface	8378	11.2	1756	8.8	0.8
		c. Chromic luvisols	70	0.1	9	0.0	0.5
		Total	75053	100.0	19874	100.0	2.3
2	Elevation (m)	2221-2450	18087	24.1	2437	12.3	0.5
		2450-2670	12521	16.7	3172	16.0	1.0
		2670-2900	12884	17.2	4067	20.5	1.2
		2900-3100	14482	19.3	4646	23.4	1.2
		3100-3370	17078	22.8	5554	27.9	1.2
		Total	75052	100.0	19876	100.0	5.1

3	Slope (percent)	0-5%	6507	8.7	715	3.6	0.4
		5-25%	38667	51.5	9076	45.7	0.9
		25-50%	26705	35.6	8943	45.0	1.3
		50-100%	3172	4.2	1142	5.7	1.4
		Total	75051	100.0	19876	100.0	3.9
4	Aspect	FLAT	5664	7.5	3377	17.0	2.3
		N	12321	16.4	5211	26.2	1.6
		NE	18075	24.1	4164	21.0	0.9
		E	22349	29.8	3310	16.7	0.6
		SE	10676	14.2	996	5.0	0.4
		S	1614	2.2	321	1.6	0.8
		SW	698	0.9	184	0.9	1.0
		W	778	1.0	429	2.2	2.1
		NW	2877	3.8	1881	9.5	2.5
		Total	75052	100.0	19873	100.0	11.9
5	Plan Curvature	a. Concave (<-0.05)	37631	50.1	9214	46.4	0.9
		b. Flat (-0.05-0.05)	11	0.0	8	0.0	2.7
		c. Convex (>0.05)	37411	49.8	10654	53.6	1.1
		Total	75053	100.0	19876	100.0	4.7
6	Distance from river(M)	a. 0-5	23724	31.6	4760	23.9	0.8
		b.5-10	18304	24.4	4560	22.9	0.9
		c.10-15	14573	19.4	4351	21.9	1.1
		d.15-20	10015	13.3	3367	16.9	1.3
		e.20-35	8440	11.2	2838	14.3	1.3
		Total	75056	100.0	19876	100.0	14.9

Table 2A. Sieve analysis for Point 1

Sieve size	Mass retained(g)	percentage retained	cumulative percentage retained(g)	Percentage finer
4.75	1095	54.75	54.75	45.25
2.36	430	21.5	76.25	23.75
1.18	50	2.5	78.75	21.25
0.6	100	5	83.75	16.25
0.3	115	5.75	89.5	10.5
0.15	160	8	97.5	2.5
0.075	35	1.75	99.25	0.75
pan	15	0.75	100	0

Table 2B. Unconfined compressive and Sieve analysis test of rock-soil for Point 2

point	Hammer rebound number	Unconfined compressive strength (Mpa)
	12.5	27.75
	13.5	28.75
	14.5	29.25
	13	28.5
	11	26.5
Point 2	13	28.5
	16	30.25
	14.5	29.25
	13	28.5
	16	30.25
	17.5	31.25
	12.5	27.75

Sieve size	Mass retained(g)	%age retained	Cum. %age retained(g)	%age finer
4.75	745	37.25	37.25	62.75
2.36	415	20.75	58	42
1.18	170	8.5	66.5	33.5
0.6	210	10.5	77	23
0.3	185	9.25	86.25	13.75
0.15	130	6.5	92.75	7.25
0.075	115	5.75	98.5	1.5
pan	30	1.5	100	0

Table 2B. Unconfined compressive and Sieve analysis test of rock-soil for Point 3

point	Hammer rebound number	Unconfined compressive strength (Mpa)
point 3	14	28.75
	14.5	29.25
	15	29.5
	16	30.25
	12.5	27.75
	15	29.5
	16	30.25
	15.5	29.75
	15	29.5
	14	28.75
	17.5	31.25
	17	31

Sieve size	Mass retained(g)	percentage retained	cumulative percentage retained(g)	Percentage finer
4.75	875	43.75	43.75	56.25
2.36	545	27.25	71	29
1.18	90	4.5	75.5	24.5
0.6	125	6.25	81.75	18.25
0.3	120	6	87.75	12.25
0.15	15	0.75	88.5	11.5
0.075	5	0.25	88.75	11.25
pan	225	11.25	100	0

Table 2C. Unconfined compressive and Sieve analysis test of rock-soil for Point 4

point	Hammer rebound number	Unconfined compressive strength (Mpa)
point 4	15	29.5
	14.5	29.25
	13	28.5
	17	31
	14	28.75
	17.5	31.25
	16	30.25

		percentage	cumulative	Percentage
Sieve size	Mass retained(g)	retained	percentage retained(g)	finer
18		31.75		
16.5		30.5		
15		29.5		
17.5		31.25		
18		31.75		

Sieve size	Mass retained(g)	percentage retained	cumulative percentage retained(g)	Percentage finer
4.75	1140	57	57	43
2.36	395	19.75	76.75	23.25
1.18	50	2.5	79.25	20.75
0.6	95	4.75	84	16
0.3	90	4.5	88.5	11.5
0.15	85	4.25	92.75	7.25
0.075	70	3.5	96.25	3.75
pan	75	3.75	100	0

Table 2D. Sieve analysis for Point 5

point	Hammer rebound number	Unconfined compressive strength (Mpa)
point 5	10.5	26
	12.5	27.5
	11.5	26.75
	17	31
	13	28.5
	14.5	29.25
	13	28.5
	16	30.25
	16.5	30.5
	17.5	31.25
	16	30.25
	18	31.75

Point 5				
Sieve size	Mass retained(g)	percentage retained	cumulative percentage retained(g)	Percentage finer
4.75	505	25.25	25.25	74.75
2.36	530	26.5	51.75	48.25
1.18	285	14.25	66	34
0.6	275	13.75	79.75	20.25
0.3	205	10.25	90	10
0.15	95	4.75	94.75	5.25
0.075	65	3.25	98	2
pan	40	2	100	0

Table 2E. Sieve analysis for Point 6

Point 6				
Sieve size	Mass retained(g)	percentage retained	cumulative percentage retained(g)	Percentage finer
4.75	816	40.8	40.8	59.2
2.36	665	33.25	74.05	25.95
1.18	130	6.5	80.55	19.45
0.6	124	6.2	86.75	13.25
0.3	100	5	91.75	8.25
0.15	65	3.25	95	5
0.075	60	3	98	2
0	40	2	100	0

Table 2F. Table generalized sieve analysis test for Rock-Soil slope stability evaluation

Soil class	Percentage finer					
	point 1	point 2	point 3	point 4	point 5	point 6
Gravel fraction (Retained on 4.75 mm sieve)	45.25	62.75	56.25	43	74.75	59.2
Sand fraction(Passes on 2.36 and Retained on .075 mm sieve)	23.75	42	29	23.25	48.25	25.95
Fine grained fraction (passes on .075 mm sieve)	0.75	1.5	11.25	3.75	2	2

Table 3A. Table for angle of repose test for Rock-Soil slope stability evaluation

Sampling points	failure slope angle in degree (in field)	Angle of repose in degree
1	44	46
2	45	43
3	40	38
4	41	40
5	39	41
6	38	36

Table 4A. Direct shear test result for soil at point 2

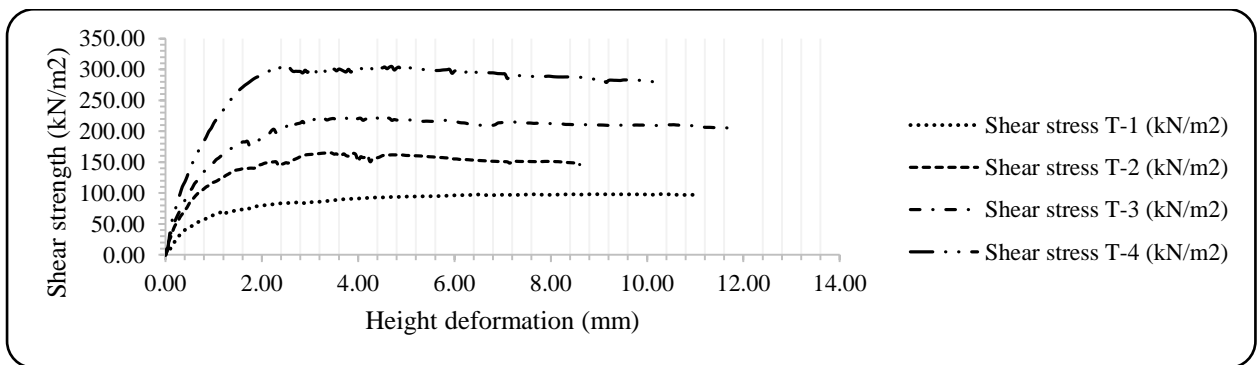| Trial	Normal Stress (kN/m2)	Max. Shear Stress (kN/m2)	Cohesion C, (kN/m2)	Angle of Friction, Ø
1	109	98.39		
2	218	164.92	28	32
3	327	221.64		
4	436	305.58		

Table 4B. Direct shear test result for soil at point 3 and 5

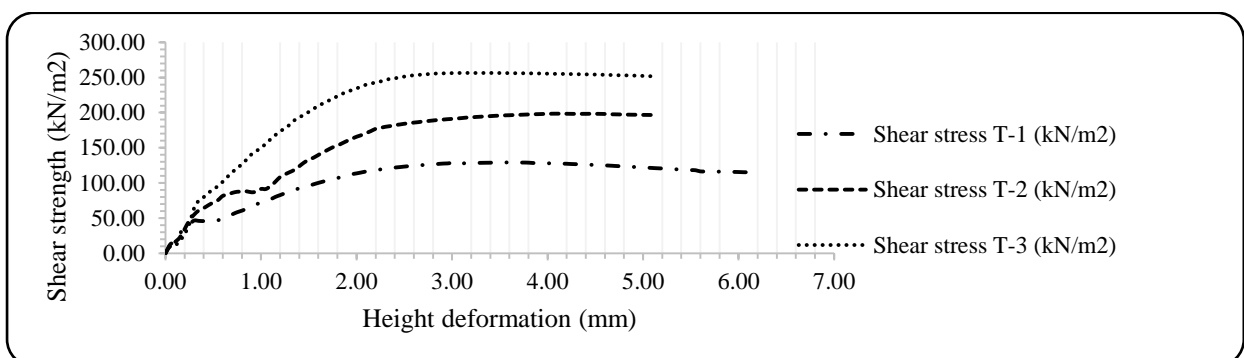| Trial	Normal Stress (kN/m2)	Max. Shear Stress (kN/m2)	Cohesion C, (kN/m2)	Angle of Friction, Ø
1	109	129.25		
2	218	198.53	68	30.
3	327	256.39		
4				

Table 4C. Direct shear test result for soil at point 4

Trial	Normal Stress (kN/m2)	Max. Shear Stress (kN/m2)	Cohesion C, (kN/m2)	Angle of Friction, Ø
1	109	73.31		
2	218	147.49	14	31
3	327	215.73		
4	436	267.19		